# THE Acoustic Sizing OF Bubbles IN Liquids

# THE ACOUSTIC SIZING OF BUBBLES IN LIQUIDS

**by Andrew John Hardwick**

of Corpus Christi College,
Cambridge



A dissertation
submitted to the University of Cambridge for the
Degree of Doctor of Philosophy.

"Sometimes, on Sundays, I hear the bells, the Lincoln, Acton, Bedford, or Concord bell, when the wind is favourable, a faint, sweet, and, as it were, natural melody, worth importing into the wilderness. At a sufficient distance, over the woods this sound acquires a certain vibratory hum, as if the pine needles in the horizon were the strings of a harp which it swept. ... The echo is, to some extent, an original sound, and therein is the magic and charm of it. It is not merely a repetition of what was worth repeating in the bell, but partly the voice of the wood: the same trivial words and notes sung by a wood-nymph."

'Walden' (Thoreau 1854)

"When caught *in flagrante delicto*, never apologise, always justify."

'The Rules of Life' (Weldon 1987)

# FOREWORD

"Bubbles.", I reply when asked about my work. "What? Bubbles?" is the normal response from anyone not doing fluid mechanics or chemical engineering. "Yes, bubbles" I confirm calmly. After a pause, the next question – "What do you, erhm, do with bubbles?" – is delivered with a disbelieving but intrigued expression. I smile slightly and say "I listen to them".

---

# ACKNOWLEDGEMENTS

The 'Acoustic Sizing of Bubbles in Liquids' project was funded by The Petroleum Science and Technology Institute, 25 Ravelston Terrace, Edinburgh. The developmental and experimental work were performed from October 1991 to September 1994 in the Physics and Chemistry of Solids Group and the Polymers and Colloids Group of the Cavendish Laboratory, Cambridge University. I am grateful to Corpus Christi College for the years I have lived on its pleasant Leckhampton site.

There are three people concerned with this project whom I am obliged to thank: Alan Walton, John Field and Tim Leighton. I thank Alan Walton, my supervisor, for co-inventing the Acoustic Bubble Capacitor, for allowing most of the development to proceed without interference, for proof-reading this work and for being a lot more cheerful and optimistic than I was about the project's progress. I thank John Field for his expertise in matters financial which enabled the project be realised; I also have a reason to thank John Field for encouragement. I thank Tim Leighton, my supervisor for only two months, for initiating the bubble sizing project which evolved into the study presented here.

I especially thank Chris Moss, who acted as my mentor in electronics, without whom the instrumentation development which lead to majority of the results presented here would have been impossible.

There are others whom I wish to thank for particular things. I thank Brian Pippard for his sharp and timely spotting of an error which would have otherwise

been highly embarrassing; with his comment it proved to be fortuitous instead. I thank Dave Powell for his instruction, patience and sarcastic humour as I bodged my way though his machine shop building equipment. I thank Adrian Panton, Howard Thompson and Roger Halls for electronics advice. I thank the P&C technicians: Pete Bone for help and advice on mechanical problems; Roger Peck for chemical advice; and both for their collection of amusing and instructive anecdotes. I thank Chris Beton for putting up with my unanswerable bubble questions and early attempts at bubble theory, and for carrying out the computer simulation to verify my two-bubble resonance theory. I thank the Cambridge Philosophical Society for an extra term's funding. I thank CUS&RC for introducing me to dance. Mi dankas Mark Rison, Edmund Grimley-Evans kaj Marriane Welle, kiuj donis al mi mian unuan sperton de neangla pensado. I thank Angela Skamvetsaki whose letter indirectly retriggered my amateur interest in art that lead to the design of this dissertation. I thank Fred, Vincent and John of central stores who have got used to me asking for thousands of small items, including several distinctly odd ones. Sheila and Cynthia, the cleaners, have had to cope with paint, solder, soap, tape, glycerine, glue, paper and two oil-spills on my floor. Kelvin Fagan reproduced the photographic plates.

I thank Chau, Karen Croot, Emma Gee, Alena Pance and Thierry Guihenuef for friendship, discussions, food, novel ways of viewing the world and many other things. I also wish to thank the many people who have been friends in the past three years including Richard Noakes, Jenny Marshall, Steve Walley, Andrew Clarke, Clive Lacy, 'PNAM' Prince, Lee Daniels, Stuart Whitcombe, George Jacques, Dana Raydan, Filotei Kolitsi, 'JD' Hatchell, 'Jis' Ham, Ruth Salomon, Michelle Webster, Ross Jones, Dave Smith, Duncan Barker, Genet Edmondson, Nikolay Todorov, Katie O'Neil, Richard Marsh, Phillippa, Steven Walker, Irene Zadnik, Kim Baskerville, Tarrick Lule, Nicolette Bethel, Chris Breach, Lucy Kinton, Guy Cecil, Anne Metherell, Anne Willoughby, Paul Prendergast, Andrew Hogg, Fiona Sneddon, Beat Kumin, Chris Daly, Tara Shears, Mike Witty, Mathew Parkin, and all those whom I have never got round to asking the names of. Additionally, I thank those who have helped in someway and are not already mentioned including Meg Staff, Nick Safford, Martin Harvey, Tom White, Jim Collett, Adrian Rennie, Andy 'Elvis' Phelps, Larry Silver, Peter Duffet-Smith, Ian Hopkinson, Matin Durrani, Stewart Palmer, Rodger Beadle, Jacqui Hardwick, Lesley Hughes and Gerry Meten.

Of course, I thank my Mum and Dad.

# PREFACE

I declare that, except where explicitly stated otherwise, this dissertation is the result of my own work and includes nothing which is the outcome of work done in collaboration. This dissertation is not substantially the same as any that I have submitted for a degree or diploma or other qualification at any other university and no part of it has been or is being concurrently submitted for any such qualification.

This dissertation contains one hundred and twelve illustrations and approximately thirty six thousand words and is therefore within the proscribed limits.

1994-12-1

# EDITION HISTORY

This dissertation has been published in 6 editions so far. This is edition 6.

**Edition 1 (1994):** Original version submitted for examination. Hardback. Alterations (mainly typos) penned in after *viva*. Only 3 copies produced.

**Edition 2 (1995):** With the *viva* alterations edited in. Hardback. Only 4 copies produced.

**Edition 3 (1995):** With photographic plates converted to half-tone screening for photocopier mass production. Hardback, paperback & unbound.

**Edition 4 (2002):** Converted to digitally transmissible form from Edition 2 by combining the original text & equation files with figures & photographs scanned at 600 dpi from the paper master copy. PDF & other printer-optimized computer file formats.

**Edition 5 (2003):** Converted to World Wide Web pages. Typos spotted during the conversion were corrected. HTML/PNG/JPEG/CSS format files.

**Edition 6 (2003):** As Edition 4 but incorporating the corrections of version 5. PDF & other printer-optimized computer file formats.

2003/2/22

# TABLE OF CONTENTS


Title Page 1
Quotes 2
Foreword 3
Acknowledgements 3
Preface 5
Edition History 5
Table of Contents 6

I. ACOUSTIC BUBBLE SIZING REVIEWED 9
I.1. Introduction 9
I.2. Applications 10
I.2.1. Petroleum and Related Industries 10
I.2.2. Sounds of Bubbles in Nature 10
I.2.3. Cavitation 13
I.2.4. Cleaning and Separation 14
I.2.5. Sonochemistry and Sonoluminescence 15
I.2.6. Food Sciences 16
I.2.7. Bubbles in Medicine and Biology 16
I.3. Mathematics 18
I.3.1. Simple Harmonic Oscillators 18
I.3.2. The Resonant Frequency of a Bubble 19
I.3.3. Sound Radiation from a Bubble 20
I.3.4. The Rayleigh Plesset Noltingk Neppiras Poritsky Equation 20
I.3.5. Damping 21
I.3.6. Boundaries and Nonspherical Bubbles 24
I.4. Activity of Bubbles 25
I.4.1. Cavity Collapse 25
I.4.2. Polytropic Index Variation 25
I.4.3. Bubble Creation 26
I.4.4. More on Boundary Effects 27
I.4.5. Motions of Bubbles in a Sound Field 28
I.4.6. Surface Waves 28
I.4.7. Subharmonic Emission 30
I.5. Overview of Techniques 31
I.5.1. Using Sound Scattering and Attenuation 31
I.5.2. Using Bubble Resonance 32

I.5.3. Using Harmonic Distortion 34
I.5.4. Using Frequency Mixing 34
I.6. Some Promising Devices 35
I.6.1. Wolf's Ultrasonic Tomographer 35
I.6.2. Farmer and Vagle's Four Frequency Echo-sounder 35
I.6.3. Breitz and Medwin's Resonator 35
I.6.4. Miller's Resonant Bubble Detector 36
I.6.5. Newhouse and Shankar's Frequency Mixing Method 36
I.6.6. Lingard and Leighton's Subharmonic Modulation Method 37

II. The ACOUSTIC BUBBLE CAPACITOR TECHNIQUE 38
II.1. Development 38
II.1.1. The Principle 38
II.1.2. The Capacitor 39
II.1.3. The Electronics 41
II.2. Testing 42
II.3. Applications 46
II.3.1. Rising Bubbles 46
II.3.2. Dissolution of Bubbles 46
II.3.3. Multiple Bubbles 48
II.4. Conclusion 49

III. The ACOUSTIC RE-EMISSION TECHNIQUE 50
III.1. Development and Testing 50
III.1.1. The Principle 50
III.1.2. Utilising a Commercial Hydrophone 50
III.1.3. Adapting The ABC 53
III.2. Further Characterisation of Bubble Resonance 56
III.2.1. The Influence of the ABC's Shape 56
III.2.2. The Damping Mechanism 57
III.2.3. The Distance Dependence 58
III.2.4. The Excitation Amplitude Dependence 58
III.2.5. Different Gases 59
III.2.6. Rising Bubbles 60
III.3. Pairs of Unequally Sized Bubbles 62
III.3.1. The Theoretical Analysis 62
III.3.2. The Simple Cases Verification 65
III.3.3. The Computational Verification 66
III.3.4. The Experimental Verification 67
III.4. Conclusion 67

IV. THE SUBHARMONIC MODULATION TECHNIQUE 69
IV.1. Background 69
IV.1.1. Earlier Research 69
IV.1.2. Preliminary Studies 69
IV.2. The Instrumentation 72
IV.2.1. Requirements 72
IV.2.2. Equivalent Representations of Modulation 73
IV.2.3. Instrumentation Mechanics 74
IV.2.4. Instrumentation Electronics 75
IV.3. The Origin of Subharmonic Modulation Explained 80
IV.3.1. The Proposed Mechanism: 80
IV.3.2. The Experimental Evidence: 80
IV.3.3. Implications: 82
IV.4. Characterising the Subharmonic Modulation 83
IV.4.1. The Sound Frequency Dependencies 83
IV.4.2. The Sound Amplitude Dependence 86
IV.4.3. Further Description of the Erratic Behaviour 88
IV.4.4. Phase Shifts 90
IV.4.5. Bubbles on Wires 91
IV.5. Conclusion 93

CONCLUSIONS 95
C.1 Comparison between the Techniques 95
C.2 Comparison to Other Techniques 96
C.3 Common Features 97
C.4 Publications 98
C.5 Final Remarks 98

APPENDICES 99
A.1. Appendix 1: Electronic Circuits 99
A.2. Appendix 2: Speaker Calibration 110
A.3. Appendix 3: Symbol Definition Summary 112
A.4. Appendix 4: Recommended Reading 115
A.5. Appendix 5: Alternative Text 116
A.6. Appendix 6: Bibliography 119
A.7. Appendix 7: Photographic Plates 130

# I. ACOUSTIC BUBBLE SIZING REVIEWED

## I.1. INTRODUCTION

When introducing the science of acoustic bubble sizing, a variety of questions arise: How does one listen to bubbles? Are bubbles important in nature? What do bubbles sound like? Do bubbles have medical implications? In what manner do bubbles respond to sound? Who is interested in measuring bubbles?

This first chapter aims to answer these questions. After a general section on situations involving bubbles to give a 'feel' for the subject, some relevant dynamics of bubbles are covered. Mathematical results which will be of use later are concisely derived. The chapter ends with a review of previously published methods of acoustic bubble sizing.

The research project originated with a discovery during a final-year undergraduate project (Lingard 1990). It was found that a bubble forced to oscillate radially can modulate scattered ultrasound at half the forcing frequency. The original aim of the project was to develop this effect into a technique for bubble sizing. The objectives were first to create an analogue signal processing system to analyse the modulation in real time and then to apply it to bubbles in various situations.

Designing the electronics transpired to be a considerable project in itself. During the design period, some other ideas for acoustic sizing were tested. The successful ideas included the Acoustic Bubble Capacitor which forms the subject of chapter II. The acoustic re-emission technique of chapter III started as an offshoot of the work on the Acoustic Bubble Capacitor. Finally the project returned to the original theme of subharmonic modulation resulting in chapter IV.

## I.2. APPLICATIONS

Many situations involve bubbles. This section briefly describes some of these to give an impression of the diverse areas for which bubble sizing could be of interest and to give a 'feel' for bubble research. Some of the following examples of bubbles and the closely related topic of cavitation are important; others are just included because they may be of interest. The selection is biased towards acoustic aspects of bubbles.

### I.2.1. PETROLEUM AND RELATED INDUSTRIES

Oil reservoirs are under high pressure from overlying rocks so gas dissolves in the oil. When the oil is brought to the surface where the pressure is much less, most of the gas comes out of the solution.

This can be a serious safety problem. Reservoir pressures are typically $10^3$ atm so any bubbles forming at the bottom of a wellbore will expand a thousandfold even without further gas coming out of solution. It is therefore important to detect gas bubbles, preferably whilst the oil is still down the hole. Similarly, it would be valuable for the downhole logging apparatus to include the a device to measure gas bubbles in the drilling mud.

In normal operation, oil pipelines carry a mixture of oil, gas, water, mud and grit. Measuring the gas bubbles in this multiphase flow is far from straightforward but situations such as oil of different qualities from different operators flowing through the same pipeline maintain a strong commercial desire for gas monitoring devices. Multiphase flow instrumentation is also wanted in many parts of the chemical industry.

### I.2.2. SOUNDS OF BUBBLES IN NATURE

Several common sounds found in the natural environment result from bubbles. The earliest one explained was that of running water:

#### *I.2.2.1. BABBLING BROOKS*

W.H.Bragg reported the work of Richard Paget (Bragg 1921a) on bubble sounds in his Royal Institution Christmas Lectures for children in 1919 and postulated (Bragg 1921b) them for the origin of the babbling sound of running water. Paget had made model open cavities to represent bubbles at the moment of formation or bursting. He blew air across the openings. They resonated in the manner of a musical ocarina. This resonating mechanism was not the correct one, instead breathing mode

oscillations of the bubble walls are dominant (Minnaert 1933), but bubbles are still accepted as the cause of babbling.

Underwater recordings of babbling brooks (Leighton and Walton 1987) show the sound to be composed of 'pings' (rapidly starting exponentially decaying sinusoids) from individual oscillating bubbles. Pumphrey c.1987 gave a quick explanation of why the oscillation is easily heard outside the water: a sound source close to the water's surface has an effective 'image' sound in the air above the surface.

#### *I.2.2.2. RAIN NOISES*

Typically, the underwater noise of rain is a broad-band sound peaking at 14 to 16 kHz. It has been postulated to come either from the impact of the water drops (see Pumphrey 1991a or 1991b for calculation) or the oscillations of newly created bubbles. These bubbles are sometimes pinched off from the bottom of the cavity formed by the raindrop as the surface wave carrying water back into the cavity overturns (Oğ uz and Prosperetti 1990a).

Liquid drop impacts into liquids were first photographed by Worthington and Cole 1897. Mallock 1919 photographed the underwater results of lead shot falling into water and, mistakenly, assumed that organ-pipe like resonances in the cavities caused the sound. When Pumphrey and Walton 1988 photographed the impact of droplets underwater and simultaneously recorded the sound, it was clear that the most significant sound was the oscillation of newly pinched-off bubbles. The formation of bubbles seemed at first to be a too random process to cause the typical structure of rain noise until regular entrainment was discovered (Pumphrey *et al* 1989). Regular entrainment is the reliable production of bubbles by droplets of certain sizes and speeds. Combined with the radius dependence of a raindrop's terminal velocity, drops of 0.8 to 1.1 mm radius will often produce oscillating bubbles. The resonances of these bubbles explain the peak in spectra of underwater rainfall noise (Pumphrey *et al* 1989, Pumphrey and Crum 1990, Pumphrey 1990, Pumphrey and Elmore 1990). Pumphrey *et al* 1989 proved this to be the mechanism by reducing the surface tension of water. This prevented regular entrainment and so reduced the power in the 14 to 16 kHz peak.

Bubble entrapment by raindrops has also been studied by mathematical analysis and numerical simulation. Examples are Longuet-Higgins 1990a and Oğ uz and Prosperetti 1991 respectively.

The underwater sound of rainfall is not just of academic interest. Potentially, it could be used to monitor rainfall into seas. This is a major part of the hydrological

cycle but part which is far less well recorded than the rain onto land because of the expense of maintaining weather stations at sea. More speculatively, bubbles themselves may be responsible for some rainfall. Bursting ocean surface bubbles eject fine droplets which evaporate to leave non-volatile particles (Blanchard 1963 estimated $10^{10}$ tonnes per year) which can nucleate raindrops.

#### *I.2.2.3. OCEAN NOISE*

The ambient noise in oceans contains a windspeed-dependent component above 100 Hz known as Knudsen noise (Pumphrey and Ffowcs Williams 1990). Knudsen noise has a maximum at 0.5 kHz followed by a fall of 5 to 6 dB per octave (Knudsen *et al* 1948). Wenz 1962 proposed oscillating bubbles as the cause of Knudsen noise. Bursting bubbles (Prosperetti and Lu 1988), collapsing bubbles (Prosperetti and Lu 1988) and bubbles which amplify turbulence noise (Prosperetti 1988a, 1988b) have been dismissed as causes on theoretical grounds.

The bubbles are created by breaking waves (see Longuet-Higgins and Turner 1974, for example, for a model of aeration by breaking waves). Even when gravity waves do not break, so no white-caps are visible, capillary waves can have sharp enough troughs to trap air (Kolaini *et al* c.1990). It is the slope of the water surface rather than the speed of the wind which is significant; waves created without wind by a plunger in a large tank still produced noise (Medwin and Beaky 1989, Medwin and Daniel 1990). The creation or division of bubbles, not merely excitation of bubbles by a passing wave, is necessary to generate the observed noise levels according to Pumphrey and Ffowcs Williams 1990.

Additional sound mechanisms have been postulated. One is that capillary waves entrain air initially as cylindrical bubbles. These then violently oscillate in shape and so radiate sound (Longuet-Higgins 1988b). Possibly bubbles also contribute to lower frequency noises since the resonant frequency for the collective oscillation of a bubble cloud is far below that for and individual bubble (Kozhevnikova and Bjørnø 1992).

#### *I.2.2.4. INFLUENCE ON OCEANIC SOUND PROPAGATION*

Bubbles scatter and dissipate sound in water. Several acoustic bubble sizing methods are based on this but for users of sonar, bubbles can be an inconvenience. Useful reflected sonar signals are attenuated and the reflection from a bubble cloud associated with a wave on the sea surface may be mistaken for a moving vessel. Conversely a ship can also create a bubble wake, in which case sound scattered from the bubbles helps with detecting the ship (Thorpe 1982).

Attenuation by bubbles is frequency dependent so the Kramers-Kronig relations (Temkin 1990) imply that the soundspeed is also frequency dependent in bubbly water. The soundspeed is lowered close to the ocean surface by bubbles so there is a possibility that some sound can be trapped near the surface. This may explain some of the maxima in the underwater ocean sound spectrum which survive between successive waves (proposed and tested by Farmer and Vagle 1989; theoretical analysis by Buckingham 1991) though alternative explanations exist (e.g. Longuet-Higgins 1990b favoured bubble shape resonances).

#### *I.2.2.5. OCEANIC GAS ABSORPTION*

The increasing concentration of carbon dioxide and certain other gases in the atmosphere has caused much concern recently. The oceans are the major removers of carbon dioxide. The rate of removal may be limited by the rate at which the gas is absorbed into the water. Many rate measurements have been attempted (e.g. Watson *et al* 1984 in the North Sea with helium-3 and sulphur hexafluoride tracers instead of carbon dioxide). Bubbles may be important because bubble plumes carry gases down below the surface with the sea-surface water currents (Thorpe 1984) and the extra pressure from the bubbles' surface tensions increases the dissolution rate.

For the 'lifestory' of a typical bubble plume, see Monahan and Lu 1990.

### I.2.3. CAVITATION

Cavitation is the formation of vaporous cavities in a liquid by a reduction in pressure. Motion of the liquid or the objects bounding it usually provide the pressure change but other sources exist, including high intensity sound. Cavitation is an important engineering subject into which a great deal of research has been performed. It is included here merely as part of the background to a work which otherwise mainly concerns gas filled cavities rather than vapour filled ones so only a few examples are mentioned.

#### *I.2.3.1. PIPES, PROPELLERS, PUMPS AND TURBINES*

If a propeller cuts through water too fast then water effectively tears and cavities spread back from the propeller hub, blade tips or blade surfaces. The extreme case is a single large cavity around the object (Plesset 1949). The propeller then has less contact with the water and the cavities impede the flow; both of these reduce the thrust. The later collapse of these cavities erodes the propeller and the thrashing of the drive system as it runs in vapour instead of liquid can damage the motor.

The unexpected loss of power with the first steam turbine driven ship, the Turbinia, led Parsons Steam Turbine Company, its designers, into the first important investigations of cavitation (Pearsall 1972a). Nine separate propellers sharing the load was their solution. Present solutions also include careful propeller designs that either deter cavitation or increase the cavity size sufficiently that the cavities move away from vulnerable surfaces before collapsing (Pearsall 1972b).

The erosive ability of cavitation is enhanced by jetting. As a cavity near a boundary collapses, the liquid on the side opposite the boundary can move most easily so that side becomes concave and eventually the liquid rapidly jets through the shrinking cavity to strike the surface (Plesset and Prosperetti 1977). The impact pressure might be increased further by a cloud of cavities. The collapsing outer parts of the cloud temporarily shield the inner cavities which collapse later. The combined pressure pulse then reaches the cloud centre (Mørch 1977).

Pumps (Pearsall 1972c) and turbines (Pearsall 1972d) cavitate similarly to propellers. Fish have been known to pass through hydroelectric turbines intact (therefore they were not hit by the blades) but nevertheless dead because of the pressures in the turbines (Pearsall 1972e).

Pipes can suffer from cavitation as well. The collapse of the Tarbella tunnel in Pakistan in 1974 resulted from cavitation damage; Trevena 1987c provides a description and photographs.

#### *I.2.3.2. LUBRICATION AND DRAG*

Contacts which are lubricated by liquid films must be carefully designed to minimise wear and energy loss. Basic hydrodynamic lubrication theory functions only at positive liquid pressures (Floberg 1964) but surfaces which are rapidly separating or sliding may create a negative pressure in the lubricant leading to cavitation (Trevena 1987b) which greatly complicates the situation.

Conversely, cavitation can reduce drag. The low pressure region behind a hydrofoil moving rapidly through water contributes to drag. A solution is to supplement the cavitation behind the hydrofoil by allowing air to be sucked down there. This reduces the low pressure responsible for drag and reduces the damage from collapsing cavities (Turin 1964).

### I.2.4. CLEANING AND SEPARATION

It was stated above that cavitation can cause erosion. This erosive ability is used in ultrasonic cleaners; the cavitation being induced acoustically (Graf and Whalen

1974). For cleaning offshore structures used in oil and gas production, a steerable version has been developed (Almas Tench *et al* 1992). The position of the maximum ultrasound amplitude was steered by controlling the phase of the 50 kHz ultrasound from each of 270 transmitters.

Ultrasound can enhance the growth rate of bubbles (see section I.4.3 on rectified diffusion) so ultrasound is used to degas liquids. The gas comes out of solution to form bubbles which rise out of the liquid.

Besides the internal gas, a bubble will carry some of the surrounding liquid as it rises. This has been used directly to melt floating ice in rivers by bringing warmer water up from below (Pounder 1965). It is also used for surfactant removal. Surfactants are attracted to interfaces of bubbles and are carried up with the bubbles (Degrois and Baldo 1974). 'Flotation' processing of ores is similar (Güth 1956). Chemicals, called 'collectors', which bind to the substance to be extracted are added to a suspension of crushed ore. The 'collector' reduces the affinity of the substance for water and extraction proceeds as for surfactants.

### I.2.5. SONOCHEMISTRY AND SONOLUMINESCENCE

Acoustic cavitation can cause high local pressures and temperatures. These can aid many chemical reactions (Mason 1993). This is 'sonochemistry'. Cavitation is also used for reducing particles to a fine powder (Mason *et al* 1992) and mixing reactants (Pearsall 1972e).

It has been observed that acoustic cavitation sometimes produces light emission ('sonoluminescence') from liquids. Many explanations including triboluminescence and various electrical theories (e.g. Degrois and Baldo 1974) have been proposed but are largely considered disproved (Walton and Reynolds 1984). The recombination of free radicals and the decay of other transient electrochemical states (as Suslick and Flint 1987 observed) comprise a more favoured explanation though there is still much disagreement (Vaughan and Leeman 1986 even dispute connection with cavitation). Thermal radiation (Noltingk and Neppiras 1950) is also widely favoured. The temperatures reached are unknown. Flint and Suslick 1991 estimated 5 kK from the spectral line profiles of sonoluminescence, though temperature itself may not be well defined since thermal equilibrium might not be reached during the short time span of sonoluminescence (Jeffies *et al* 1992). Recently several popular articles – in Nature (Maddox 1993), in The Scientific American (Yam 1993) and even on British prime-time television (Tucker *et al* 1994) – have increased the general interest in sonoluminescence. Note that not all glows from insonated liquids are strictly sonoluminescence, but may arise from light producing sonochemical reactions (e.g.

hydroxyl radicals from hydrogen peroxide reacting with 3-aminophthalhydrazide ('luminol') was the basis of the spectacular demonstration in Tucker *et al* 1994).

### I.2.6. FOOD SCIENCES

Stable gas bubbles are important in the food industry. Besides the obvious application in effervescent beverages, the control of bubbles is crucial in achieving pleasant textures in many products. For example, bread must be made from dough deformable enough that the carbon dioxide produced by yeast inflates it yet tough enough to prevent the gas escaping uselessly before the bread is cooked (McGee 1991a).

### I.2.7. BUBBLES IN MEDICINE AND BIOLOGY

#### *I.2.7.1. DECOMPRESSION SICKNESS*

The most well known medical problem involving bubbles is decompression sickness ('the bends'). When deep under water for prolonged periods, the high pressure increases the dissolution of nitrogen in the diver's blood. Upon resurfacing, the nitrogen forms bubbles which obstruct bloodflow, cause pain in joints and can be fatal. Much of the medical research into bubble detection is connected with this.

A slightly similar effect is responsible for the cracking sound when knuckle joints are pulled. The sound is from bubbles forming in the synovial fluid where the separating finger-bones momentarily reduce the pressure (reviewed in Trevena 1987b).

#### *I.2.7.2. IMPLICATIONS FOR MEDICAL ULTRASOUND*

Therapeutic ultrasound is commonly used as an aid to healing though its effect may be largely as a placebo (Hashish and Harvey 1987). The power used for this is usually too low for flesh to be thermally damaged (though ultrasound can thermally destroy tissue if desired (Frizzel *et al* 1977)) unless the energy is somehow concentrated. Recently there has been concern about the possibility that oscillating bubbles could provide the concentration and lead to long term medical problems from cavitation damage or free radical production.

Direct cavitation damage from therapeutic ultrasound seems unlikely (Gross *et al* 1985) but a study of sonoluminescence left open the possibility of free radical production (the papers Leighton *et al* 1988, Pickworth *et al* 1988, Pickworth *et al* 1989b, Pickworth *et al* 1989c, Leighton *et al* 1990d, and the abstracts Leighton *et al* 1987, Pickworth *et al* 1989a, Pickworth *et al* 1989d). The study found that a therapeutic ultrasound unit could produce sonoluminescence in water at ultrasound

antinodes but no sonoluminescence was observed when the test was repeated with a human cheek. It explained the increase in sonoluminescence when the ultrasound was pulsed (Leighton 1989a) as due to transient bubble oscillation (Leighton 1989b) or the prevention of bubbles clustering which shields some bubbles (Leighton *et al* 1989a). For a concise review of medical ultrasound hazards and sonoluminescence, see Dendy 1988.

#### *I.2.7.3. LITHOTRIPSY*

In extracorporeal shock-wave lithotripsy, sound pulses from outside the patient's body are used to break kidney and gall stones. The exact mechanism of break-up is uncertain; Pfeiler *et al* 1989 lists crushing, cavitation in the stone and cavitation in the liquid around the stone. A common style of lithotripter, which creates the pulse by sparking, gives a series of smaller shocks after the main shock. Bubbles may grow near the stone during the rarefaction which follows the main shock. Possibly these bubbles break the stone when the subsequent shocks collapse them (Coleman 1991). Williams *et al* 1989 detected bubbles produced by a lithotripter pulse in both water and blood *in vitro* but not *in vivo*.

#### *I.2.7.4. BLOOD PRESSURE*

Contrary to popular belief, small quantities of gas injected into a bloodstream are not necessarily fatal (Gresham c.1983). Fairbank and Scully 1977 proposed measuring the blood pressure inside the heart by acoustically detecting the changes in size of such bubbles. If the bubbles are ~4 μm or less in diameter (Nishi 1975) then the cellular structure of blood may need to be taken into account in the acoustics.

#### *I.2.7.5. ZOOLOGY*

The final example in this applications section is the muskrat. Muskrats swimming under ice appear to waste air exhaling too soon. This is not actually wastage, MacArthur 1992 discovered, but the creation of a reservoir of bubbles to breathe on later trips.

## I.3. MATHEMATICS

This section presents several derivations whose results are used later in this dissertation. (There is a summary of symbol definitions in Appendix 3.)

### I.3.1. SIMPLE HARMONIC OSCILLATORS

Though very well known, a review of some aspects of simple harmonic motion (SHM) will clarify many of the arguments used later in this dissertation.

The dynamics of a linear oscillation in a variable $\zeta$ about $\zeta = 0$ obeys the equation

$$m\ddot{\zeta} + \chi\zeta = 0 \qquad \{1.1\}$$

with $m$ as the inertial parameter and $\chi$ as the stiffness parameter. It has the oscillatory solution

$$\zeta = \alpha\cos\omega_0 t + \beta\sin\omega_0 t \qquad \{1.2\}$$

where $\alpha$ and $\beta$ are arbitrary constants and $\omega_0 = \sqrt{\chi/m}$ is the resonant angular frequency. For a bubble in radial oscillation, the liquid supplies the inertia and the gas supplies the stiffness. $\zeta$ will be taken as $R - R_0$, the departure of the radius from equilibrium, though pressure or volume departures could have been chosen. (Angular frequencies (in rad/s) will be denoted by $\omega$ with subscripts and conventional frequencies (in Hertz) will be denoted by $\nu$ (=$\omega$/2π) with corresponding subscripts.)

A damped oscillator such as a bubble has another term:

$$\ddot{\zeta} + (Q^{-1}\omega_0)\dot{\zeta} + (\chi/m)\zeta = 0\,. \qquad \{1.3\}$$

$Q^{-1}$ is called the 'damping constant' and $Q$ is called the 'Quality'. A decaying sinusoid is produced.

The sizing methods of chapters II to IV all involve acoustically exciting (forcing) the bubbles into oscillation. Adding a forcing term at $\omega$ with amplitude $(\chi/m)\Gamma$ gives

$$\ddot{\zeta} + (Q^{-1}\omega_0)\dot{\zeta} + (\chi/m)\zeta = (\chi/m)\Gamma\sin\omega_e t\,. \qquad \{1.4\}$$

which has the steady state solution

$$\zeta = \frac{-\Gamma}{\sqrt{\left(1-(\omega_e/\omega_0)^2\right)^2 + Q^{-2}(\omega_e/\omega_0)}}\cos\left(\omega_e t + \arctan\left(\frac{1-(\omega_e/\omega_0)^2}{(\omega_e/\omega_0)}\right)\right). \qquad \{1.5\}$$

The important features are that the response is a maximum at the resonant frequency (i.e. $\omega_e = \omega_0$) and that the response changes from in phase with the

stimulus if $\omega_e << \omega_0$ to quadrature if $\omega_e = \omega_0$ to antiphase if $\omega_e >> \omega_0$. $Q$ can be considered in several ways:

$Q$ + damping constant reciprocated {1.6}
+ $2\pi$ total oscillation energy / energy loss per cycle if unforced {1.7}
+ number of radians for amplitude to decay to $e^{-1}$ if unforced {1.8}
+ $\nu_e$ / peak width at half maximum power in response to forcing {1.9}
+ response amplitude if excited at resonance / $\Gamma$. {1.10}

### I.3.2. THE RESONANT FREQUENCY OF A BUBBLE

The resonant frequency of volume-mode oscillations can be derived for spherical bubbles in an unbounded incompressible liquid by the method of Minnaert 1933. A small, and therefore linear, radial oscillation of amplitude $R_a$,

$$R = R_0 + R_a \sin \omega_0 t, \qquad \{1.11\}$$

causes the surrounding liquid to have radial velocity

$$v = \dot{R}(R_0/r) \qquad \{1.12\}$$

at distance *r* from the bubble's centre. Integrating the liquid's kinetic energy over all the liquid (of density $\rho$) produces

$$Kinetic\ Energy = 2\pi R_0^{\,3} \rho R_a^{\,2} \omega_0^{\,2} \cos^2 \omega_0 t. \qquad \{1.13\}$$

$\kappa$, the so-called polytropic index of the gas, is defined such that $pV^{\kappa}$ = constant models the behaviour of the gas; it would assume the value the value of 1 or $\gamma$ were the oscillations strictly isothermal or adiabatic (Walton 1976). The pressure inside the bubble thus varies from its static equilibrium value like

$$p = p_0 - 3\kappa p_0 \left( \frac{R - R_0}{R_0} \right). \qquad \{1.14\}$$

Subtracting the ambient pressure $p_0$, multiplying this by the surface area $4\pi R^2$ and integrating from $R_0$ to the value of *R* in equation {1.11} gives

$$PotentialEnergy = 6\pi\kappa R_0 p_0 R_a^{\,2} \sin^2 \omega_0 t. \qquad \{1.15\}$$

With no damping, the total of potential and kinetic energy must be constant. Enforcing this implies

$$\omega_0 = \frac{1}{R_0} \sqrt{\frac{3\kappa p_0}{\rho}} \quad \text{and} \qquad \{1.16\}$$

$$TotalEnergy = 6\pi\kappa R_0 p_0 R_a^{\,2} = 2\pi\rho R_0^{\,3} \omega_0^{\,2} R_a^{\,2}. \qquad \{1.17\}$$

For bubbles of a fixed gas and pressure, equation {1.16} is conveniently rewritten:

$$\nu_0 R_0 = M_M \qquad \{1.18\}$$

where $M_M$ is a constant (often called the 'Minnaert constant'). $M_M$ equals 3.24 Hz m for adiabatic air bubble oscillation in water.

### I.3.3. SOUND RADIATION FROM A BUBBLE

The sound field radiated from a bubble into an unbounded liquid can be calculated in the manner of Pippard 1989 as follows. With a radial liquid displacement $\Lambda$, a spherical shell of liquid at radius $r$ suffers a relative volume dilation of $(2\Lambda/r)+(\partial\Lambda/\partial r)$. As the bulk modulus = $\rho c$ where $c$ is the sound speed in the liquid,

$$p - p_0 = -\rho c\left(\frac{2\Lambda}{r} + \frac{\partial\Lambda}{\partial r}\right) = -\frac{\rho c}{r^2}\frac{\partial}{\partial r}\left(r^2\Lambda\right). \qquad \{1.19\}$$

The radial force per unit volume is $-\partial p/\partial r$ so Newton's third law of motion gives

$$\rho\frac{\partial^2\Lambda}{\partial t^2} = -\frac{\partial p}{\partial r} \qquad \{1.20\}$$

which combines with {1.19} yielding

$$\frac{\partial^2 p}{\partial t^2} = \frac{c^2}{r^2}\frac{\partial}{\partial r}\left(r^2\frac{\partial p}{\partial r}\right). \qquad \{1.21\}$$

The solution to this that obeys the boundary condition {1.14} on a resonating bubble is

$$p = p_0 - 3\kappa p_0\left(R_a/r\right)\sin(\omega_0(t - r/c)) \qquad \{1.22\}$$

from which $v = \partial\Lambda/\partial t$ is obtainable by the equation of motion {1.20}:

$$v = \frac{3\kappa p_0 R_a}{\omega_0\rho}\left(\frac{1}{r^2}\cos(\omega_0(t - r/c)) + \frac{\omega_0}{rc}\sin(\omega_0(t - r/c))\right). \qquad \{1.23\}$$

These results shows the transition between the dominance of $1/r^2$ velocity dependence close (much less than a wavelength) to the bubble and the $1/r$ dependence further away. The former, the 'induction' field, is as if the liquid were incompressible and transmits no net energy because the velocity and pressure are in quadrature. This is the most significant component for chapters II to IV because all measurements are made much less than one wavelength of the acoustic excitation away from the bubbles. The latter, the 'radiation' field, is a radiative sound field with pressure and velocity in phase.

### I.3.4. THE RAYLEIGH PLESSET NOLTINGK NEPPIRAS PORITSKY EQUATION

This is one of the most commonly used equations for the non-linear dynamics of a forced spherical bubble. Neppiras 1980 provides a full analytic derivation but

the following short version is, except the viscous term, from Leighton *et al* 1990c (based on Walton and Reynolds 1984).

Repeating the derivation of kinetic energy, {1.13}, but without assuming sinusoidal motion gives $2\pi\rho R^3\dot{R}^2$ as the kinetic energy.

The internal pressure in a static bubble in equilibrium must balance both the external pressure $p_0$ and the surface tension $\tau$ and so equals $p_0+2\tau/R_0$. If the liquid has vapour pressure $p_V$ then the partial pressure of the permanent gas inside the bubble is $p_0+2\tau/R_0-p_V$. As the radius changes to *R*, this will be multiplied by $(R_0/R)^{3\kappa}$. The pressure immediately outside the bubble is therefore that minus $2\tau/R_0$ and minus the effect of viscosity, $4\mu\dot{R}/R$. (The $4\mu\dot{R}/R$ can be derived very crudely as follows. The area $4\pi r^2$ of a shell of liquid will change with time like $8\pi rv=8\pi\left(\dot{R}R^2/r\right)$ as the fluid moves. This varies with radial position as $-8\pi\left(\dot{R}R^2/r^2\right)$ which is $-8\pi\dot{R}$ at the bubble surface. This area increase gradient is occurring over a length of order $2\pi R$ giving a speed gradient of $4\dot{R}/R$ and thus stress $4\mu\dot{R}/R$.)

The difference between the work done by this pressure at the bubble's surface and that done by an applied distant time varying pressure $p_\infty[t]$ will be the change in kinetic energy:

$$2\pi R^3\dot{R}^2=\int_R^{R_0}\left(\left(p_0+\frac{2\tau}{R_0}-p_V\right)\left(\frac{R_0}{R}\right)^{3\kappa}-\frac{2\tau}{R}-\frac{4\mu\dot{R}}{R}-p_\infty[t]\right)4\pi r^2\,dr\,. \qquad \{1.24\}$$

This, differentiated with respect to *R*, is the Rayleigh Plesset Noltingk Neppiras Poritsky equation:

$$R\ddot{R}+\frac{3}{2}\dot{R}^2=\frac{1}{\rho}\left(\left(p_0+\frac{2\tau}{R_0}-p_V\right)\left(\frac{R_0}{R}\right)^{3\kappa}-\frac{2\tau}{R}-\frac{4\mu\dot{R}}{R}-p_\infty[t]\right). \qquad \{1.25\}$$

Substantial use will not be made of this equation because it neglects the important thermal damping mechanism and, for most of the experimental work, linear models will suffice.

### I.3.5. DAMPING

#### *I.3.5.1. VISCOUS DAMPING*

Damping is very important, especially for forced oscillation at resonance where it prevents the amplitude increasing without limit. Damping is usually divided into three mechanisms – viscous, radiation and thermal – in the manner of the standard review (Devin 1959). The following derivations are substantially shorter than Devin's

and restrict consideration to the important regime near resonance. The damping constants simply add:

$$Q_{total}^{-1} = Q_{viscous}^{-1} + Q_{radiation}^{-1} + Q_{thermal}^{-1} \qquad \{1.26\}$$

Viscous damping seems intuitively important but actually is small for radial oscillation. Linearising the Rayleigh *et al* equation {1.25} and comparing to SHM {1.4} gives

$$\omega_0 = \frac{1}{R_0}\sqrt{\frac{1}{\rho}\left(3\kappa\left(p_0 + \frac{2\tau}{R_0} - p_V\right) - \frac{2\tau}{R_0} - \frac{4\mu^2}{\rho {R_0}^2}\right)}, \qquad \{1.27\}$$

which is slight refinement to the Minnaert result {1.16}, which assumed $\sigma = \mu = p_V = 0$, and

$$Q_{viscous}^{-1} = 4\mu\omega_0 / 3\kappa p_0 . \qquad \{1.28\}$$

Even in the worst case used, the vegetable oil of chapter II where $\mu = 0.08$ Pa s, $Q_{viscous}^{-1}$ is less than 0.001.

### *I.3.5.2. RADIATION DAMPING*

Sound radiated, or – more precisely – reradiated if the bubble is being acoustically forced, dissipates energy. The liquid velocity in the far field ($r >> R_0$) is, from {1.23},

$$v = \frac{{R_0}^2 \omega_0^2 R_a}{rc} \sin(\omega_0 (t - r/c)) \qquad \{1.29\}$$

at resonance. If multiplied by the acoustic pressure {1.22} and the area $4\pi r^2$, this gives the power flowing out so the energy loss per cycle is:

$$Energylosspercycle = \frac{2\pi}{\omega_0} 4\pi r^2 \langle v.(p - p_0) \rangle = \frac{6\pi\kappa\omega_0 {R_0}^2 {R_a}^2 p_0}{c} . \qquad \{1.30\}$$

Dividing this by $2\pi$ times the total energy {1.17} gives the damping constant (by Q relationships {1.6} and {1.7}):

$$Q_{radiation}^{-1} = \omega_0 R_0 / c = 2\pi M_M / c = \text{constant} . \qquad \{1.31\}$$

This shows that $Q_{radiation}^{-1} \approx 0.015$ which is substantially higher than $Q_{viscous}^{-1}$ and could be significant.

### *I.3.5.3. THERMAL DAMPING*

The conversion of mechanical energy to heat and its subsequent loss from a bubble can dominate the damping. The full derivation of Devin 1959 (based on Pfriem 1940) is long and self-inconsistent; the following alternative is purely for large resonant bubbles and contains gross approximations but is simpler to visualise and

substantially shorter. (For a more rigorous but much more complex derivation see Prosperetti 1977.)

The bubble is below equilibrium radius for half its cycle, a time $2/\nu_0$, during which time the gas will be denser than at equilibrium so the heat capacity $w$ will increase by, at maximum,

$$w_a = 3w_0 R_a/R_0 \qquad \{1.32\}$$

and temperature $T$ by

$$T_a = 3(\gamma-1)T_0 R_a/R_0 \qquad \{1.33\}$$

because of adiabatic compression; $w_0$ and $T_0$ are the equilibrium gas heat capacity (at constant volume, per unit volume) and temperature.

In time $2/\nu_0$ heat will typically diffuse a distance $\sim\sqrt{2K/\nu_0 w_0}$, where $K$ is the thermal conductivity of the gas. Consider the cooling to be the outer $\sqrt{2K/\nu_0 w_0}$ of the bubble returning to $T_0$ from a mean temperature $(T_0 + T_a/2)$ so

$$Heatloss \simeq 4\pi(R_0 - R_a)^2 (T_a/2)(w_0 + w_a)\sqrt{2K/\nu_0 w_0}\,. \qquad \{1.34\}$$

Similarly, in the other half cycle,

$$Heatgain \simeq 4\pi(R_0 + R_a)^2 (T_a/2)(w_0 - w_a)\sqrt{2K/\nu_0 w_0} \qquad \{1.35\}$$

and the difference, using {1.32} and {1.33}, is to second order in small quantities,

$$Netheatloss \simeq 12\pi T_0 w_0 R_a^{\,2}\sqrt{2K/\nu_0 w_0}\,. \qquad \{1.36\}$$

Once again, dividing this by $2\pi$ times the total energy {1.17} gives the damping constant which, after simplification by Minnaert's equation {1.16}, is

$$Q_{thermal}^{-1} \simeq \frac{2^{3/2}\pi}{\gamma^{3/2}}\sqrt{\frac{K\rho\nu_0}{3p_0 w_0}}\,. \qquad \{1.37\}$$

The result of Devin 1959 is the same except for the γ-dependent prefactor:

$$Q_{thermal}^{-1} = \frac{3\pi^{1/2}(\gamma-1)}{\gamma}\sqrt{\frac{K\rho\nu_0}{3p_0 w_0}}\,. \qquad \{1.38\}$$

The resulting Q for bubbles of two gases with $\nu_0 = 500$ Hz (using data from Tennet 1971) in the table below shows that helium bubbles are more damped than air bubbles and thermal damping is plausibly the dominant mechanism. The dominance of thermal damping and the difference between the gases will be experimentally verified in chapter III. The difference in numerical value between {1.37} and {1.38} is not significant at this level of approximation.

| Gas | $K/\mathrm{Wm^{-1}K^{-1}}$ | $w_0/\mathrm{Jm^{-3}K^{-1}}$ | $Q_{thermal}$ by {1.38} | $Q_{thermal}$ by {1.37} |
|---|---|---|---|---|
| Air | 0.0241 | 915 | 99 | 28 |
| Helium | 0.142 | 565 | 23 | 11 |

#### *I.3.5.4. OTHER MECHANISMS AND OFF-RESONANCE DAMPING*

According to Eller 1970, thermal damping is dominant if a bubble is acoustically excited well below its resonant frequency and radiation damping is dominant if well above. The minimum in damping between these extremes is close to but not precisely at $\nu_0$.

Other damping mechanisms have been hypothesised, for example energy transfer to damped shape oscillations(Longuet-Higgins 1992), but are not regarded as significant.

### I.3.6. BOUNDARIES AND NONSPHERICAL BUBBLES

A way of amending the Minnaert result {1.17} for more complicated cases than spherical bubbles has been invented (Strasberg 1953). It involves converting the problem to one in electrostatics.

Since both the velocity potential ($\int \underline{v} \bullet d\underline{r}$) of irrotational fluid flow and the electrostatic potential ($-\int \underline{E} \bullet d\underline{r}$) in free space obey Laplace's equation, they have similar solutions. The kinetic energy in the Minnaert calculation {1.13} is proportional to the integral of $v^2$ over all the liquid. For a charged isolated conducting object, the equivalent quantity is the integral of $E^2$ over all external space which is proportional the energy stored in electric field and thus the object's capacitance. The upshot of this is that the necessary adjustment factor in the equation for the bubble's kinetic energy is proportional to the capacitance for the electrical analogy. The result is therefore simply that

$$\nu_0 \propto \sqrt{Capacitance of an isolated conductor of the same shape as the bubble}\,. \qquad \{1.39\}$$

For an oblate bubble with $\xi =$ ratio of major to minor axes, standard electrostatics (Smythe 1968a) then gives

$$\nu_0 = \frac{M_M}{R_0}\sqrt{\frac{\sqrt{\xi^2-1}}{\xi^{2/3}\arctan\sqrt{\xi^2-1}}}\,. \qquad \{1.40\}$$

Fortunately, nonsphericity does not greatly effect $\nu_0$; for example it is only increases by 2 % for $\xi = 2$.

Another application is for a pair of equal size spherical bubbles separated by $s$ (see Smythe 1968b for capacitance). It gives approximately

$$\nu_0 = \frac{M_M}{R_0} \Bigg/ \sqrt{1 + \frac{R_0}{s} - \left(\frac{R_0}{s}\right)^4} \ . \qquad \{1.41\}$$

This also applies to a spherical bubble next to a rigid boundary due to the effective image bubble (or, equivalently: the flow from two identical bubbles is symmetric about the plane midway between them so no liquid crosses that plane so $\nu_0$ would not be affected by inserting a rigid boundary there).

## I.4. ACTIVITY OF BUBBLES

This section continues from the previous section into aspects of bubble activity of which some knowledge will be useful but detailed discussion and mathematical analysis will not be needed.

### I.4.1. CAVITY COLLAPSE

The analysis by Rayleigh 1917 of an empty collapsing cavity is a special case of the Rayleigh *et al* equation {1.25} with σ, $R_0$ and μ zero, and $p_\infty[t] = p_0$:

$$R\ddot{R} + \frac{3}{2}\dot{R}^2 = \frac{p_0}{\rho} \ . \qquad \{1.42\}$$

Multiplying by $R^2$ and integrating over time gives

$$\dot{R}^2 = \frac{p_0}{\rho}\left(\left(\frac{R_{initial}}{R}\right)^2 - 1\right) \qquad \{1.43\}$$

where $R_{initial}$ is the radius when the bubble starts collapsing. $\dot{R}^{-1}$ integrated from $R = R_{initial}$ to $R = 0$ gives the time for collapse as $0.915 R_{initial}\sqrt{\rho/p_0}$ .

In the above theory, $\dot{R} \to \infty$ as $R \to 0$. This is unrealistic but can be avoided by assuming the cavity contains some gas, in which case the cavity rebounds. The bubble may become a cloud of smaller bubbles, since the spherical shape is unstable during collapse (Plesset 1964). These can then dissolve or act as nuclei for the growth of later bubbles. Viscosity or viscoelasticity (Ryskin 1990) in the liquid would also keep $\dot{R}$ finite. In acoustic cavitation (where $p_\infty$ has a sinusoidally varying component), the dynamics get more complicated (Noltingk and Neppiras 1950).

### I.4.2. POLYTROPIC INDEX VARIATION

The polytropic approximation, $pV^\kappa$ = constant in a bubble, was introduced when deriving equation {1.14}. The bubbles studied in chapters II to IV were large compared to the thermal diffusion length in water so it would have been expected

that the heat transfers from the gas to the liquid during a period of oscillation were small. Therefore the oscillations would be almost adiabatic and so $\kappa \approx \gamma$. Smaller bubbles oscillating at higher frequencies would have transferred more heat to the liquid, been nearer to isothermal and have had $\kappa \approx 1$ (Plesset 1964).

Though useful, the polytropic approximation is basically just an *ad hoc* convenience. To calculate $\kappa$, it is necessary to use other approximations, such as uniform internal pressure (Prosperetti 1991), asymptotically matched internal and external fluid dynamics (Miksis and Ting 1984) or numerical simulation of the gas (Prosperetti *et al* 1988). The requirements of causality, the well-known Kramers-Kronig relations, obviously imply that $\kappa$ varies from $\gamma$ to 1 via the complex plane (Pippard 1984). This is another way of understanding the thermal damping of section I.3.5.3.

### I.4.3. BUBBLE CREATION

Bubbles were blown individually with a syringe for the static bubble experiments reported later in this dissertation. For the rising bubble experiments, gas was simply released from a nozzle. If the gas-flow is slow, bubbles grow quasistatically and successive bubbles are identical (Longuet-Higgins *et al* 1991 gives an analytic analysis) but at high flow rates the fluids become turbulent so bubbling is no longer simple (photographs in Leighton *et al* 1991b). Other researchers have used less mundane means to produce bubbles including sparks (Vorkurka 1988a, 1988b), laser pulses (Vorkurka 1988a, 1988b), tribonucleation (Trevena 1987b), electrolysis (Kozhevnikova and Bjørnø 1992), neutron bursts (West and Howlett 1969), and rapid impact to the liquid's container (Hansson *et al* 1982).

Bubbles will, of course, grow in liquid which is over-saturated with a gas but the bubbles need first to be nucleated. This is because the surface tension of a bubble increases the internal pressure to above that of the surrounding liquid. If the liquid was not over-saturated, the bubbles would dissolve. Even when over-saturated, there is a minimum size below which bubbles are unstable and dissolve (Keller 1964). The nucleation requirement explains why an unshaken champagne bottle outgasses gently but a shaken one, which contains many bubbles to act as nuclei, froths dramatically (McGee 1991b).

Considering that bubbles large enough not to dissolve in water at atmospheric pressure will rapidly rise out (Epstein and Plesset 1950), it is somewhat difficult to explain why bubbles then grow if the pressure on such water is then reduced. Two hypotheses are that small bubbles stabilised by surfactants survive and that dust motes trap gas. 1 $mm^3$ of tap water contains ~100 motes (Apfel 1981). Surface tension

keeps any air in the crevices in the motes below the pressure in the liquid because the interface is concave not convex like a normal bubble. This prevents the air dissolving (Apfel 1970). When the ambient pressure is reduced, the interface bows out and more gas comes out of solution into the crevice. A bubble is pinched off and the cycle repeats (Atchley and Prosperetti 1989).

Adding sound complicates bubble growth considerably. Even the simple calculation of how much the ambient pressure must be reduced (the 'Blake Threshold') to cause a bubble of permanent gas to grow indefinitely becomes an extended analysis resulting in an interrelated set of thresholds in $R_0$, $p_0$, $\nu_e$ and $p_e$ (Neppiras and Noltingk 1951). An additional mechanism for gas to come out of solution exists for oscillating bubbles, 'rectified diffusion'. Gas diffuses into a bubble when the internal pressure is highest and diffuses out when it is lowest but the bubble's surface area is highest when its internal pressure is lowest so the net gas flow is into the bubble (Eller and Flynn 1965). Extra factors complicate the mechanism, e.g. convection is important (Hsieh and Plesset 1961). The oscillation and growth of bubbles in sound fields is easily observed (Leighton *et al* 1990b, Leighton *et al* 1989b).

### I.4.4. MORE ON BOUNDARY EFFECTS

The reduction in a bubble's resonant frequency due to a neighbouring rigid boundary was discussed in section I.3.6. Conversely, a free boundary, as at a surface open to the atmosphere, increases the resonant frequency because less liquid needs to move as the bubble oscillates. The strength of the radiation from a naturally oscillating bubble is also affected. If the boundary is free and planar then the radiation will be dipole not monopole in character (Pumphrey and Crum 1990). The form of the boundary also has an effect. The shape of the dent above a bubble created by an impacting raindrop (Longuet-Higgins 1990b) can increase the radiation from the bubble by a factor of three (Longuet-Higgins 1990c), though the increase is less significant if the bubble is a few radii below the dent as is normally the case (Oğuz and Prosperetti 1990b).

For acoustic purposes, considering bubbles in a cluster to have the same dynamics as isolated ones can be useful even for void fractions up to 25 % (Arakeri and Shanmuganathan 1985). The changes in dynamics do, however, need to be accounted for in precise applications such as bubble-sizing. As the void fraction approaches 100 % and the bubble cluster becomes a foam, the inertia of the liquid ceases to be as significant and the relevant dynamics change totally (Glazier and Weaire 1992) of course.

### I.4.5. MOTIONS OF BUBBLES IN A SOUND FIELD

Without applied sound or flow, bubbles rise because of buoyancy; the drag force on them may be less than that predicted by Stokes' Law (Stokes 1851) due to circulation of the gas inside (Clift *et al* 1978) or more than that if the bubbles oscillate in shape.

In a sound field, there is an additional force called the 'Bjerknes force' (Blake 1949) arising from bubble oscillations. Consider a non-uniform sound field of amplitude $p_e[x]$, i.e. $p[x,t]=p_0+p_e[x]\sin\omega_e t$. The pressure gradient is $\nabla p[x,t]=\nabla p_e[x]\sin\omega_e t$. The volume of a bubble with $\omega_0 >> \omega_e$ will vary like $V = V_0 - V_a \sin\omega_e t$ where $V_a \propto p_e$. The instantaneous translational force on the bubble is proportional to $-V\nabla p$. The average of this over an acoustic period is proportional to $p_a \nabla p_a$ which is in the direction of increasing $p_a$, i.e. the bubble is forced towards regions of greater sound amplitude. This force is sometimes useful for holding bubbles in a sound field against buoyancy.

Conversely, bubbles with $\omega_0 << \omega_e$ vary like $V = V_0 + V_a \sin\omega_e t$ and so are forced towards regions of lower sound amplitudes. Similarly bubbles experience Bjerknes forces in each other's sound fields; pairs with both $\omega_0 > \omega_e$ or both $\omega_0 < \omega_e$ are attracted together, pairs with one $\omega_0 > \omega_e$ and one $\omega_0 < \omega_e$ repel (Bjerknes 1906). (Note that the preceding theory is linearised – large amplitude non-linear oscillations can reverse the force direction (Oğ uz and Prosperetti 1990a).)

### I.4.6. SURFACE WAVES

Many factors can distort bubbles from the spherical. These include nearby boundaries and straining liquid motion (Ryskin and Leal 1984c, Kang and Leal 1988); even just buoyant rising (Ryskin and Leal 1984a, 1984b) can distort bubbles into toruses (Lundgren and Mansour 1991). More important for the current study are oscillatory deformations of bubbles. These shape oscillations are equivalent to surface waves on the bubbles and are also known as capillary waves (Landau and Lifshitz 1987). Surface waves do not need spatially inhomogeneous fields to excite them. A uniformly oscillating planar surface is unstable when the acceleration is directed from the gas to liquid if the amplitude of oscillation is sufficiently high (Taylor 1950, Benjammin and Ursell 1954). A spherical bubble surface behaves similarly except that the diverging streamlines stabilise the bubble surface in expansion so instability occurs in the contraction phase (Plesset 1954).

The normal modes for surface waves are the spherical harmonics $Y_n[\theta,\phi]$. $n$ is the number of nodal planes; when seen by the naked eye it is the pattern of nodes and antinodes which give the shimmery appearance to bubbles exhibiting high-order

surface waves (Kornfiled and Suvorov 1944). The modes with $n = 0$ and $n = 1$ are inapplicable because they are the breathing and translational modes respectively. The natural frequencies of modes with $n > 0$ are

$$\sqrt{(n^2-1)(n+2)\tau/\rho R_0^3} \qquad \{1.44\}$$

where $\tau$ is the surface tension (Lamb 1874). This does not take into account the effects of mass diffusion (Fanelli *et al* 1984) or contaminants on the bubble surface (Benjammin 1964).

The modes which are preferentially excited are those with natural frequency close to half the excitation frequency as is the case for an initially planar surface (Faraday 1831, Benjammin and Ursell 1954). (Section VI.3.2 includes qualitative explanations of this.)

The emission of sound from surface oscillations is principally multipole in character because there is no net volume change and therefore no net motion of liquid to or from the bubble at any time if the liquid is incompressible. Effectively, liquid just flows between oppositely displaced areas around the bubble (Stokes 1868). The sound pressure at distance $r$ from a bubble oscillating with amplitude $a_n$ in the $n$th mode is

$$(n-1)(n-2)(\tau/R_0)(a_n/r)(R_0/r)^n Y_n[\theta,\phi] \qquad \{1.45\}$$

close to the bubble or if the liquid is incompressible, and

$$(2^n n!(n-1)(n^2-1)(n+2)^{1+(n/2)}/2n)(\tau/R_0)(\tau/R_0\rho c^2)^{n/2}(a_n/r)Y_n[\theta,\phi] \qquad \{1.45\}$$

far from the bubble (Strasberg 1953) so surface waves emit much less sound that the breathing mode. For example, a breathing mode oscillation of a 0.33 mm radius air bubble in water at one atmosphere (natural frequency 1 kHz) gives a sound pressure at 10 cm which is $\sim 10^7$ times higher than an $n = 2$ surface wave (natural frequency 25 Hz) of the same amplitude.

There is another mechanism by which a surface wave may radiate more sound. Bernoulli's equation for fluid flow implies a change in pressure proportional to the fluid speed squared which would give monopole emission from a surface wave, albeit at a frequency twice that of the surface wave. The emission is enhanced for shape mode resonances close to half the breathing mode resonance in frequency (Longuet-Higgins 1988a, 1988b). This is effectively the converse phenomenon to the excitation of surface waves at half the frequency of the forcing sound. This theory has proved to be surprisingly controversial (e.g. Ffowcs Williams and Gou 1991, Longuet-Higgins 1991).

Though radiation from surface waves is not significantly relevant to this dissertation, another acoustic effect of surface waves will feature highly in the fourth chapter. Discussion of that effect will await section IV.3 so that it does not proceed the background which justifies its relevance.

### I.4.7. SUBHARMONIC EMISSION

Von Esche 1952 examined the spectrum of sound re-emitted by acoustic cavitation caused by a sound at frequency $\nu_e$. Not only were spectral components found at the harmonics, $\nu_e, 2\nu_e, 3\nu_e, \ldots$, but also at $\frac{1}{2}\nu_e, \frac{1}{3}\nu_e, \frac{3}{2}\nu_e, \frac{2}{3}\nu_e, \frac{1}{4}\nu_e$ etc.. The components at $\frac{1}{n}\nu_e$ are called 'subharmonics' of $\nu_e$. The origin of subharmonics is still unknown and intensely debated. Hypotheses include collapse shockwaves, surface waves, oscillatory collapse and breathing mode period bifurcation:

The shockwave from a collapse has many spectral components but gives no particular preference to subharmonics (Neppiras 1969) though maybe a shock could excite other bubbles into breathing mode subharmonic oscillation (Prosperetti 1991).

Surface waves, as stated in the previous section, are preferentially excited at $\frac{1}{2}\nu_e$ but they radiate relatively little sound. (The monopole radiation mechanism of Longuet-Higgins 1988a is unlikely to help because it doubles the frequency back to $\nu_e$.)

On collapse in a sound field, simulation shows that it is possible that a bubble may repeatedly rebound during several forcing periods before a final collapse (West and Howlett 1969) but the threshold does not fit with that found by Neppiras 1969 for subharmonics in bubbly water.

Period doubling in the breathing mode is becoming a fashionable explanation. If a non-linear oscillator is excited sufficiently strongly, it may 'overshoot' during one cycle and miss the start of next cycle so the period of the oscillation is double that of the excitation. Oscillating bubbles have been photographed exhibiting this behaviour (Leighton *et al* 1991c). Oscillation at $\frac{1}{2}\nu_e$ is most readily excited when $\nu_e = 2\nu_0$ so the bubble oscillates at its own natural frequency (Güth 1956, Eller and Flynn 1969). Part of the current popularity of this explanation stems from its connection with chaos theory. If the excitation amplitude is increased, the oscillation becomes progressively more complex (Lauterborn 1976) with more period doublings occurring until the motion never repeats (Kamath and Prosperetti 1989); this is called 'chaos'. The successive period doublings have been observed in the sound from forced bubbles (Lauterborn and Holzfuss 1991). The transition to chaos is, of course,

dependent upon the excitation frequency as well as amplitude; see Parlitz *et al* 1990. For a moderately detailed introduction to acoustic chaos exemplified by bubbles see Lauterborn and Parlitz 1988.

Note that this subharmonic *emission* effect is not the same as the subharmonic *modulation* effect (also known as the subharmonic sum-and-difference effect (Leighton *et al* 1991a)) that is the subject of chapter IV. The former is the production of $\frac{1}{2}\nu_e$ detected from excitation at $\nu_e$; the latter is the production of $\nu_i \pm \frac{1}{2}\nu_e$ from simultaneous excitation at $\nu_e$ and $\nu_i$ with $\nu_i >> \nu_e$. These very different effects have been confused (e.g. Incognito 1994) in the past causing unnecessary problems. Unlike with subharmonic emission, the origin of subharmonic modulation has now been discovered and is revealed in section IV.3.

## I.5. OVERVIEW OF TECHNIQUES

This section introduces different acoustic techniques for detecting and measuring bubbles. It progresses from basic techniques to more involved ones.

There are, of course, numerous non-acoustic sizing methods available. Some are simple and mechanical but are inconvenient to use in practical situations. Optical methods – including light shadowing (Hwang *et al* 1990), light scattering (Stavs and von Stochar 1985b), optical interference (Kingsbury and Marston 1981, Holt and Crum 1991), laser Doppler anemometry (Yu and Varty 1988) and holography (Ran and Katz 1991) – work for some applications but are useless in opaque media. Only acoustic methods will feature in the following.

### I.5.1. USING SOUND SCATTERING AND ATTENUATION

The acoustic impedances of gases are usually much lower than those of liquids so sound is reflected well by gas-liquid boundaries. The reduction in straight-through transmission of ultrasound reveals bubbles (Stavs and von Stochar 1985b). The technique of ultrasonic tomography combines the ultrasonic attenuation information from different directions to construct an image of the bubbles in a slice through the liquid sample (Wolf 1988).

The backscattered sound, instead of the shadows, may be used to detect bubbles (Roy *et al* 1990, Crum *et al* 1992). If the bubbles are moving, then the backscatter from bubbles can be distinguished from the reflection from static obstacles by the Doppler shift (Belcher 1980, Nishi 1972). This can be observed in the spectrum of the backscatter (Kisman 1977) or as 'chirps' in the Doppler output (Gillis *et al* 1968). The Doppler shift also gives the bubbles' speeds.

The variation of the backscatter or attenuation of ultrasound over time provides additional information. Even in a detection system where large spurious changes in the strengths of detected signals are unavoidable, rapid fluctuations can be used as an indicator of bubbles passing (e.g. for detecting boiling in pressured water vessels (Hulshof and Schuink 1985)). Some bubble size information is obtainable because a few large bodies would produce less rapid fluctuations than the same total volume in the form of many smaller bodies (Smith 1974). It might be possible to use the detail of the change in scattering as a single bubble passes the sensors to estimate its size (Stavs and von Stochar 1985a).

The echo-sounder principle, using determining a distance by the time a sound takes to reach a target and return, has been used to measure distances to bubbles (e.g. Aleksandrov and Vaindruck 1974, Crawford and Farmer 1987, Thorpe 1982). A conventional medical ultrasound scanner can image bubbles. From a series of scans of freely rising bubbles, their rise-rates are calculable so, by Stokes' Law, the bubbles sizes can be estimated (Watmough *et al* 1991).

### I.5.2. USING BUBBLE RESONANCE

A bubble interacts with sound most strongly at its breathing mode resonant frequency $\nu_0$. Since $\nu_0$ is related to the bubble radius in a simple manner (equation {1.18}), the resonance is especially useful for measuring bubble sizes.

When a bubble is created, it oscillates at its natural frequency giving off a 'ping' sound. Figure 1.1 is a trace of the sound from a 1.39 ml air bubble released from a nozzle in water at atmospheric pressure. The sound was detected by a Brüel & Kjær 8103 hydrophone and recorded on a digital storage oscilloscope. The smaller, 0.56 ml, bubble used for figure 1.2 had a higher resonant frequency as is obvious from the traces.

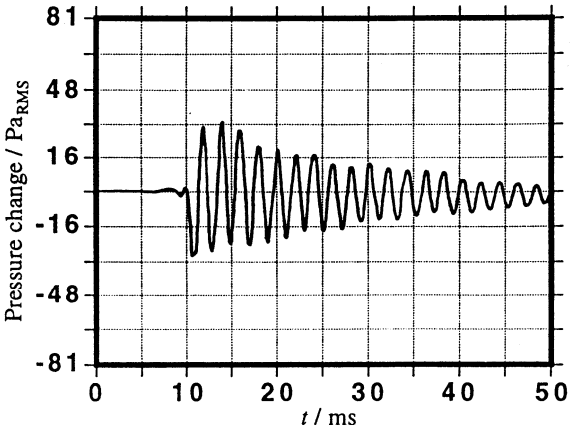



**Fig. 1.1:** Trace of the sound emitted from the natural oscillation of a 1.39 ± 0.005 ml air bubble in water.

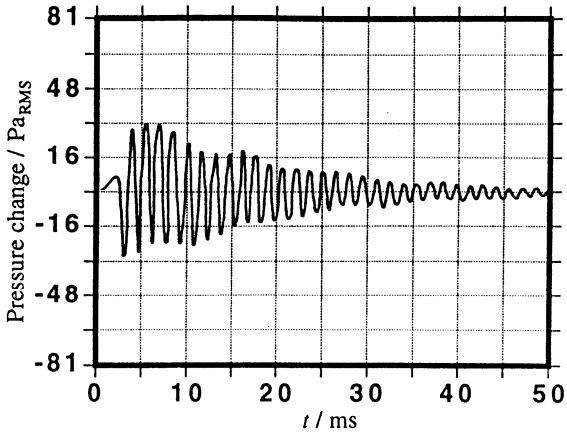



**Fig. 1.2:** Trace of the sound emitted from the natural oscillation of a 0.56 ± 0.005 ml air bubble in water.

Of course, passively monitoring the sound from bubbles is only useful is something excites the bubbles into oscillation; in the above case, it was the pinching-off of the bubbles from the air in the nozzle. Besides passively listening to a bubble to find $\nu_0$, a bubble can be actively excited into oscillation by a sound transduced into the medium at a frequency $\nu_e$. The bubble responds most strongly when $\nu_e = \nu_0$. To measure different bubble sizes, $\nu_e$ can be varied or many frequencies can be used at once, for example by using the harmonics of non-sinusoid excitation sound (Medwin 1977a, 1977b) or the spectrum from a broad-band excitation (Fairbank and Scully 1977). Detecting when a bubble is responding to the sound may appear to be difficult since the acoustic re-emission (scattering) from the bubble will be masked by the original excitation sound which is at the same frequency. If the bubbles are small enough for the wavelength in the liquid at $\nu_0$, and therefore at $\nu_e$, to be much less than the dimensions of the system then the problem can be avoided by pulsing the sound then recording the re-emission at a later time (Fairbank and Scully 1977, Medwin 1977a). If the bubbles are larger so the sound source and receiver are no more than a few wavelengths apart then it seems, at first, as if the acoustic re-emission would be almost totally undetectable in the presence of the excitation. This is not actually so, as is demonstrated in chapter III which is on this subject. An alternative solution is monitor the bubble's response by some other non-acoustic method while still exciting it acoustically; an example of this is the subject of chapter II.

Although a bubble responds most strongly when $\nu_e = \nu_0$, bubbles do respond somewhat when $\nu_e \neq \nu_0$; in particular, a large bubble not at resonance can scatter sound as strongly as a smaller bubble at resonance. This has lead to overestimates of the numbers of smaller bubbles in oceans in the past (Commander and Moritz 1989).

This is not a problem if the interrogated region contains so few bubbles that each distinct peak in the frequency response corresponds to an individual bubble. If necessary, the problem can be alleviated by numerically fitting a bubble size distribution to the experimental data to match the frequency response (e.g. Commander and McDonald 1991).

### I.5.3. USING HARMONIC DISTORTION

An ideal bubble can expand without limit but obviously cannot contract below zero radius. This implies that a bubble is not a perfectly linear oscillator and the sound it re-emits when excited at $\nu_e$ will contain harmonics ($2\nu_e$,$3\nu_e$,$4\nu_e$, etc.). Detecting the re-emission at $2\nu_e$ instead of $\nu_e$ has several advantages (Miller 1981): the excitation sound field does not mask the re-emission (provided that the transducers do not create significant harmonics themselves); the response peaks more sharply about $\nu_e = \nu_0$ facilitating accurate $\nu_0$ measurement; and a large non-resonant bubble which would scatter more at $\nu_e$ than a smaller resonant one emits relatively little at $2\nu_e$. The main disadvantage is that the excitation pressure needs to be strong enough to make non-linear behaviour noticeable.

### I.5.4. USING FREQUENCY MIXING

Another non-linear effect possible in multiphase media is frequency mixing (Koreav and Naugol'nykh 1980). In addition to the excitation at $\nu_e$, a second sound is provided at another frequency $\nu_i$ and the intermixing products at $\nu_i \pm \nu_e$ are monitored. Once again, the response is a maximum when $\nu_e = \nu_0$ (Newhouse and Shankar 1984). It is convenient to make $\nu_i$ much higher than $\nu_e$. This prevents the complication of any bubbles resonating at $\nu_i$. Also, if $\nu_i$ is of megahertz order, the corresponding wavelength will be short enough for spatial information to be obtained from the signal; this is why $\nu_i$ is sometimes called the 'imaging' frequency.

Another frequency mixing method has both input frequencies much higher than $\nu_0$. The response should be greatest when the difference between them equals $\nu_0$ (Butkovsky *et al* 1986) but experimental results are not encouraging (Doskoi *et al* 1984). In theory, this could be combined with the preceding method to give a three-frequency technique (Bunkin *et al* 1983).

An additional variant was discovered when Lingard *et al* 1990 attempted to replicate the $\nu_i \pm \nu_e$ technique. They reported additional emission at $\nu_i \pm \frac{1}{2}\nu_e$. The instrumentation, characterisation and explanation of this effect is the subject matter of chapter IV.

## I.6. SOME PROMISING DEVICES

This introductory chapter concludes with descriptions of some of the acoustic bubble sizing devices which have been invented in the recent past. The selection covers a range of different techniques which have been claimed as successful. It includes brief details concerning their principles of working, development and reported abilities.

### I.6.1. WOLF'S ULTRASONIC TOMOGRAPHER

Ultrasonic tomography was explained in section I.5.1. The device of Wolf 1988 consisted of 36 transducers in circular array around a pipe. Each could act as transmitter or receiver. The data from the transmission between various pairs was processed by a computer to give an image of the bubble flow in the pipe. Wolf 1988 only reports it detecting streams of bubbles not the individual bubbles within the streams. The main drawback is the expense of having numerous transducers.

### I.6.2. FARMER AND VAGLE'S FOUR FREQUENCY ECHO-SOUNDER

Farmer and Vagle 1989 used an upwardly pointing echo-sounder to measure the positions of bubbles near sea surfaces. This gave distance information with 10 cm resolution. To give an estimate of the size distribution of the bubble populations, the device operated at four frequencies (two at a time: 50 and 200 kHz together and 28 and 88 kHz together). A computer fitted a probable size distribution to the strengths of the returning signals at the four frequencies.

This system was used by Farmer and Vagle 1989 both suspended 24 m below a float in the Caribbean Sea and tethered to the sea bottom near Vancouver Island. They used the resulting vertical bubble distributions to explain some of the features of the noise of breaking waves.

### I.6.3. BREITZ AND MEDWIN'S RESONATOR

The resonant cavity consisted of two flat 25 cm diameter plates separated by 12.6 cm; the other sides were open to the surrounding water. One plate acted as a sound source, the other as a reflector. A hydrophone was in the cavity close to the centre of the sound source. White noise emitted from the transducer excited the resonances of cavity. Resonances between 27 and 64 kHz were monitored in the hydrophone output. The reduction in amplitude of these cavity resonances when bubbles were introduced into the cavity was attributed to bubbles resonant at these frequencies.

This device (Breitz and Medwin 1989) was tested on a known distribution of bubbles and the average attenuations from the bubbles agreed with theory to within 1 %. The region within 4 cm of the central axis apparently accounted for 90 % of the absorption. It was used at sea to rapidly measure the 30 to 270 μm radii bubble distributions from breaking waves. The minimum size limit was set by the spectrum analyser, the maximum size limit by the dimensions of the cavity.

### I.6.4. MILLER'S RESONANT BUBBLE DETECTOR

The resonant bubble detector (Miller 1981) utilised harmonic distortion by monitoring the re-emission at $2\nu_e$ when the sample was excited at $\nu_e$. In the original device, one piezo-electric transducer, emitting at 40 $kPa_{RMS}$ at its resonance of 1.64 MHz, excited the bubbles and second transducer, resonant at 3.28 MHz, detected the $2\nu_e$ re-emission. The transducers were arranged to fit around a 4 mm diameter pipe or blood vessel. These frequencies were suitable for detecting 4.2 μm diameter bubbles; for other sizes, additional sets of transducers working at other frequencies would be needed (Miller *et al* 1984). A spectrum analyser extracted the $2\nu_e$ component from the detected signal (a lock-in amplifier is a simpler alternative (Vacher *et al* 1984)).

The device was first tested on 4.2 μm diameter bubbles in the presence of non-resonant but much larger 500 μm diameter bubbles (Miller 1981). Though the re-emission amplitude at $\nu_e$ from a larger bubble was 50 times that from a smaller one, a smaller size bubble produced 43 times more than a larger one at $2\nu_e$.

The resonant bubble detector has since been used for practical studies. Miller *et al* 1984 observed the reduction of bubble numbers by ultrasound exposure (coalescence was probably the mechanism). Gross *et al* 1985 searched for bubbles in dog's blood by assembling the device around their aortas (no pre-existent bubbles were found). Williams *et al* 1989 investigated bubbles produced in lithotripsy (bubbles were found *in vitro* but not *in vivo*).

### I.6.5. NEWHOUSE AND SHANKAR'S FREQUENCY MIXING METHOD

This method relies upon monitoring the strength of the $\nu_i \pm \nu_e$ components produced by bubbles when excited at $\nu_e$ in the presence of an additional sound at $\nu_i$, where $\nu_i >> \nu_e$. The mixing is a maximum for bubbles with $\nu_e = \nu_0$. The first trial system had $\nu_i$ = 2.25 MHz and $\nu_e$ = 8 to 28 kHz. It demonstrated that the method could distinguish bubble streams with different resonant frequencies (Newhouse and Shankar 1984), though it was much less effective when more than one size were present at once (Chapelon *et al* 1985), and could detect changes in resonant frequencies caused by changes in the ambient pressure (Shankar *et al* 1986).

A similar system has been applied to smaller bubbles by increasing the frequencies to $\nu_i$ = 10 MHz and $\nu_e$ = 1 MHz (Schmitt *et al* 1987, Siegert *et al* 1987).

Later the spectrum analyser which extracted the $\nu_i \pm \nu_e$ components was replaced by an analogue electronic demodulator (Chapelon *et al* 1988). The method was extended with simultaneous monitoring of other features at frequencies near $\nu_i$: the Doppler shift gave bubble speed information (Chapelon *et al* 1988); and the return time gave bubble distance information (Cathignol *et al* 1990). The method is currently claimed to be able to produce bubble size distributions from a distance of two metres (Shankar 1991, Li *et al* 1992).

### I.6.6. LINGARD AND LEIGHTON'S SUBHARMONIC MODULATION METHOD

This method (Leighton *et al* 1991a) similarly involves exciting at $\nu_e$ in the presence of another sound at $\nu_i$ but, in addition to the $\nu_i \pm \nu_e$ components of the response, the $\nu_i \pm \frac{1}{2}\nu_e$ components were also monitored. Chapter IV of this dissertation is devoted to a study of this technique which included the creation of an analogue electronic signal processing system, a detailed characterisation of the effect and the discovery of the mechanism responsible for it.

A parallel project has developed a digital signal processing system for this method but has yet to yield any significant results (Phelps and Leighton 1993, 1994a, 1994b, 1994c). An effort, which aimed to combine this method with a steerable ultrasonic array for imaging multiphase flow, has recently been abandoned (Leighton 1994b).

# II. The ACOUSTIC BUBBLE CAPACITOR TECHNIQUE

## II.1. DEVELOPMENT

### II.1.1. THE PRINCIPLE

The Acoustic Bubble Capacitor (abbreviated to ABC) is based on the combination of two pre-existent methods. One method uses capacitance measurement (Cheremisinoff c.1960) where the fluids act as a dielectric. Liquids usually have higher dielectric constants than gases so the presence of gas in the sample reduces the capacitance. Because this characterises the system by a single parameter – the capacitance – ambiguities arise since it fails to distinguish one large bubble from several smaller ones. Its response for a given bubble also depends very highly on the shape of the bubble; its extent across the electric field is far more significant than the extent parallel to the field.

It is also possible to utilise the response of the bubble to a variable frequency sound field. A gas filled bubble in a liquid can oscillate naturally at a frequency $\nu_0$ which depends on the radius, see equation {1.18}. As with any simple harmonic oscillator, the response – in this case the amplitude of the volume oscillations – is a maximum when the impressed frequency matches the natural frequency $\nu_0$.

This new technique employs elements of both the capacitative and frequency response techniques. A variable frequency sound field excites a bubble located within a capacitor and the resonance is identified by monitoring the consequent capacitance oscillations. The question of how the bubble radii deduced via equation {1.18} from the measured resonant frequencies relate to actual bubble sizes will be addressed later.

### II.1.2. THE CAPACITOR

#### *II.1.2.1. FAILED PROTOTYPES*

The first attempt (ABC Mark 1) was a naïvely designed pair of copper disks supported by glued polymethylmethacrylate shown in fig. 2.1. The capacitor and the wires together formed a loop which acted as a antenna that picked up so much electromagnetic emission from the loudspeaker that the design was useless.

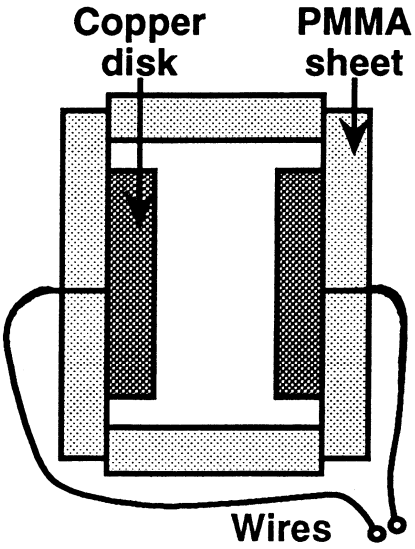



**Fig. 2.1:** ABC Mark 1. Full size.

ABC Mark 2 was coaxial, with the connection to the active plate running through the centre of the earthed plate, which eliminated most of the loop (fig. 2.2). Its width was greater than the plate separation to screen out electromagnetic interference further but spurious signals from vibrations of the plates themselves masked the bubble signal.

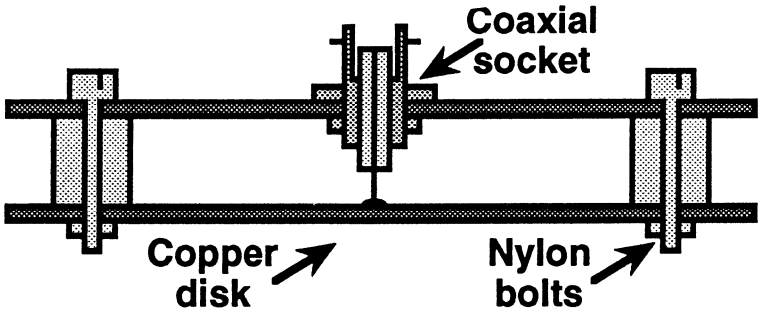



**Fig. 2.2:** ABC Mark 2. Full size.

#### *II.1.2.2. WORKING DESIGNS*

Better screening and elimination of stray capacitance from the cabling (which is much greater than that of the ABC itself) was achieved by active screening. Mark 4 incorporated this (Mark 3 was merely a partial mock-up to test the mechanics of the electrical connections). The capacitor consisted of a circular central active plate surrounded by a guard ring maintained at the same potential as the central plate. An outer ring, for additional screening, and the bottom plate are both earthed. Figure 2.3 shows the construction of the capacitor except that the nylon screws which held the layers together and the brass bars which attached the earthed plate are omitted for clarity. The capacitor, screens and intervening insulators were constructed massively

and rigidly from brass and nylon to reduce the extent of the vibrations of the capacitor itself. This particular model has the diameter of the active plate 8 cm, the overall diameter 11 cm and the plate separation 0.5, 1.5 or 2.5 cm. Its stray capacitance was 156 pF and, in the oil used as the liquid for this chapter, the useful capacitance was 20 ± 1 pF. It weighed 4.25 kg (which is considerably higher than normal 20 pF capacitors!).

The bubble, located within the active volume of the capacitor, was excited by a loudspeaker (Gearing & Watson UW60 – the best mass-produced underwater loudspeaker obtainable; it is marketed largely for synchronised swimming). The speaker was driven by an audio-frequency signal generator whose frequency could be swept . The size of ABC Mark 4 was sufficient to distort the sound field (see the speaker calibration in Appendix 2). The variation of applied sound pressure $p_e$ with frequency $\nu_e$ at the centre of the ABC is shown in figure 2.4. The 200 Hz peak from the speaker and the 900 Hz capacitor resonance could cause complications so most of the measurements were made between 300 and 800 Hz.

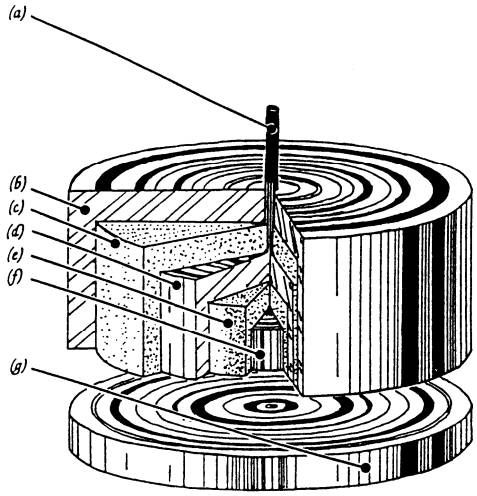



**Fig. 2.3:** ABC Mark 4. Cutaway view.(a) Triax cable; (b) earthed screen; (d) active screen; (f) active capacitor plate; (g) earthed plate; (c) and (e) insulators.

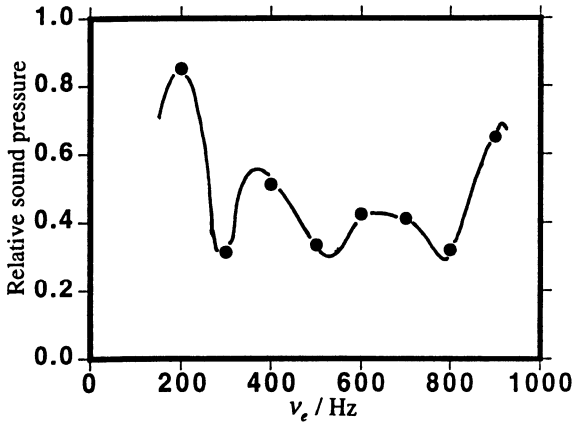



**Fig. 2.4:** Frequency response of excitation in ABC Mark 4

To test repeatability, and to determine if such a bulky size was necessary, a smaller version (ABC Mark 5) was machined. This had overall diameter 43 mm, active plate diameter 18 mm, mass 156 g and plate separation 1 to 15 mm. The earthed plate was attached by brass screws to a projecting flange. See figure 2.5.

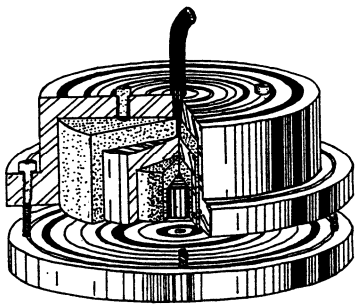


**Fig. 2.5:** ABC Mark 5 Cutaway view. Note the drawing scale is larger than for Mark 4.

### II.1.3. THE ELECTRONICS

Changes in capacitance needed to be measured fast enough to detect changes at $\nu_e$. Numerous designs with high frequency a.c. bridge circuits, sinusoid inductor-capacitor oscillators and digital relaxation oscillators all proved to be very difficult to construct because of the low capacitance involved. A simple method based on one used by my supervisor to measure contact potential differences (Schott and Walton 1977) worked for some liquids. This requires a constant bias voltage to be across the plates. This was empirically chosen to be between 20 and 160 V; the bias circuit is described in appendix 1. The voltage was applied via a 1 GΩ resistor, sufficient to ensure that the time constant of the bias circuit was significantly greater than the period of the bubble oscillations. This maintained a charge on the capacitor. Since the capacitance changed periodically as a result of the bubble oscillations, an oscillatory voltage of the same period was superimposed on the bias voltage; the time constant of the biasing circuit being too high for these to be smoothed away. This oscillation was recorded via a 1 nF capacitor, which blocked the bias voltage, and a high-impedance amplifier (Brookdeal 432) with a gain of 40 dB (This amplifier also provided the current to feed the active screen.). The signal path is wired with triax (triply coaxial) cable to retain the active screening throughout. See figure 2.6.

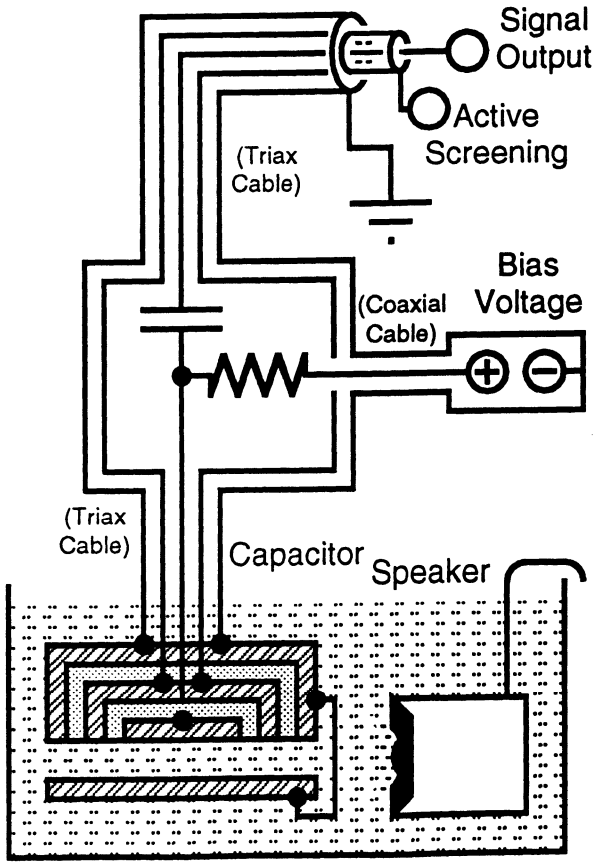



**Fig. 2.6:** The ABC capacitance monitoring.

To succeed, this method requires that the ABC's time constant, which equals the electric permittivity of the liquid $\varepsilon$ divided by its conductivity $\sigma$, is significantly greater than the oscillation period. Otherwise conduction in the liquid becomes important.

The output from the amplifier was monitored by a CRO and voltmeter and was fed to a chart recorder via a sinusoid-to-RMS voltage converter (see appendix 1 for its construction) which together recorded the RMS of the signal amplitude. An accurately automated frequency sweep was used for the frequency response chart recordings whereas the resonant frequency measurements were attained by manually tuning in $\nu_e$. The flow of information and control, and the auxiliary components, are shown below.

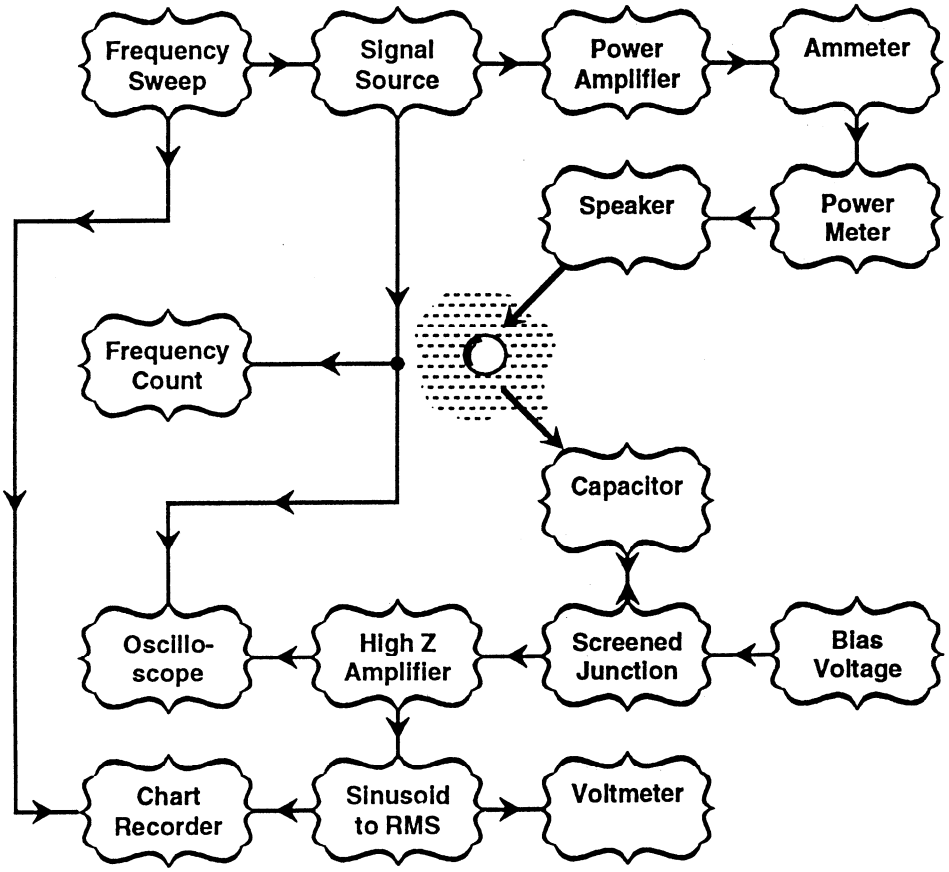



**Fig. 2.7:** Block diagram of ABC setup.

## II.2. TESTING

The ABC was tested in W.A.S.P. vegetable oil ($\mu$ = 0.7 to 0.9 Pa s, $\sigma$ ~ 0.02 nS/m; $\rho$ = 914 kg/m$^3$; $\varepsilon/\sigma$ ~ 2 s). Except where otherwise stated, all experiments were performed using ABC Mark 4. The speaker was driven at 50 mW giving an RMS acoustic pressure of approximately 20 Pa (the ABCs worked similarly at higher and lower sound pressures). The capacitor was mounted, plates horizontally, 4 cm from the speaker with 1.5 cm separation (figure 2.8) and a single bubble was introduced

between the plates using a 1 ml hypodermic syringe. The volume of the bubble was read directly from the syringe graduations, giving volume accurate to ± 5 μl. Because the tank used in these studies was open, the gas pressure in the bubble was essentially atmospheric (the pressure due to the hydrostatic head was around one percent of atmospheric pressure).

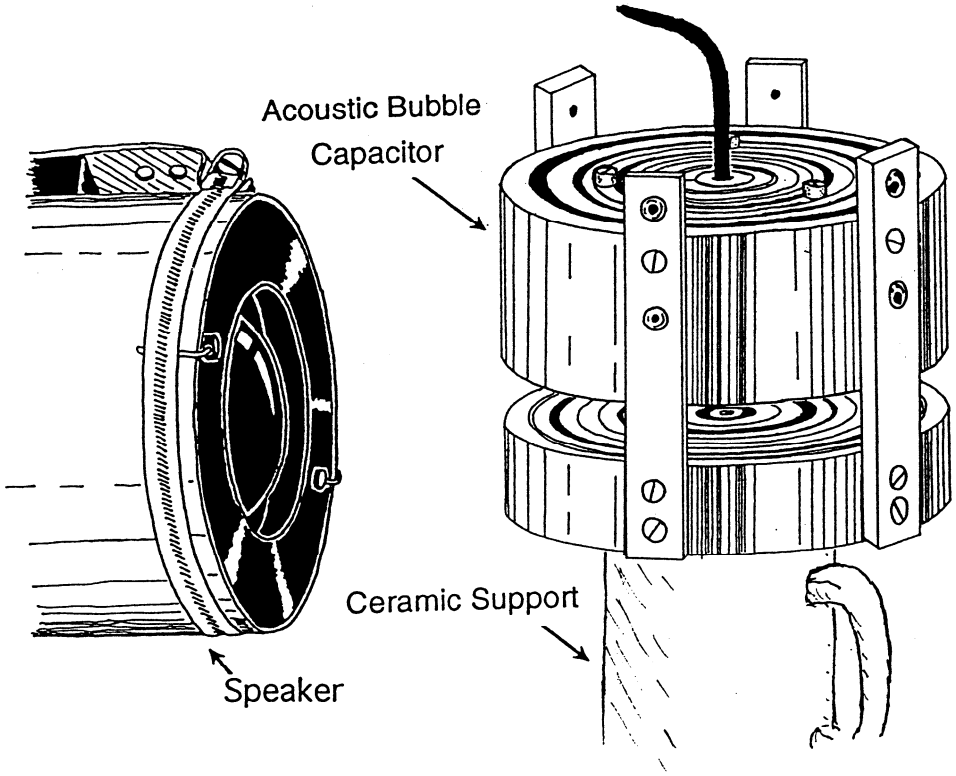



**Fig. 2.8:** Sketch of the ABC Mark 4 in use.

The output signal was a sinusoid at $\nu_e$ with insignificant levels of harmonics ($n\nu_e$, $n = 1,2,3...$), no subharmonics ($n^{-1}\nu_e$), and ~0.1 $V_{RMS}$ broadband noise. Figure 2.9 shows the frequency response curves obtained on the chart recorder for individual air-filled bubbles of volumes 0.30 ml, 0.90 ml, and 1.50 ml. These curves are those expected for a forced simple harmonic oscillation and demonstrated that the bubbles have a quality factor Q of approximately 20. The expected phase shift of π rad on passing through resonance was also obtained (using Lissajous figures). On repeating the measurements with new bubbles of similar size at the same location, the resonant frequencies were reproduced to better than ~ 2 Hz and the response curves were of identical shape. The traces of output signal strength $S_e$ in figure 2.9 clearly show how the response, in particular the resonant frequency, changes with the size of the bubble. This variation is plotted out in figure 2.10 which is of the form to be expected from {1.18}, Minnaert's result. However, the bubbles studied are not spherical and are in a bounded liquid which are contrary to the assumptions made by Minnaert. An effective radius $R_{eff}$ can be defined such that $V = 4\pi R_{eff}{}^3/3$ is the actual bubble volume. Figure 2.11 shows a graph of the measured resonant

frequency $\nu_0$ plotted against $R_{eff}^{-1}$ for air and helium filled bubbles. Although the dependence is proportionality as expected, the measured gradient ($M = 2.38 \pm 0.02$ Hz m) does not agree with the value of $M_M = 3.42$ Hz m predicted from equation {1.16} assuming $\kappa = 1.4$. The relation is, instead, of the form

$$\nu_0 R_{eff} = M \qquad \{2.1\}$$

which is the same as {1.17} but with a different constant $M \neq M_M$.

This discrepancy amounts to bubble volumes, calculated via equation {1.16}, which are three times the measured volume and cannot be accommodated by any plausible value of $\kappa$. Most of the discrepancy arises because the rigid boundaries which are the capacitor plates effectively created 'image' bubbles oscillating in phase with the corporeal bubbles so increasing their effective volume. Effects due to the nonspherical nature of the bubbles appear negligible here as does the finite size of the plates (fortuitous cancellation of these influences is more likely, given the results for changing the plate separation that follow in section III.2.1). For practical applications, these complications are not of great concern since the device would normally be calibrated against bubbles of known size.

Bubbles of this size are thought to oscillate almost adiabatically because there is insufficient time for heat to flow in and out during an acoustic cycle so $\kappa = \gamma$ and so equation {1.16} gives resonant frequencies proportional to $\gamma^{1/2}$. The ratios of heat capacities $\gamma$ differ between air and helium but changing the gas from air to helium (figure 2.11) affected $\nu_0$ by less than three percent. Bubbles in water (section III.2.5) do display the expected gas dependence. This odd gas independence has not yet been adequately explained.

The variation in output strength $S_e$ at resonance ($\nu_e = \nu_0$), figure 2.12, is qualitatively easily understood. Larger bubbles effected the capacitance more than smaller ones so the strength increased as the volume increased. The minimum in the sound pressure around 300 Hz (figure 2.4) caused the drop in output above 2 ml.

The smaller ABC Mark 5 behaved similarly. The resonant frequencies were slightly (9%) lower because of an extra boundary – a plastic corral which was needed to retain the bubble in this small version – but figure 2.13 shows that the resonant frequencies were proportional to $R_{eff}^{-1}$ as above.

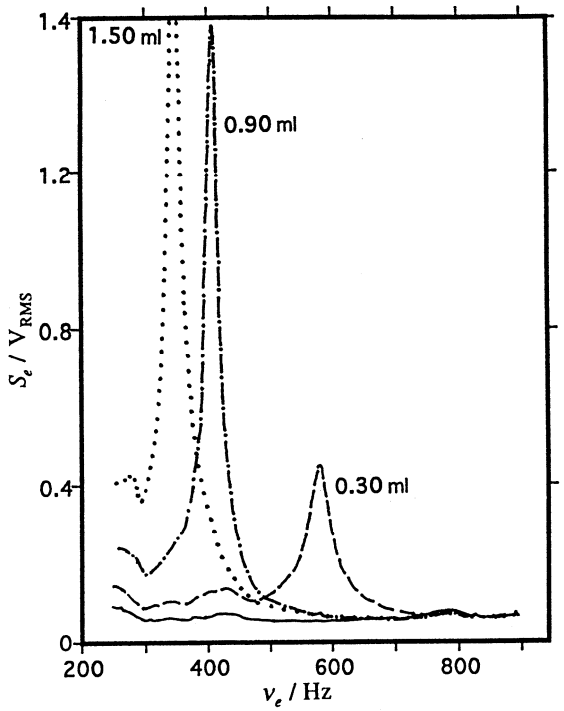



Fig. 2.9: Frequency responses for three sizes of air bubbles in oil. The solid line is the response in the absence of bubbles.

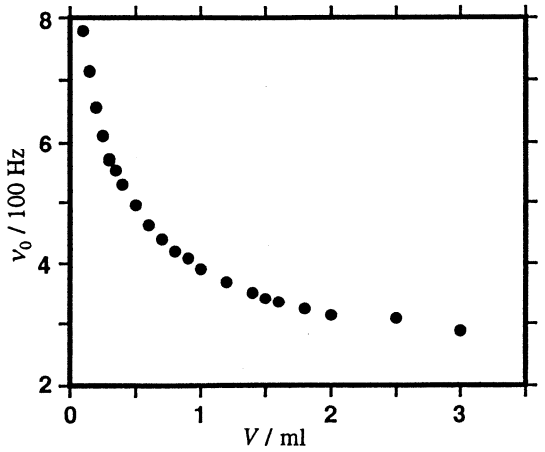



Fig. 2.10: Resonant frequency as a function of bubble volume for air bubbles in oil.

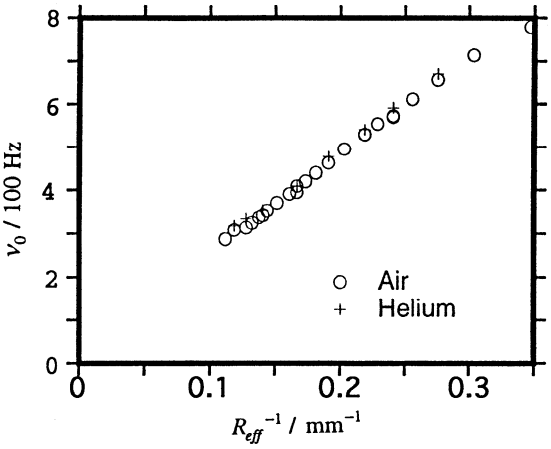



Fig. 2.11: Peak response frequency versus the reciprocal of the bubbles' effective radii in ABC Mark 4.

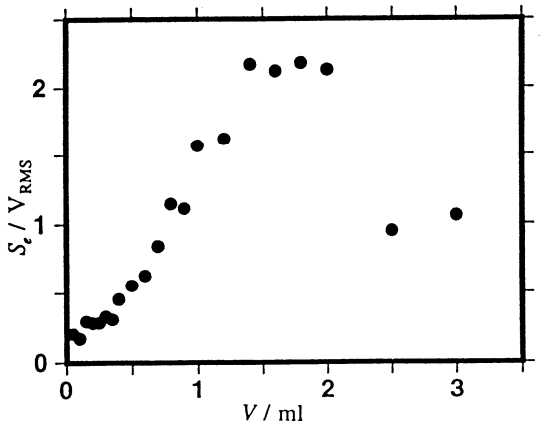



Fig. 2.12: Maximum output signal strength versus bubble volume in ABC Mark 4.

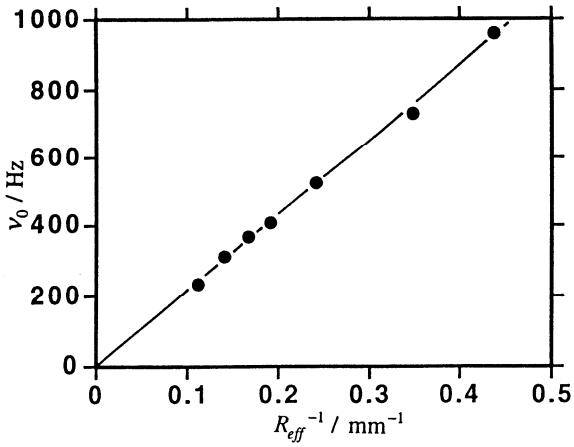



Fig. 2.13: Peak response frequency versus the reciprocal of the bubbles' effective radii in ABC Mark 5.

## II.3. APPLICATIONS

Several other studies were done on bubbles utilising the ABC Mark 4. Three interesting ones are presented below. Many of those done by the acoustic reradiation method and presented in section III.2 could also have been done by the ABC instead.

### II.3.1. RISING BUBBLES

To study the performance of the ABC with moving bubbles, it was mounted with the plates vertical. A steady stream of air-filled bubbles, each of volume 0.76 ± 0.01 ml, passed diametrically between the plates at a rate of one bubble every 1.15 s. A peristaltic pump supplied the air pressure; a reservoir then smoothed the flow; and a clamp on the air pipe controlled the airflow to the nozzle. The nozzle was satisfactorily made from a syringe body angled downwards. To ensure that the bubbles rose uniformly in a straight line, the plate separation was increased to 2.5 cm. A high-pass filter with 1 kHz 3 dB point was used because 50 Hz mains pickup from nearby power cables was otherwise significant in this orientation. At any instant there was only one bubble between the plates. Figure 2.14 shows the measured response of the bubble train. Each peak arises from a single bubble; the envelope of these peaks is essentially the response curve of a single bubble of volume 0.76 ml. The extended high-frequency tail evident in figure 2.14 arises from the geometry of the capacitor; when this portion of the data was being recorded the loudspeaker sweep frequency was high and each bubble responded when it was close to the edge of the capacitor where it had a higher natural frequency since it was oscillating in a less constrained medium.

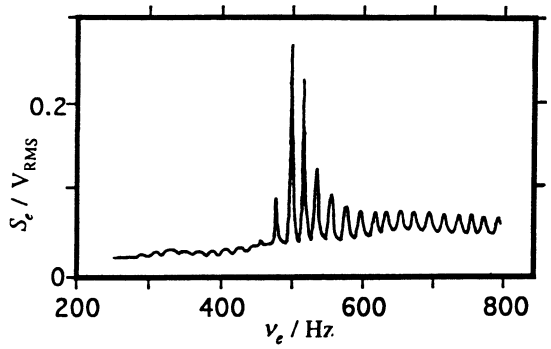



**Fig. 2.14:** The frequency response of a stream of rising bubbles taken over 33 s.

### II.3.2. DISSOLUTION OF BUBBLES

Instead of measuring the different sizes of different bubbles, the Acoustic Bubble Capacitor can, obviously, measure the changing size of one bubble as it grows or shrinks. The following examples are selected from a study of bubbles dissolving in the vegetable oil and make use of the ability of the liquid fat to dissolve

many common gases. Exceptions include the inert helium and the air, which are non-polar and have sufficiently small molecules for van der Waals bonding to oil to be weak, that were used for the testing above. For variety, figures 2.15 to 2.17 have been selected from different example gases.

Figure 2.15 shows how the volume of a nitrous oxide bubble decreases over 50 minutes. The recording was not automated, though it could have been, and the resonance $\nu_0$ was found by manually tuning $\nu_e$. The calibration on the volume scales was not certain because the bubbles dissolve slightly before the first measurement since it took at least 6 s to inject a bubble and make the first reading without dripping oil over the apparatus. The constant $M$ was assumed to be the same as for air (and so also almost the same as for helium). This assumption is reasonable because the dissolution curves of figures 2.15 to 2.17 extrapolate back to 0.90 ml at zero time which was the volume originally injected.

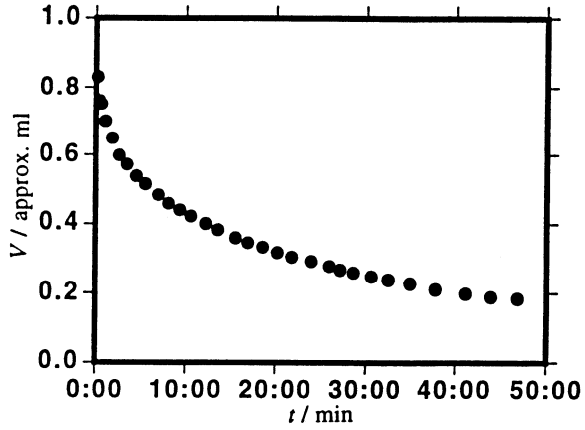



**Fig. 2.15:** Dissolution of a dinitrogen oxide (nitrous oxide, Sainsbury's whipped cream propellant, $N_2O$) bubble in vegetable oil.

The difference in dissolution rates between the different gases used was less significant than the difference between different experiments on the same gas. This was due to the changing local concentration of gas already dissolved in the oil. Figure 2.16 shows three dissolutions of 0.90 ml bubbles of the same chlorofluorocarbon (composition unspecified but probably largely Freon-11 or Freon-12). The lower line (fastest dissolution) was obtained with no predissolved chlorofluorocarbon in the oil. The upper (slowest) one was after several bubble dissolutions had been done at that point in the oil and the rate was virtually the same for subsequent bubbles. The middle line was an intermediate case.

The dissolution profiles can be made repeatable by manually flushing oil through the bubble position between each experiment. This prevents the build-up of dissolved gas there. The square and circular data points of figure 2.17 are from two such runs with 0.90 ml butane bubbles. Also apparent on figure 2.17 is the transition

from the faster initial dissolution, when the rate is limited by the passage of gas from the bubble to the liquid, to the slower later dissolution, when the liquid has become locally saturated so the diffusion of gas away through the liquid bulk is the dominant limiter.

Dissolutions for which the loudspeaker was initially switched off and only later switched on for a measurement revealed no significant changes in the dissolution rates compared to those obtained when the sound was continuous. Therefore it is reasonable to conclude that the dissolving bubbles were measured non-invasively.

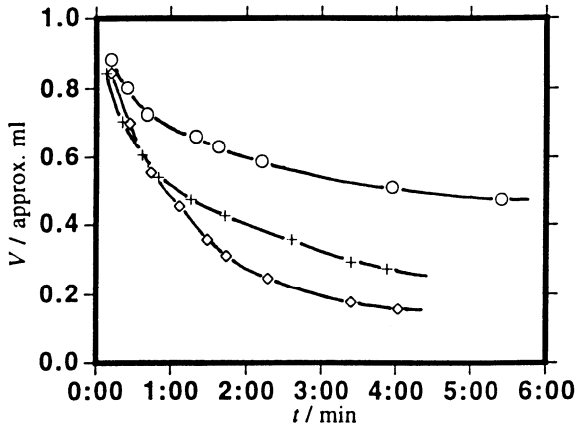



**Fig. 2.16:** Dissolution of three CFC (RS Air Duster spay, probably mainly Freon) bubbles in vegetable oil with different concentrations of predissolved gas.

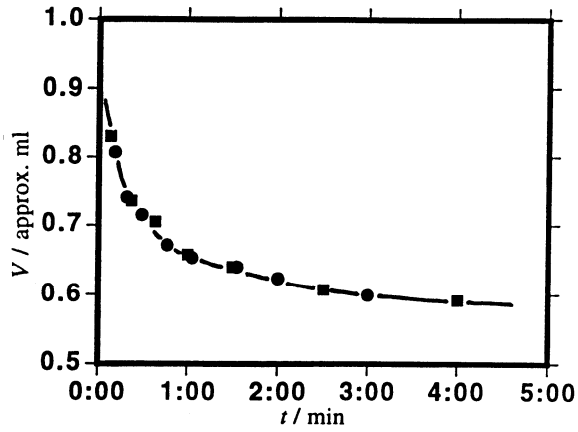



**Fig. 2.17:** Dissolution of two butane ('Ronson HiHeat', $C_4H_{10}$) bubbles in vegetable oil.

### II.3.3. MULTIPLE BUBBLES

Figure 2.18 shows the measured response curves for two differently sized bubbles, recorded separately and together, at a separation of 6 cm. The frequency shifts evident with both bubbles demonstrates the expected coupling allowed by the liquid. The coupled oscillation shifted the two resonant frequencies apart in a manner which will be calculated in section III.3.1. As anticipated, the resultant frequencies of the pair approached the free bubble values as the pair separation increased. With multiple bubble arrays the amplitudes of the resonant peaks of the interior bubbles decreased due to partial shielding of the sound field by the outer bubbles but are nevertheless detectable as figure 2.19 demonstrates. The three bubbles of figure 2.19 also show considerable shifting of the resonances.

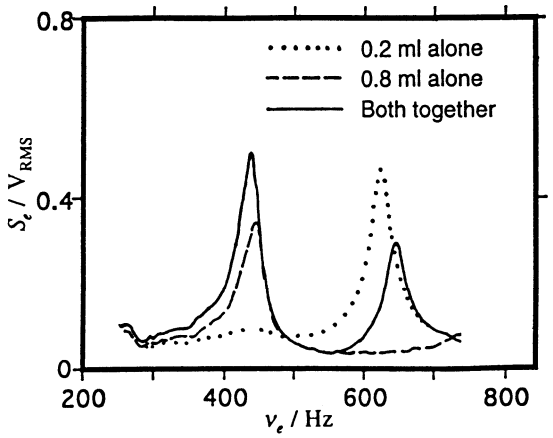



**Fig. 2.18:** Frequency response for a pair of bubbles separated by a few centimetres compared to the responses for the same bubbles when alone.

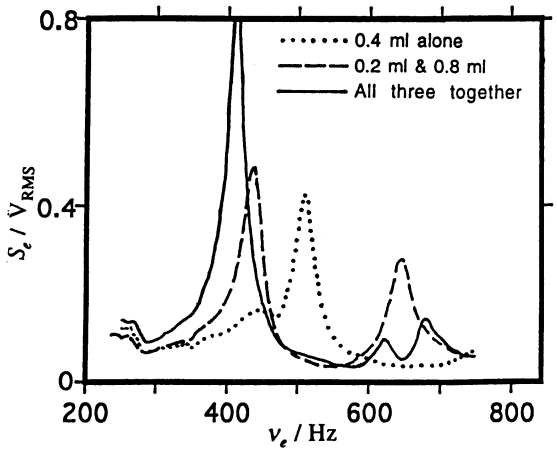



**Fig. 2.19:** Frequency response for the pair of bubbles as shown on the previous figure and after the addition of a further bubble.

## II.4. CONCLUSION

A full conclusion will await the description of the techniques of chapters III and IV so comparisons can be made but a brief conclusion here is desirable.

This technique avoids the main ambiguity inherent in passive capacitative techniques; it gives the volume of individual bubbles rather than an uncertainly combined volume if several bubbles are present. The coupling of the bubbles' oscillations will need to be studied further to predict the frequency shifts though. It has certain major advantages over active techniques which involve the generation and detection of subharmonics which will become apparent in chapter IV which explores them in detail. By contrast the technique described here relies on stable first-order effects. Newhouse and Shankar 1984 have observed these first-order oscillations by interrogating a bubble with a megahertz sound field and detecting the bubble oscillations as sidebands as described in section I.6.5. However the technology required for that is much more sophisticated than that employed here.

# III. The ACOUSTIC RE-EMISSION TECHNIQUE

## III.1. DEVELOPMENT AND TESTING

### III.1.1. THE PRINCIPLE

When bubbles oscillate, they emit sound. This includes bubbles which are being forced to oscillate by an applied sound field. Thus a bubble could be measured in a similar way to the Acoustic Bubble Capacitor (ABC) of chapter III but using the maximum in re-emitted sound instead of the maximum in capacitance oscillation to test when the applied sound frequency $\nu_e$ is at the bubble's resonance $\nu_0$.

In some respects this is an obvious idea but there is also an obvious (but mistaken) intuitive objection. This is that the technique is not worth even trying because the re-radiated sound must be less intense than the incident sound which is at the same frequency and so will be totally obscured. It is possibly this sophism that has deterred previous experimental research on this technique and diverted attention to modifications such as the dual frequency technique of chapter IV.

### III.1.2. UTILISING A COMMERCIAL HYDROPHONE

#### *III.1.2.1. THE SYSTEM*

The sound emitted by the bubble was detected by a hydrophone (Brüel & Kjær 8103, sensitivity 30 μV/Pa) placed a few centimetres below the bubble. The rest of the analysing setup, figure 3.1, is the same as for the ABC of chapter II with the ABC itself and the bias circuitry replaced by the hydrophone. The high impedance amplifier was replaced with a low noise amplifier (Brookdeal 450). The 'Spurious Signal Canceller' allowed a portion of the speaker driving signal to be added to the hydrophone output. Except where specified otherwise, the bubbles were in tap water and the 'Spurious Signal Canceller' was not used.

The UW60 loudspeaker was set up as for the ABC studies, providing an RMS acoustic pressure of ~ 10 $Pa_{RMS}$, unless otherwise stated, and the bubbles were held under a 3½ " diameter watchglass as in figure 3.2.

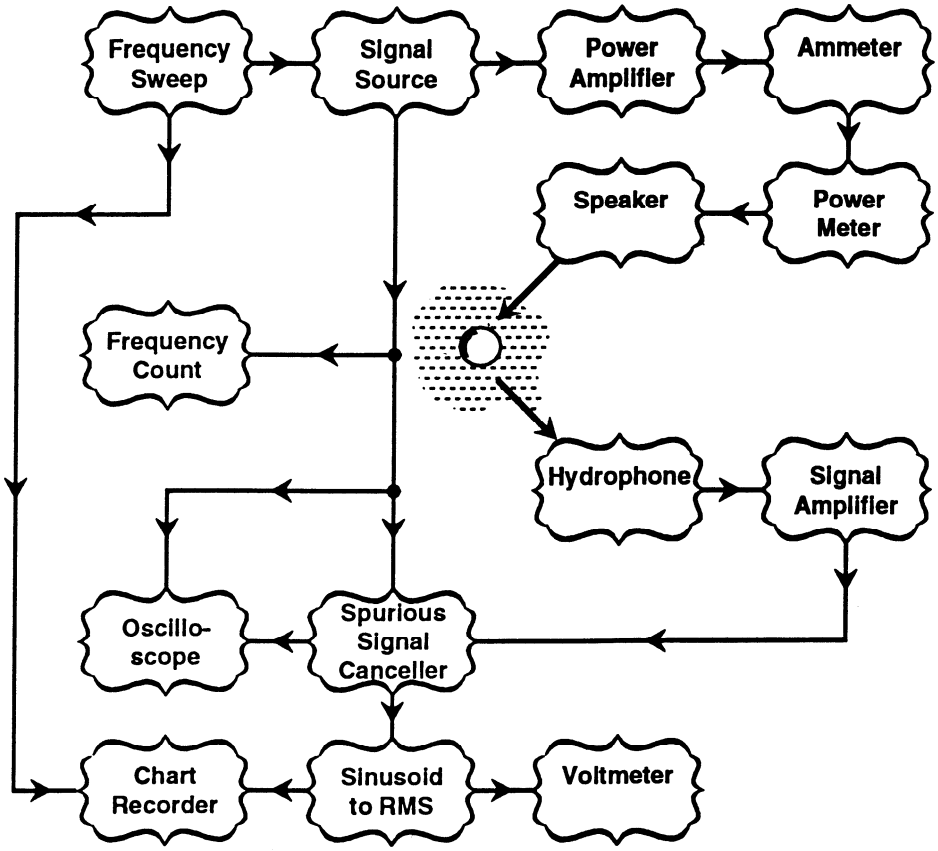



**Fig. 3.1:** Block diagram of the acoustic re-emission setup.

### *III.1.2.2. TESTING*

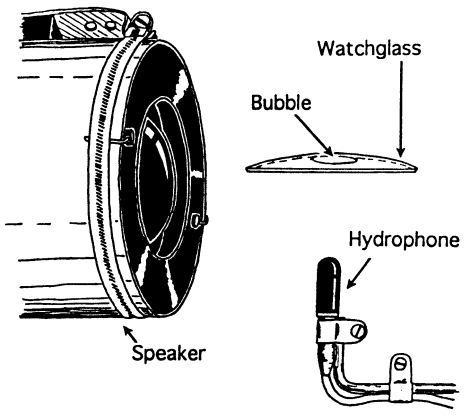



**Fig. 3.2:** A bubble held for forced oscillation.

The testing proceeded as for the ABC. Figure 3.3 shows the frequency response curves obtained for individual air-filled bubbles of three different volumes. The output underwent a phase shift of $\pi$ rad on passing through resonance as expected for forced simple harmonic oscillation. It is this phase shift which is responsible for the dip to nearly zero after each peak. The dip arises, of course, because the hydrophone picks up both the sound field produced by the speaker (amplitude $p_e$) and the phase–shifted sound produced by the bubble (amplitude $q_e$). Thus they add in phase for $\nu_e << \nu_0$ (giving amplitude $q_e + p_e$), add in quadrature for $\nu_e = \nu_0$ (giving amplitude $\sqrt{q_e^2 + p_e^2}$), and add in phase for $\nu_e >> \nu_0$ (giving amplitude $q_e - p_e$) This dip disappears when part of the loudspeaker drive signal is mixed in antiphase with the

hydrophone signal to cancel the part of the signal caused by the speaker's sound field. On repeating the measurements with new bubbles of similar size at the same location, the responses were identical and the resonant frequencies were reproduced to better than ~ 2 Hz. Changing the rate and direction of the frequency sweep did not reveal any hysteresis in the frequency response.

Unlike the bubbles in oil in chapter II, bubbles in water did show shifts of resonant frequency for different gases (figure 3.4). Were the behaviour to be strictly adiabatic, $\nu_0$ would be proportional to $\gamma^{1/2}$ and hence to $(1+(2/N))^{1/2}$ where $N$ is the number of degrees of freedom in the gaseous molecules (from equation {1.16}). Figure 3.6 shows that the gradient does indeed decrease with increasing molecular complexity. For further discussion on the gas dependence, see section III.2.5.

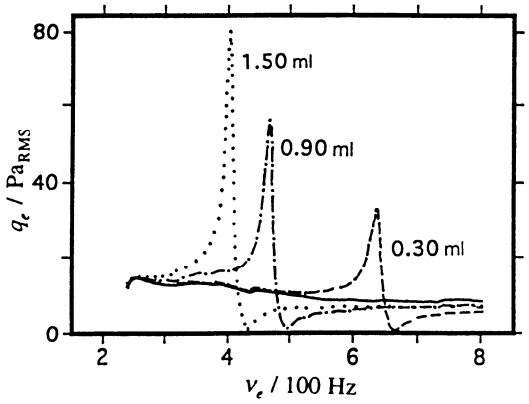



**Fig. 3.3:** Frequency responses for three sizes of air bubbles in water. The solid line is the response in the absence of bubbles.

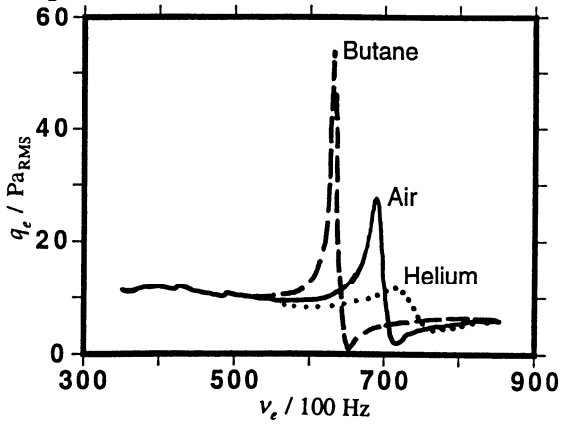



**Fig. 3.4:** Frequency responses for 0.30 ml bubbles of three gases in water.

The variation of $\nu_e$ with volume in figure 3.5 looks Minnaert-like (i.e. $\nu_0 R_{eff} \propto M$, equation {2.1}) but though plotting $\nu_e$ against the effective bubble radius $R_{eff}$ reciprocated, figure 3.6, produces a straight line, it seriously misses the origin.

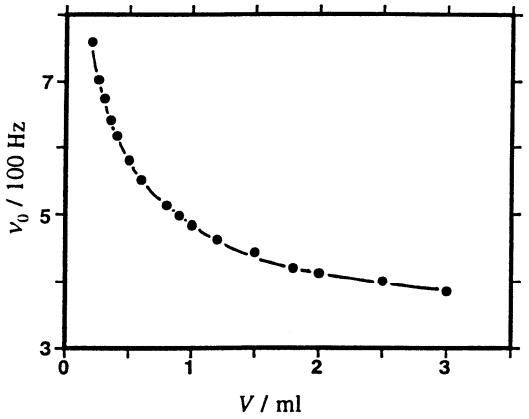



**Fig. 3.5:** Resonant frequency of air bubbles in water plotted against volume.

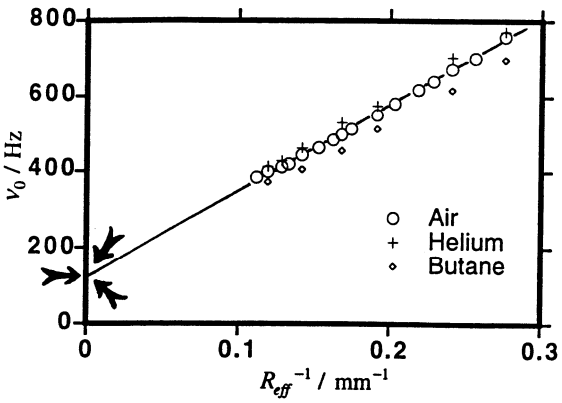



**Fig. 3.6:** Resonant frequency of bubbles in water plotted against reciprocal effective radius.

This ought to be expected since the bubbles in practice were neither in an unbounded medium nor spherical as assumed in equation {1.18}. The behaviour of such bubbles has been discussed in section I.3.6 with equation {1.40} as the result for oblate bubbles. If the ratio of major to minor diameters $\xi$ is large, this approximates to

$$\nu_0 R_{eff} = M\xi^{1/6} . \qquad \{3.1\}$$

The bubbles appeared to have the same vertical extent (which is the minor diameter) so $\xi$ is approximately proportional to $V^{1/2}$. $V$ is proportional to $R_{eff}{}^3$ so

$$\nu_0 R_{eff}{}^{3/4} = M . \qquad \{3.2\}$$

The efficacy of equation {3.2} is confirmed in figure 3.7 for bubbles filled with air, helium and butane. (Though the equation works, it should be noted that its derivation is in fact somewhat invalid. $\xi \approx 1$ for some of the smallest bubbles so the large $\xi$ approximation is very poor yet removing this simplification and actually measuring the $\xi$ values gave a worse fit than {3.2}.)

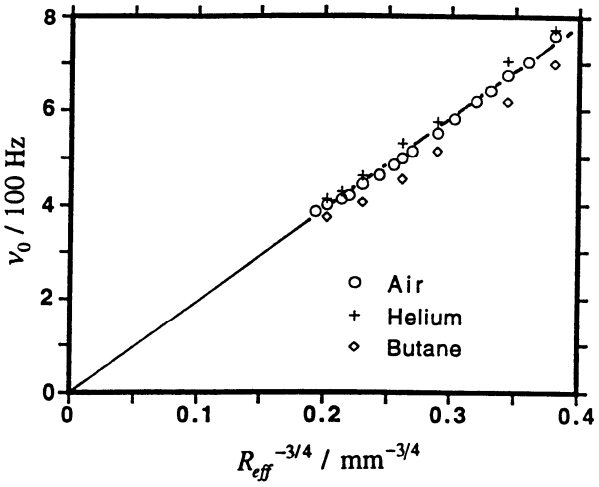



**Fig. 3.7:** Resonant frequency of bubbles in water.

### III.1.3. ADAPTING THE ABC

#### *III.1.3.1. THE SYSTEM*

The resonance of bubbles is affected by the geometry of neighbouring boundaries so it would be convenient if the above trials were repeated using a hydrophone which had the same geometry as the ABCs of the previous chapter. Fortunately it was possible to modify the ABCs themselves into such hydrophones.

The capacitor part of an ABC system consisted of two plates (one earthed, one active) composed of metal and a dielectric composed of the liquid which contained the bubbles. This was converted into a form of capacitive microphone simply by no longer using the liquid as the dielectric. Instead a solid dielectric was fixed to the active plate and an earthed conductor was fixed to the other side of this dielectric. The sensor was then reduced to a simple capacitor. The dielectric and earthed conductor were made both thin and flexible (from silicone sealant and aluminium foil respectively) so this simple capacitor compressed and extended in response to sound pressure. Thus the sound was manifested as periodic capacitance variations. These variations were detected in exactly the same way as for the unmodified ABC

(figures 2.6 and 2.7). The old inflexible earthed plate of figure 2.3 was no longer necessary but was retained to maintain the same geometry as in chapter II.

When used in water, which conducted electricity far better than oil, the foil was omitted since conduction through the water itself was sufficient. By smearing out the silicone dielectric under a thin polymer film ('clingfilm'), it was reduced to less than 0.2 mm thick but retained a resistance of 30 GΩ. Effectively it was a capacitive microphone with water acting as one of the capacitor plates.

The sound pressure response in the ABC Mark 4 in water, shown in figure 3.8, was obtained by placing the Brüel & Kjær hydrophone within the ABC and applying a constant RMS voltage amplitude to the speaker whilst sweeping the frequency. As in oil, there is a maximum at 0.9 kHz from the acoustic resonance of the ABC. The comparison in figure 3.9 demonstrates that the modified ABC acts as an adequate hydrophone.

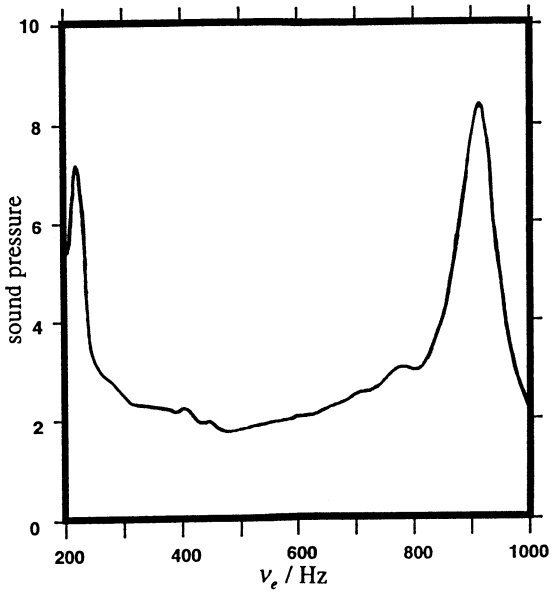



**Fig. 3.8:** Relative excitation pressure versus frequency in the ABC Mark 4 in water measured by a Brüel & Kjær 8103 hydrophone.

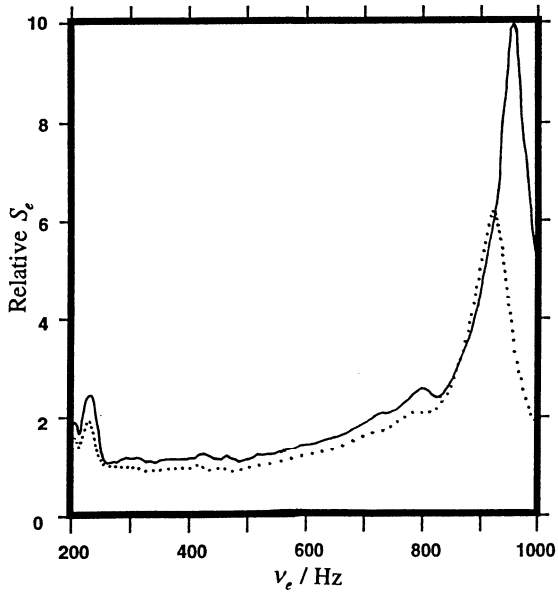



**Fig. 3.9:** Output of ABC Mark 4 adapted as a hydrophone (solid line) compared to a Brüel & Kjær 8103 (dotted line) with the same filtering.

### *III.1.3.2. TESTING*

The frequency responses for three different sizes of air bubbles in water (figure 3.10) and for three different gases (figure 3.11) appear to exhibit much simpler and clearer peaks than for the earlier figures (3.3 and 3.4) but this is just because the 'Spurious Signal Canceller' was used in these cases to compensate for pickup of the excitation sound field. The plate separation was 1.5 cm.

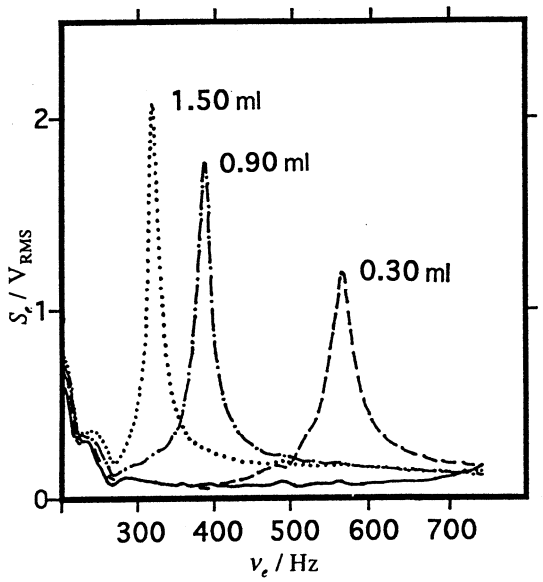



**Fig. 3.10:** Frequency responses for three sizes of air bubbles in water. The solid line is the response in the absence of bubbles.

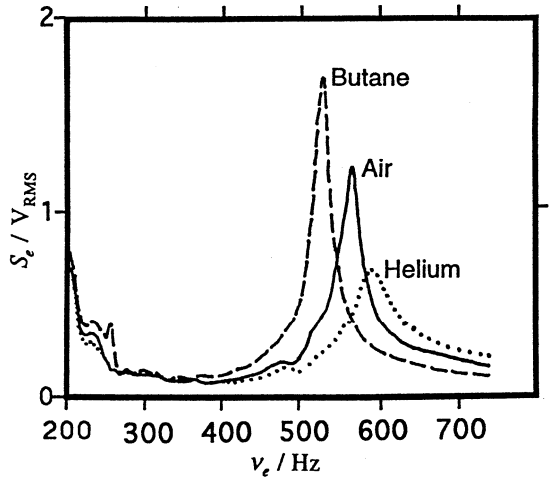



**Fig. 3.11:** Frequency responses for 0.30 ml bubbles of three different gases.

The variation of $\nu_0$ with volume is shown for air, helium and butane in figure 3.12. Plotting against $R_{eff}^{-1}$ yields a straight line which passes through the origin as it did earlier for bubbles in oil (figure 2.11) in the ABC Mark 4 but not in water (figure 3.6) under a watchglass. Therefore this property is a result of the shape of the ABC rather than the choice of liquid; it will be dealt with below. For air the slope, ignoring the two smallest bubbles, is $M = 2.291 \pm 0.005$ Hz m. The ratio of this to the equivalent slope found for oil ($2.38 \pm 0.02$ Hz m) is $1.04 \pm 0.01$ which equals the ratio $(\rho[\text{water}]/\rho[\text{oil}])^{1/2} = 1.045$, predicted by Minnaert's equation {1.16}.

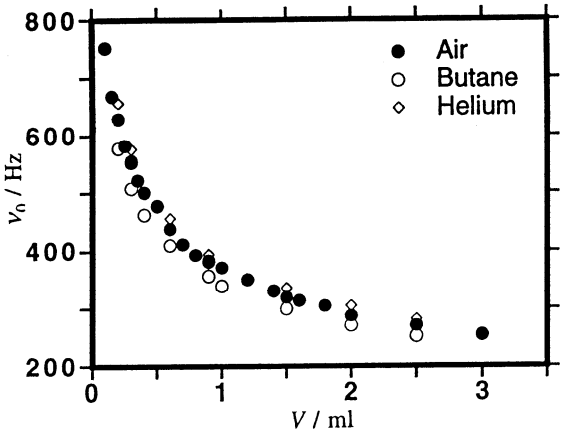



**Fig. 3.12:** Resonant frequencies of bubbles in water in the adapted ABC Mark 4 plotted against volume.

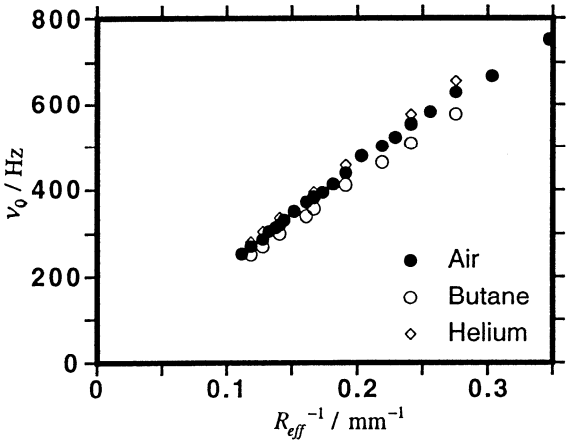



**Fig. 3.13:** Resonant frequency of bubbles in water in the adapted ABC Mark 4 plotted against reciprocal effective radius.

Testing was also carried out using a second, similar, hydrophone made by converting from the smaller ABC Mark 5 which was described in chapter II.

The results of this testing were substantially similar to those of from the larger Mark 4 described earlier. Figure 3.14 is an example, $\nu_0$ versus $R_{eff}^{-1}$.

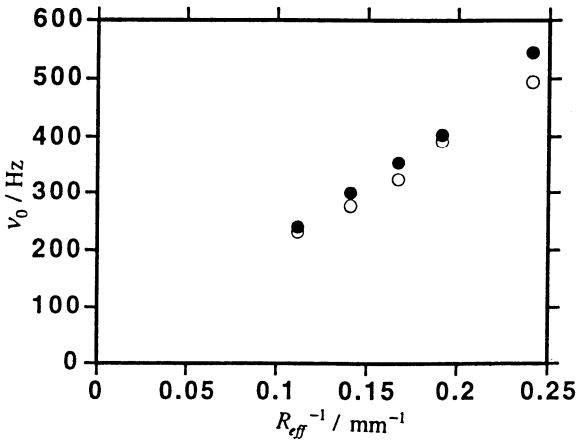



**Fig. 3.14:** Resonant frequency of bubbles in water in adapted ABC Mark 5 plotted against reciprocal effective radius.

## III.2. FURTHER CHARACTERISATION OF BUBBLE RESONANCE

### III.2.1. THE INFLUENCE OF THE ABC'S SHAPE

If a bubble is close to the edge of the (adapted) ABC Mark 4, it is less constrained by the rigid boundaries and so oscillates at a higher frequency than if it were near the centre. This is shown on diagram of the ABC for two sizes of bubbles in figure 3.15. The bubbles were individually sealed, with a quantity of water, in loose PVC sacks so they could be repositioned reliably.

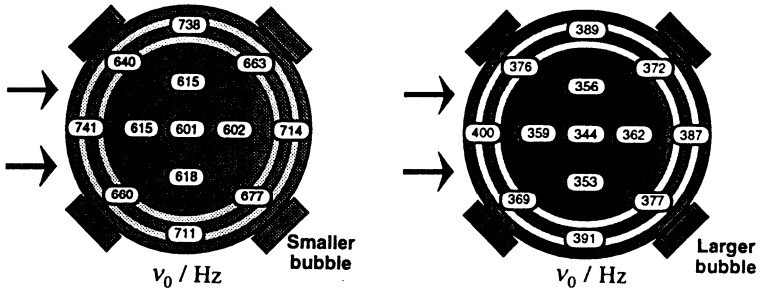



**Fig. 3.15:** Resonant frequency of two air bubbles in water in different positions in the adapted ABC Mark 4 .

Changing the separation of the plates revealed why bubbles obeyed a $\nu_0 \propto R_{eff}^{-1}$ relation in the ABC when they did not in other environments. The possibility of three separations was designed into the ABC; an 'infinite' (actually 14 cm, to the bottom of the tank) separation was achieved by removing the earthed plate which was not necessary when the device was being used as a hydrophone. The value of $\nu_0$ attained as $R_{eff} \to \infty$ (i.e. $R_{eff}^{-1} \to 0$) by extrapolating the $\nu_0$ versus $R_{eff}^{-1}$ plot (figure 3.16) increases as the plate separation increases. At some separation the intercept must be zero. This happens to be very close to the 1.5 cm separation which was chosen as a convenient standard setting for the testing. The close fit to a Minnaert-like result in

the ABC was largely a chance effect! The frequency increase due to increasing oblateness as bubble volumes were increased was counteracted by the frequency decrease due to the decrease in the ratio of plate separation to bubble radius.

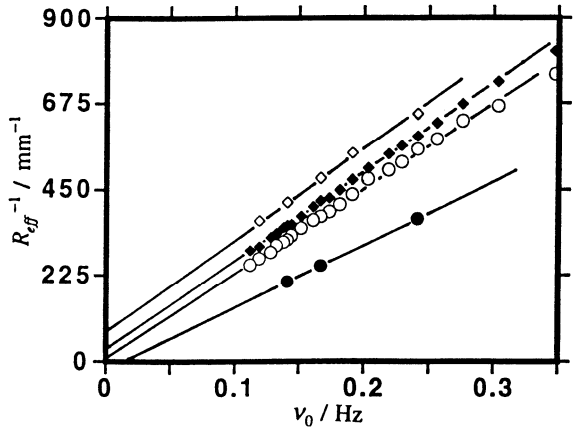



**Fig. 3.16:** Resonant frequency of bubbles in water in adapted ABC Mark 4 plotted against reciprocal effective radius. Plate separation is 0.5 cm (filled circles), 1.5 cm (circles), 2.5 cm (filled squares) and infinity (squares).

### III.2.2. THE DAMPING MECHANISM

The damping mechanism determines the form of the function which relates the amplitude of the acoustic re-emission amplitude at resonance to the bubble size. The amplitude response of a simple harmonic oscillator forced at its resonance is proportional to its Q (equation {1.10}). Also, by dimensional analysis, the radial response amplitude $R_a$ of a spherical bubble will be proportional to its radius $R_0$ so $R_a \propto R_0 Q$. The detected signal is proportional to the pressure amplitude at a point which is (by equation {1.22}) proportional to $R_a$ and thus to $R_0 Q$. $Q$ is proportional to $R_0$ for viscous damping, proportional to $R_0^{1/2}$ for thermal damping, and independent of $R_0$ for radiation damping (results {1.28}, {1.37} and {1.31}). The volume $V \propto R_0^3$ so the output at resonance would be proportional to $V^{2/3}$, $V^{1/2}$ and $V^{1/3}$ respectively.

Using the Brüel & Kjær 8103 for air, helium and butane bubbles under the watchglass, $V^{1/2}$ was found to fit well. Therefore the damping was predominantly thermal. Figure 3.17 is the result for air bubbles.

The standard thermal damping result, {1.38}, gives a Q which is far too high ($Q = 99$ for an air bubble in water with $\nu_0 = 500$ Hz). The actual values observed, e.g. on figure 3.3, are closer to the cruder approximation, {1.37}, ($Q = 28$ for $\nu_0 = 500$ Hz).

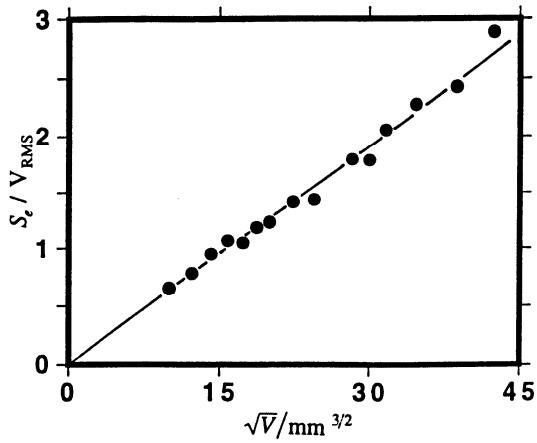



**Fig. 3.17:** Sound re-emission at resonance compared to bubble volume.

### III.2.3. THE DISTANCE DEPENDENCE

The re-emitted acoustic pressure amplitude was inversely proportional to the distance from the centre of the bubble as predicted in {1.22}. Figure 3.18 shows this for a 0.90 ml bubble driven at resonance. The excitation sound was independently measured with the bubble absent and deducted from the recorded amplitude using the knowledge that they were in phase quadrature. The origin of distance is slightly uncertain because of the relatively large size of the Brüel & Kjær 8103 hydrophone (see figure 3.2 for a scale drawing of the hydrophone compared to the rest of the system).

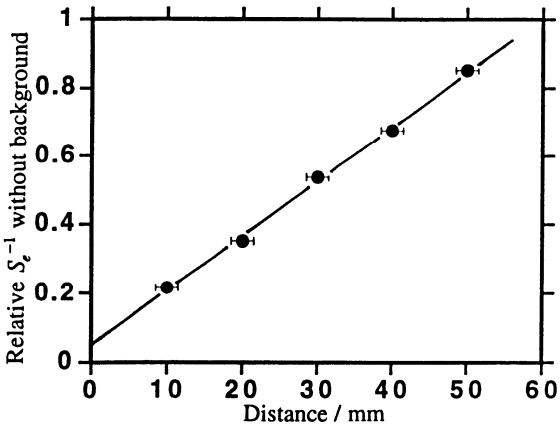



**Fig. 3.18:** Reciprocal sound re-emission amplitude versus the distance between bubble and hydrophone tip.

### III.2.4. THE EXCITATION AMPLITUDE DEPENDENCE

Figure 3.19 shows how the output amplitudes of five individual bubbles of various size varied with the amplitude of the excitation (which is proportional to the square root of the power consumed by the speaker $W_e$). The situation was somewhat complicated and unreproducible at high amplitudes but two main effects could be discerned.

The main effect is simply that the output amplitude is proportional to the excitation amplitude as always results from a linear system. The 0.90 ml bubble of figure 3.19 (detail in figure 3.20) approximates to this. The second effect is that high

excitation intensities move the bubbles either gradually or in an irreversible jump. The 1.50 ml bubble results of figure 3.19 (detail in figure 3.21) exhibits a typical glitch on its plot as the bubble was displaced to a position further from the speaker.

The highest excitation amplitudes used required the experimenter to wear ear protectors so it is not surprising that the bubbles were also affected by the strength of the sound. Fortunately both the acoustic re-emission and the ABC techniques work well at sound pressures much lower than those used for figure 3.19 so these complications are not a serious problem. These results were obtained in the adapted ABC Mark 4 acting as a hydrophone; similar behaviour occurred in the unmodified ABC in oil.

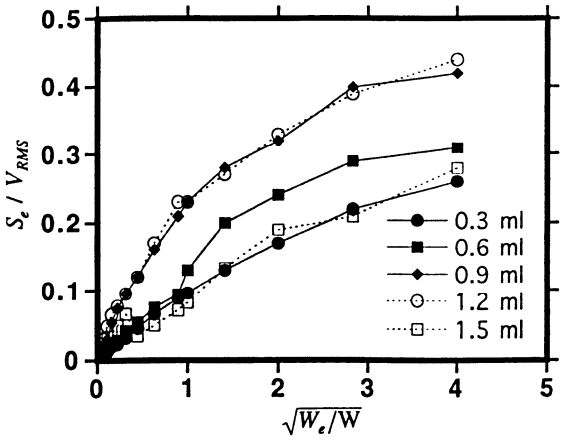



**Fig. 3.19:** Relative output amplitude versus excitation amplitude for five separate air bubbles in water.

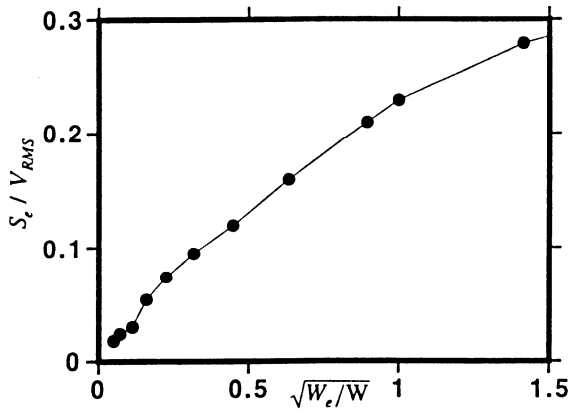



**Fig. 3.20:** Relative output amplitude versus excitation amplitude for a 0.90 ml bubble.

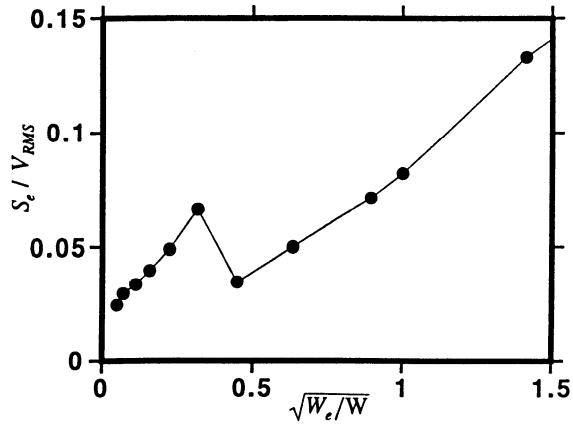



**Fig. 3.21:** Relative output amplitude versus excitation amplitude for a 1.50 ml bubble.

### III.2.5. DIFFERENT GASES

Figures 3.4 and 3.11 showed that, in water, the type of gas in the bubble affected the resonant frequency. The ratio of slopes from figure 3.13 is M[butane] : M[air] : M[helium] = 0.933 ± 0.005 : 1.000 : 1.052 ± 0.005 which is in the sequence as the Minnaert prediction from {1.16}, 0.976 : 1.000 : 1.091, but does not fit quantitatively. Bubbles of mixed gases show intermediary values, for example the air/butane mixtures in the adapted ABC graphed as figure 3.22 below.

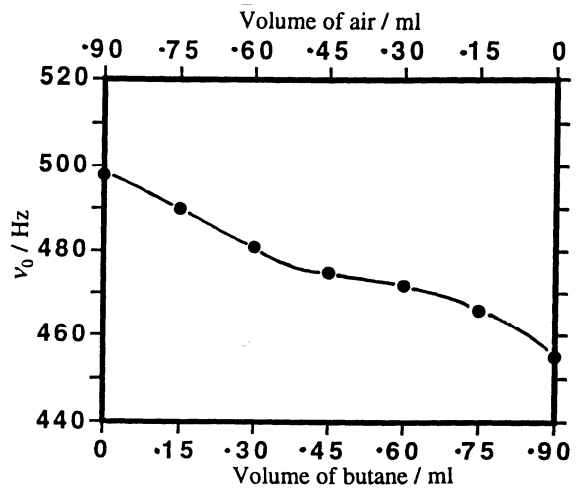



**Fig. 3.22:** Resonant frequencies of 0.90 ml bubbles of different air/butane mixtures in water.

The Q falls when changing from butane to air to helium because thermal conductivity rises increasing the thermal damping.

### III.2.6. RISING BUBBLES

The acoustic re-emission technique was applied, like the ABC earlier, to rising bubbles. Figure 3.23 shows the composite response curve for thirty two bubbles (each of volume 1.36 ± 0.01 ml); this being the number of bubbles interrogated by the sound field in the sweep time of the audio frequency. The sound was detected by the Brüel & Kjær hydrophone which is small compared to the ABC Mark 4 so the high-frequency tail evident in figure 2.14, which was caused by the ABC's bulk, is absent. When $\nu_e > \nu_0$, the re-emitted and driving sounds cancel as for figure 3.3.

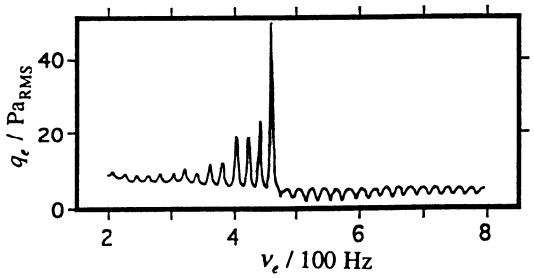



**Fig. 3.23:** The frequency response for a stream of rising bubbles, each of volume 1.36 ml, taken over 36 s.

The output of the system was also recorded on a digital storage oscilloscope to record it on shorter time scales than the chart recorder could manage. Doing this for air bubbles rising in water through the adapted ABC Mark 4 and printing the display onto an X-Y plotter produced figures 3.24 to 3.27. The upper trace on each is the output of the sinusoid to RMS converter which normally went to the chart recorder.

The lower trace is the raw unprocessed oscillatory signal. The resonant frequency $\nu_0$ was 403 Hz.

Figure 3.24 shows the small response for two successive bubbles when $\nu_e = 300\text{Hz} < \nu_0$. Figure 3.25 shows a larger response when $\nu_e = \nu_0$. Figure 3.26 shows the case when $\nu_e = 421\text{Hz} > \nu_0$ with the partial cancellation of the background sound as the bubbles passed through the centre and peaks on each side of it from the same bubbles when at the edges of the ABC plates and so resonating at a higher frequency. The increase in sound amplitude as a bubble entered the device is shown in figure 3.27 on an expanded scale.

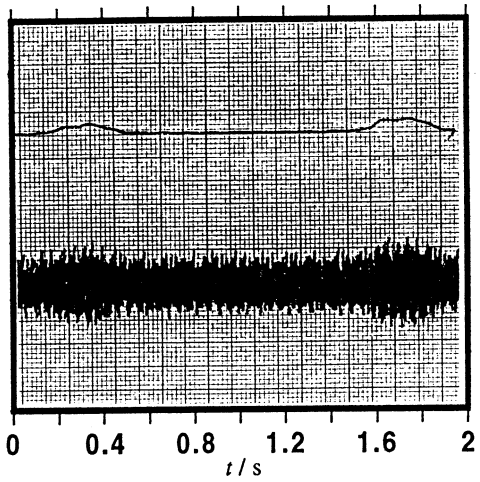



**Fig. 3.24:** Trace from rising bubbles excited below resonance.

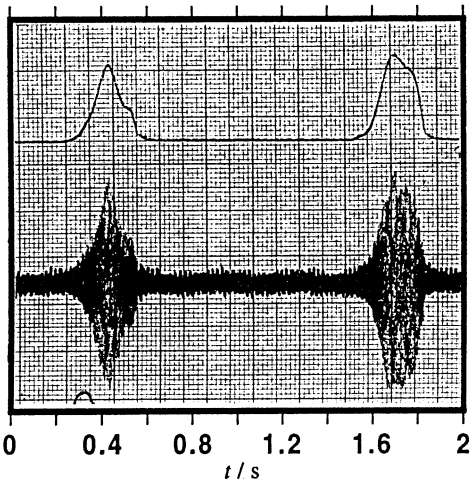



**Fig. 3.25:** Trace from rising bubbles excited at resonance.

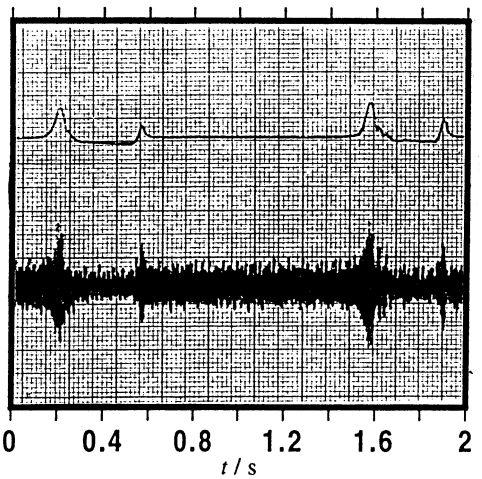



**Fig. 3.26:** Trace from rising bubbles excited above resonance.

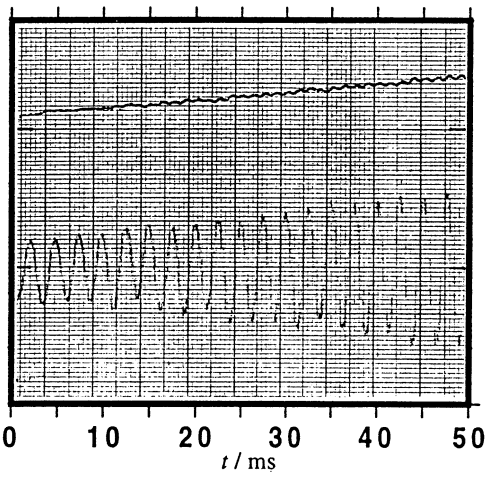



**Fig. 3.27:** As 3.25 but on a shorter time scale.

## III.3. PAIRS OF UNEQUALLY SIZED BUBBLES

Complications arise when bubbles are close to other bubbles: the resonant frequencies shift (figure 2.18). This seriously limits the usefulness of all sizing techniques which rely on acoustic resonance unless a way is found to calculate the shift. The problem is exemplified by figure 3.28 for which the watchglass of figure 3.2 was replaced by a 140 mm by 90 mm dural plate with indentations to hold bubbles. Identically sized bubbles were created in a line with 15 mm between centres. As more bubbles were added the resonant frequency fell.

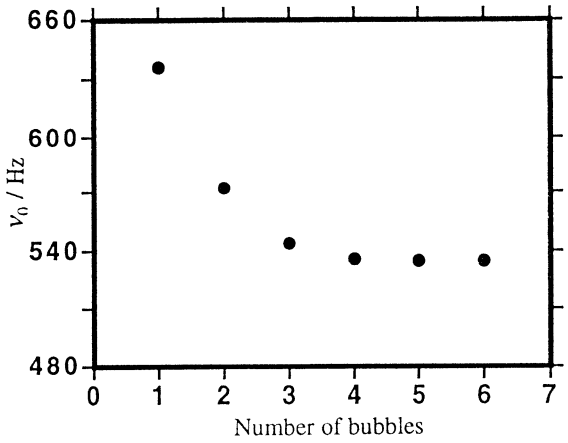



**Fig. 3.28:** Change of resonant frequency of 0.30 ml air bubbles as more 0.30 ml bubbles were added.

### III.3.1. THE THEORETICAL ANALYSIS

The natural frequency of two bubbles oscillating in phase, with centres separated by distance $s$, that is given by {1.41} only applies to identical spherical bubbles. It is also unhelpful for giving a mental picture of the derivation because of its roundabout route through capacitance calculations (which involves several tricks and considerable algebra if done in full). The case for differently sized bubbles additionally needs to include the second normal mode – with the bubbles oscillating in antiphase – since this will have a monopole component and so couple with sound field as well. A new theory needed to be created.

Several early attempts either degenerated into algebraically inelegant sprawls or simply gave absurd results for the two known cases, i.e. identical bubbles at any separation and any bubbles at a large separation. Modelling the SHM of bubbles as masses and springs failed when the coupling was strong because the dimensionality of the problem was wrong: doubling a bubble's radiation mass does not divide its $\nu_0$ by $2^{1/2}$ but $2^{1/3}$.

The following, successful, derivation starts from Newton's Second Law of Motion applied to an infinitesimal volume of liquid (this is, equivalently, a linearised inviscid Navier-Stokes equation):

$$\nabla p = -\rho \dot{\underline{v}} \qquad \{3.3\}$$

where $p$ is the pressure, $\underline{v}$ is the liquid velocity and $\rho$ is the liquid density. Let the radii of the two spherical bubbles $R_1$ and $R_2$ oscillate as

$$\begin{cases} R_1 = R_{10} + R_{1a}\sin\omega_0 t \\ R_2 = R_{20} + R_{2a}\sin\omega_0 t \cdot \end{cases} \qquad \{3.4\}$$

If the flow is incompressible and unbounded then the time derivatives of {3.4} can give the liquid velocities in the medium . The liquid velocity at $\underline{r_1}$ from the centre of the first bubble due to the first bubble alone is

$$\underline{v_1} = \frac{{R_{10}}^2 R_{1a}\omega_0 \cos\omega_0 t}{{r_1}^2}\hat{\underline{r}}_1 \qquad \{3.5\}$$

and so the acceleration is

$$\dot{\underline{v}}_1 = -\frac{{R_{10}}^2 R_{1a}{\omega_0}^2 \sin\omega_0 t}{{r_1}^2}\hat{\underline{r}}_1 . \qquad \{3.6\}$$

Similarly, the second bubble causes

$$\dot{\underline{v}}_2 = -\frac{{R_{20}}^2 R_{2a}{\omega_0}^2 \sin\omega_0 t}{{r_2}^2}\hat{\underline{r}}_2 . \qquad \{3.7\}$$

Substituting the total acceleration $\dot{\underline{v}} = \dot{\underline{v}}_1 + \dot{\underline{v}}_2$ into {3.3} gives the pressure gradient in the liquid:

$$\nabla p = \rho{\omega_0}^2\left( R_{1a}\frac{{R_{10}}^2}{{r_1}^2}\hat{\underline{r}}_1 + R_{2a}\frac{{R_{20}}^2}{{r_2}^2}\hat{\underline{r}}_2 \right)\sin\omega_0 t . \qquad \{3.8\}$$

Making the polytropic approximation ($pV^{\kappa}$ = constant), as for {1.14}, the pressures in the bubbles, and at their surfaces, are

$$\begin{cases} p_1 = p_0 - 3\kappa p_0 (R_{1a}/R_{10})\sin\omega_0 t \\ p_2 = p_0 - 3\kappa p_0 (R_{2a}/R_{20})\sin\omega_0 t \cdot \end{cases} \qquad \{3.9\}$$

The pressure at the centre point between the bubbles $p_c$ can be obtained from the pressure of the first bubble:

$$p_c = p_1 + \int_{bubble1}^{centre} \nabla p \bullet d\underline{r} . \qquad \{3.10\}$$

Substituting $\nabla p$ from {3.8} produces

$$p_c = p_1 + \rho{\omega_0}^2\left( \int_{bubble1}^{centre} R_{1a}\frac{{R_{10}}^2}{{r_1}^2} \bullet d\underline{r}_1 + R_{2a}\int_{bubble1}^{centre}\frac{{R_{20}}^2}{{r_2}^2} \bullet d\underline{r}_2 \right)\sin\omega_0 t . \qquad \{3.11\}$$

The simplest path to integrate along is the line joining the bubble centres. At the centre point $r_1 = r_2 = s/2$. For the first integral, the boundary of the first bubble is taken as its equilibrium position; i.e. $r_1 = R_{10}$. For the second integral, the bubble separation will suffice; i.e. $r_2 = s$. Thus

$$p_c = p_1 + \rho\omega_0^2\left( R_{1a}R_{10}^2\left[\frac{-1}{r_1}\right]_{R_{10}}^{s/2} + R_{2a}R_{20}^2\left[\frac{-1}{r_2}\right]_{s_{10}}^{s/2}\right)\sin\omega_0 t \qquad \{3.12\}$$

$$= p_1 + \rho\omega_0^2\left( R_{1a}R_{10}^2\left(\frac{1}{R_{10}} - \frac{2}{s}\right) + R_{2a}R_{20}^2\left(\frac{-1}{s}\right)\right)\sin\omega_0 t\,. \qquad \{3.13\}$$

Similarly $p_c$ can be calculated from the pressure in the secondbubble giving

$$p_c = p_2 + \rho\omega_0^2\left( R_{1a}R_{10}^2\left(\frac{-1}{s}\right) + R_{2a}R_{20}^2\left(\frac{1}{R_{20}} - \frac{2}{s}\right)\right)\sin\omega_0 t\,. \qquad \{3.14\}$$

These must give the same $p_c$ (this imposes the boundary condition whereby each bubble is affected by the other's sound). This implies

$$\frac{R_{1a}}{R_{10}}\left(4\pi^2 M_M^2 - \omega_0^2 R_{10}^3\left(R_{10}^{-1} - s^{-1}\right)\right) = \frac{R_{2a}}{R_{20}}\left(4\pi^2 M_M^2 - \omega_0^2 R_{20}^3\left(R_{20}^{-1} - s^{-1}\right)\right) \qquad \{3.15\}$$

where $M_M$ is the familiar Minnaert constant of {1.16}.

It is convenient to use the symmetric combination of {3.13} and {3.14} for $p_c$,

$$p_c = p_0 + \left( \begin{array}{c} \frac{\rho\omega_0^2}{2}\left( R_{1a}R_{10}^2\left(\frac{1}{R_{10}} - \frac{3}{s}\right) + R_{2a}R_{20}^2\left(\frac{1}{R_{20}} - \frac{3}{s}\right)\right) \\ -3\kappa p_0\left(\frac{R_{1a}}{R_{10}} + \frac{R_{2a}}{R_{20}}\right) \end{array} \right)\sin\omega_0 t\,, \qquad \{3.16\}$$

to calculate the pressures elsewhere. The pressure far from the bubble is obviously the atmospheric pressure $p_0$, i.e.

$$p_0 = p_c + \int_{centre}^{\infty} \nabla p \bullet d\underline{r} \qquad \{3.17\}$$

$$= p_c + \rho\omega_0^2\left( R_{1a}R_{10}^2\left[\frac{-1}{r_1}\right]_{s/2}^{\infty} + R_{2a}R_{20}^2\left[\frac{-1}{r_2}\right]_{s/2}^{\infty}\right)\sin\omega_0 t \qquad \{3.18\}$$

$$= p_c + \frac{2\rho\omega_0^2}{s}\left(R_{1a}R_{10}^2 + R_{2a}R_{20}^2\right)\sin\omega_0 t\,. \qquad \{3.19\}$$

Using the expression {3.16} for $p_c$ gives

$$\frac{R_{1a}}{R_{10}}\left(4\pi^2 M_M^2 - \omega_0^2 R_{10}^3\left(R_{10}^{-1} + s^{-1}\right)\right) = -\frac{R_{2a}}{R_{20}}\left(4\pi^2 M_M^2 - \omega_0^2 R_{20}^3\left(R_{20}^{-1} + s^{-1}\right)\right). \qquad \{3.20\}$$

The original Minnaert single bubble results,

$$R_{10}\omega_{10} = R_{20}\omega_{20} = 2\pi M_M \qquad \{3.22\}$$

where $\omega_{10}$ and $\omega_{20}$ are the resonant angular frequencies of the two bubbles when isolated, can be derived from {3.20} by insisting that there is no restriction on the ratio of oscillation amplitudes $R_{1a}/R_{2a}$ after $s \to \infty$.

The two expressions which relate $\omega_0$ to $R_{1a}/R_{2a}$, {3.15} and {3.20}, are readily solved. First divide one by the other:

$$\frac{4\pi^2 {M_M}^2 - {\omega_0}^2 {R_{10}}^3 \left({R_{10}}^{-1} + s^{-1}\right)}{4\pi^2 {M_M}^2 - {\omega_0}^2 {R_{10}}^3 \left({R_{10}}^{-1} - s^{-1}\right)} = -\frac{4\pi^2 {M_M}^2 - {\omega_0}^2 {R_{20}}^3 \left({R_{20}}^{-1} + s^{-1}\right)}{4\pi^2 {M_M}^2 - {\omega_0}^2 {R_{20}}^3 \left({R_{20}}^{-1} - s^{-1}\right)}. \qquad \{3.23\}$$

Then remove $M_M$ from {3.23} by using Minnaert relations {3.22}. Since $\omega_{10}$ and $\omega_{20}$ are measurable quantities, this removes the influence of all the approximations (including the polytropic one) in Minnaert's argument except linearity. It also simplifies the appearance:

$$\frac{{\omega_{10}}^2 - {\omega_0}^2 \left(1 + \left(R_{10}/s\right)\right)}{{\omega_{10}}^2 - {\omega_0}^2 \left(1 - \left(R_{10}/s\right)\right)} = -\frac{{\omega_{20}}^2 - {\omega_0}^2 \left(1 + \left(R_{20}/s\right)\right)}{{\omega_{20}}^2 - {\omega_0}^2 \left(1 - \left(R_{20}/s\right)\right)}. \qquad \{3.24\}$$

This is multiplied out,

$${\omega_0}^4 \left(1 - \frac{R_{10}R_{20}}{s^2}\right) - {\omega_0}^2 \left({\omega_{10}}^2 + {\omega_{20}}^2\right) + {\omega_{10}}^2 {\omega_{10}}^2 = 0, \qquad \{3.25\}$$

and solved to give the two values of $\omega_0$, called $\omega_+$ and $\omega_-$:

$$\omega_\pm = \sqrt{\frac{{\omega_{10}}^2 + {\omega_{20}}^2 \pm \sqrt{{\omega_{10}}^4 - 2\left(1 - \frac{2R_{10}R_{20}}{s^2}\right){\omega_{10}}^2 {\omega_{20}}^2 + {\omega_{20}}^4}}{2\left(1 - \frac{R_{10}R_{20}}{s^2}\right)}}. \qquad \{3.26\}$$

The lower frequency $\omega_-$ corresponds to the bubbles oscillating in phase; the higher frequency $\omega_+$ to oscillations in antiphase. The latter is higher because the mass of liquid moved is lower – a portion of the liquid is shunted back and forth between the bubbles. Equations {3.15} and {3.20} can be solved to give the ratio of amplitudes $R_{1a}/R_{2a}$ if desired.

### III.3.2. THE SIMPLE CASES VERIFICATION

Two special cases of {3.26} are readily verified. For infinite bubble separation, it gives $\omega_\pm \to \omega_{10}, \omega_{20}$ as required. For $\omega_{10} = \omega_{20}$, it reduces to

$$\omega_- = \omega_{10} \Big/ \sqrt{1 + \left(R_{10}/s\right)} \qquad \{3.27\}$$

which differs from Strasberg's result ({1.41}), which was

$$\omega_- = \omega_{10} \Big/ \sqrt{1 + \left(R_{10}/s\right) + \left(R_{10}/s\right)^4}, \qquad \{3.28\}$$

by less than 2 %.

For bubbles of equal volume, the oscillation at $\omega_+$ is purely dipole and so does not couple well with sound fields.

### III.3.3. THE COMPUTATIONAL VERIFICATION

Equation {3.26} is trivially converted from angular to conventional frequencies:

$$\nu_{\pm} = \sqrt{\frac{\nu_{10}{}^2 + \nu_{20}{}^2 \pm \sqrt{\nu_{10}{}^4 - 2\left(1 - \frac{2R_{1eff}R_{2eff}}{s^2}\right)\nu_{10}{}^2\nu_{20}{}^2 + \nu_{20}{}^4}}{2\left(1 - \frac{R_{1eff}R_{2eff}}{s^2}\right)}} \quad . \qquad \{3.29\}$$

Figure 3.29 was provided by C.W.H.Beton who used a Boundary Element Method to simulate the dynamics of bubbles including axisymmetric shape changes (Beton 1994). The points on the figure are the main frequencies found to be present in the natural oscillations of simulated bubble pairs. The lines are the predictions of {3.29}.

The slightly greater divergence of natural frequencies found in the simulation was probably due to the bubbles being allowed to approach each other under the influence of Bjerknes forces in the simulation.

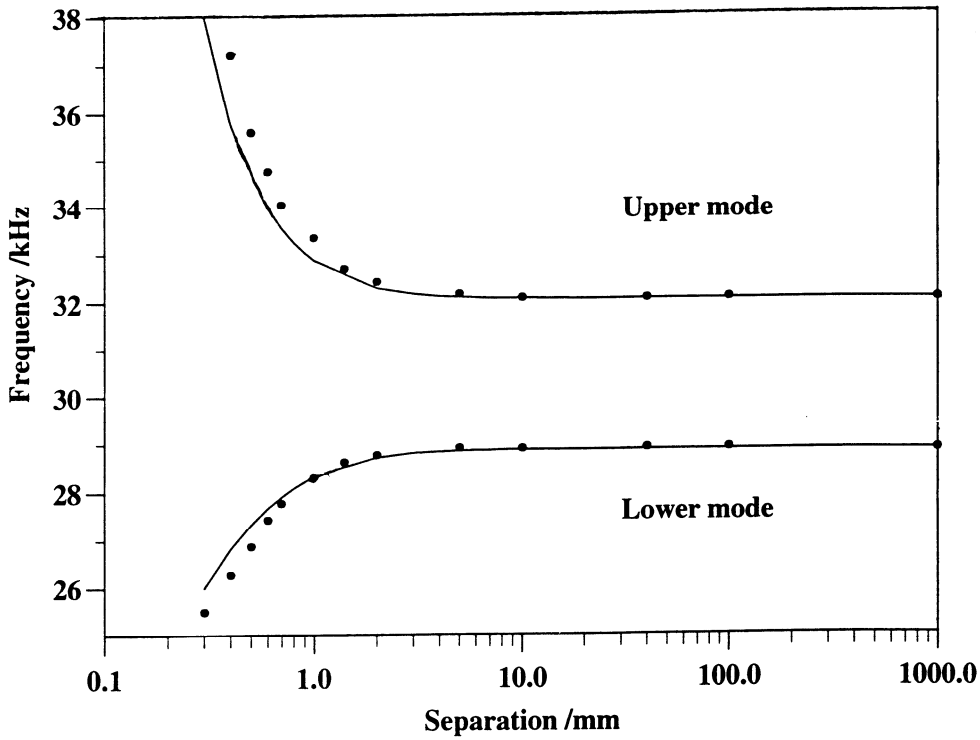



**Fig. 3.29:** Natural frequencies of two air bubbles in water versus separation of centres. Radii are 0.10 and 0.11 mm. The line is from {3.29}. The points are from BEM simulations. (This is part of figure 3.18 of Beton 1994, photocopied with permission.)

### III.3.4. THE EXPERIMENTAL VERIFICATION

After the above theory was created, the case of $\omega_{10} \neq \omega_{20}$ was tested experimentally by using bubbles of two different sizes held under the metal plate as for figure 3.28. The bubbles were of determined volume so their radii where approximated by effective radii $R_{1eff}$ and $R_{2eff}$ as for the other experiments.

When the theoretical values and the experimental data were plotted together (figures 3.30 and 3.31), the degree of correspondence was remarkable. The fit could have been slightly improved by increasing the effective radii *ad hoc* by ~10 % to represent the bubbles being slightly oblate under the plate but the original first plots are those shown here. There were no free parameters optimised to achieve the fit. Only the readily measured $\omega_{10}$, $\omega_{20}$, volumes and separation were used with the above theory.

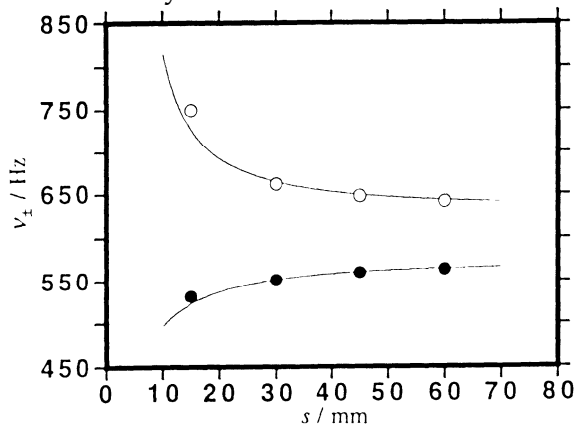



**Fig. 3.30:** Resonant frequencies of two air bubbles in water versus separation of centres. Volumes are 0.50 and 0.30 ml. The line is from {3.29}. The points are experimental.

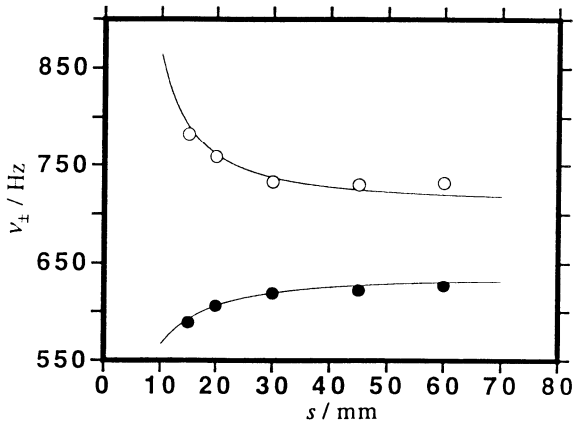



**Fig. 3.31:** Resonant frequencies of two air bubbles in water versus separation of centres. Volumes are 0.30 and 0.20 ml. The line is from {3.29}. The points are experimental.

## III.4. CONCLUSION

This is a conceptually simple method of acoustically sizing bubbles. It can be implemented using only commercially available devices. It requires just a hydrophone, a loudspeaker that works in the liquid used and standard monitoring electronics as desired.

Most of the conclusions which applied to the ABC apply equally to this technique except that the electrical conductivity of the liquid does not affect the ease of electronic design for this technique. Extraneous acoustic noise may complicate the detection of re-emitted sound in industrial applications but the frequency (and, at resonance, the phase) of the re-emission is known so tight filtering or coherent detection could be applied to remove most of the noise.

Though it works experimentally and the mathematics is well known (Pippard 1989), there may be some unease over how it seems that a sound can actually be made louder by adding a damping object such as a bubble. This is largely due to confusion between the intensity of a sound (proportional to the flux of energy) and the energy density of a sound (which includes energy stored in standing waves, which have no net flux, as well as in travelling waves). Because the hydrophone is less than a wavelength from the bubble, the extra sound pressure (i.e. energy density) detected is mainly the bubble's induction field. The pressure and velocity oscillations in the liquid are in almost quadrature; there is relatively little net flow of energy. The net flow of sound energy is, of course, inwards to the bubble where it is lost by thermal damping. For this reason the word 're-emission', rather the more euphonious 're-radiation', has been used throughout this chapter.

# IV. THE SUBHARMONIC MODULATION TECHNIQUE

## IV.1. BACKGROUND

### IV.1.1. EARLIER RESEARCH

As described in chapter I, when Newhouse and Shankar 1984 reflected ultrasound (at 'imaging' frequency $\nu_i$) from air bubbles in water whilst the bubbles were being independently excited into oscillation by a separate sound source (frequency $\nu_e$, $\nu_e << \nu_i$), they found that the reflected ultrasound was partly modulated at $\nu_e$. The explanation was that the size of the scatterers, the bubbles, was periodically varying at $\nu_e$. Like the methods of chapters II and III, the bubble's resonance $\nu_0$, and hence size, could therefore be found by varying $\nu_e$. The response, the degree of modulation in this case, would be maximum when $\nu_e = \nu_0$. When this was repeated as an undergraduate project (Lingard *et al* 1990, published as Leighton *et al* 1990a, 1991a), an additional effect was found in the spectrum of the ultrasound. This was sidebands at $\nu_i \pm \nu_e/2$ which indicated that modulation at $\nu_e/2$, a subharmonic of the excitation frequency, could also exist.

The origin of this subharmonic modulation was unknown and intriguing. One explanation was merely that the bubbles' breathing-mode oscillations themselves had a subharmonic component resulting from non-linearities in the bubbles' dynamics; a non-linear oscillator can exhibit subharmonics if driven sufficiently hard. Another candidate was surface waves (shape oscillations) on the bubbles; that they could be somehow involved was hinted at by the well-known fact that surface waves are preferentially excited at half the forcing frequency (Faraday 1831) but how they could be effective was unclear. Because the dipole nature of surface oscillations leads to little radiation compared to the breathing mode (Strasberg 1956), the former explanation – subharmonic radial oscillations – became favoured.

### IV.1.2. PRELIMINARY STUDIES

These studies were performed on air bubbles in tap water using an Electro-Medical Supplies Therasonic 1030 (a therapeutic ultrasound unit) to provide ultrasound at $\nu_i = 3.35\text{MHz}$ and a Mylar® RS-248-325 (a general purpose cheap 85 mm diameter plastic cone type) loudspeaker to provide sound at $\nu_e$. The ultrasound transducer was kept outside the water tank behind an acoustic window. The loudspeaker was originally simply immersed in water. The speakers' lifetimes were later extended by adding waterproof backing of plastic or dural.

A Dapco NP10-3 Needle Hydrophone and a Marconi Instruments TF2370 spectrum analyser detected and monitored the ultrasound. All control and recording was manual. Figure 4.1 is a schematic of this simple system.

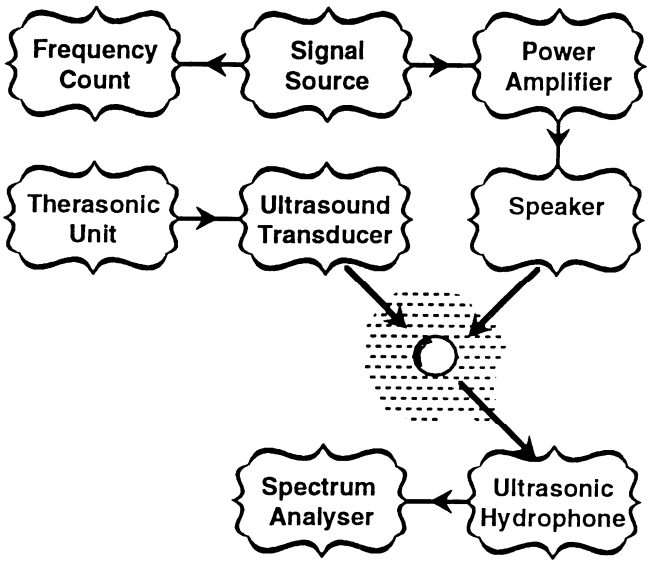



**Fig. 4.1:** Schematic of the preliminary subharmonic analysis system.

The bubbles, which were much smaller than those of chapters II and III, were blown by a drawn glass pipette and held on a greased vertical wire as in figure 4.2. Their volumes were measured by first dislodging each bubble into a water-filled glass cell then measuring their principle diameters with a travelling microscope The bubbles were approximated to ellipsoids for their volumes to be calculated. The purpose of the Brüel & Kjær 8103 hydrophone was to test for the presence of sound emission from the bubble at $\nu_e/2$ itself. A typical output from the spectrum analyser when the effect was being exhibited by the bubble is shown on figure 4.3; the subharmonic modulation sidebands at $\nu_i \pm \nu_e/2$ are indicted by arrows.

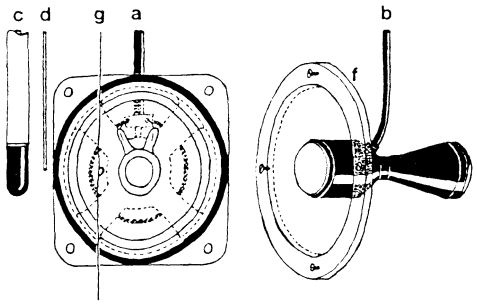



**Fig. 4.2:** Detail of tank contents: (a) loudspeaker, (b) ultrasound source, (c) Brüel & Kjær audio hydrophone, (d) Dapco ultrasonic hydrophone, (f) acoustic window and (g) wire holding a bubble.

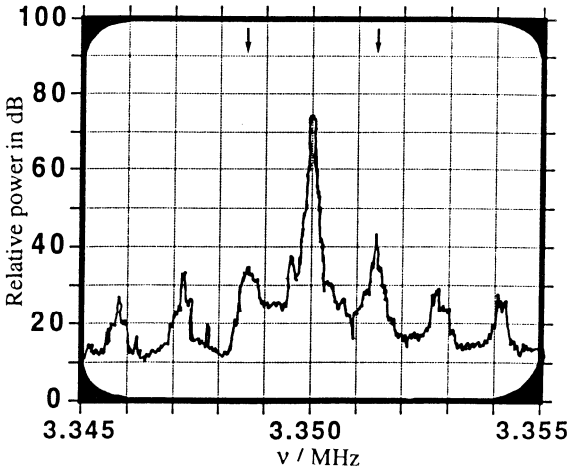



**Fig. 4.3:** Spectrum of subharmonic modulation from a bubble on a wire forced at resonance at 2.7 kHz.

The results from this system were rather unsatisfactory. Often the bubbles were lost from the wire whilst recording the frequency response, the modulation amplitudes varied greatly between experiments (frequently being totally absent) and the amplitudes of the sidebands on either side of $\nu_i$ – which should be symmetric for

pure modulation – differed in amplitude. One of the tidiest frequency responses is shown in figures 4.4 and 4.5! Figure 4.4 displays the unprocessed amplitudes of the various sidebands ($S_{\pm 1}$ are the signal amplitudes at $\nu_i \pm \nu_e$ and $S_{\pm 1/2}$ are those at $\nu_i \pm \nu_e/2$). It looks neater after averaging the corresponding sidebands and making cosmetic changes (figure 4.5).

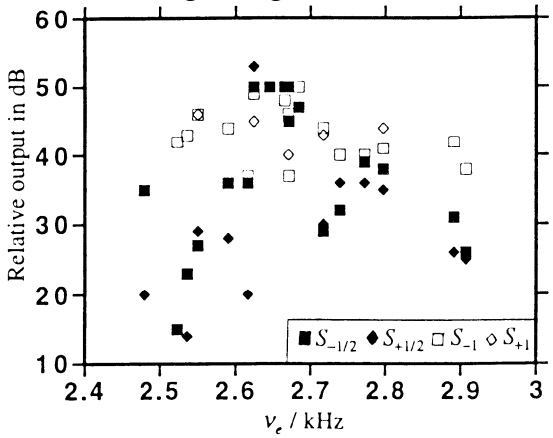



**Fig. 4.4:** Amplitude of sidebands versus the excitation frequency for a 1.04 ± 1 mm radius bubble.

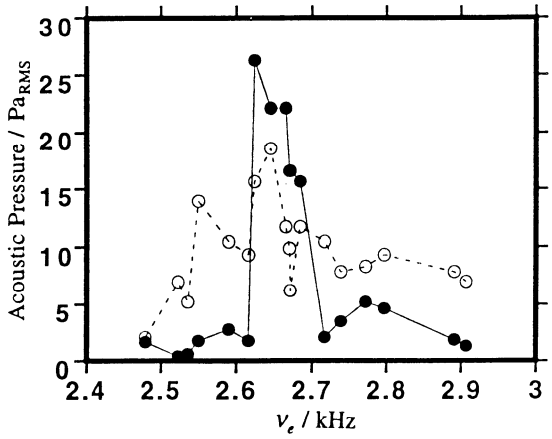



**Fig. 4.5:** The same as figure 4.4 but after some processing to make it look better. (Solid points are at $\nu_i \pm \nu_e/2$, hollow at $\nu_i \pm \nu_e$).

This system did reveal that the subharmonic modulation had a threshold in the excitation amplitude $p_e$ (as predicted by Shankar 1991) demonstrated in figure 4.6.

The most encouraging results by that time had been obtained by Leighton *et al* 1991a using virtually the same setup. Their figure 6 (redrawn as figure 4.7 below) is for an array of four bubbles and "The resonance of each bubble is arrowed" (Leighton *et al* 1991a). The variety of Mylar® speaker used was not designed for use underwater and had a very uneven frequency response (see Appendix 2). The response has been found to include four maxima in the 3 to 6 kHz region so loudspeaker resonances are a more likely explanation of the peaks than bubble resonances.

Inadequacies of the speaker were also responsible for the $\nu_e/2$ signal reported in Hardwick *et al* 1992 and originally mistakenly attributed to a doubling of the bubbles breathing mode. Speakers have long been known as a source of subharmonics (Pedersen 1935).

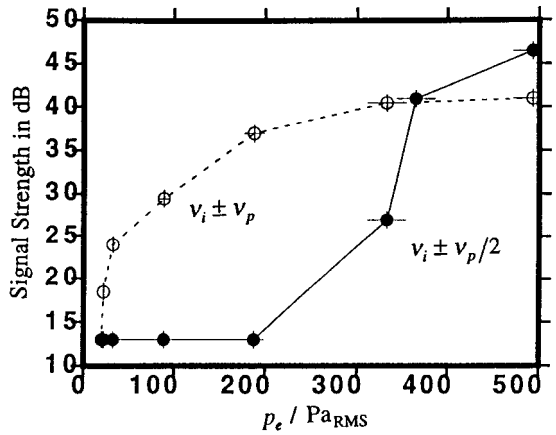



**Fig. 4.6:** Amplitude of sidebands versus the excitation for a bubble resonant at 4.05 kHz.

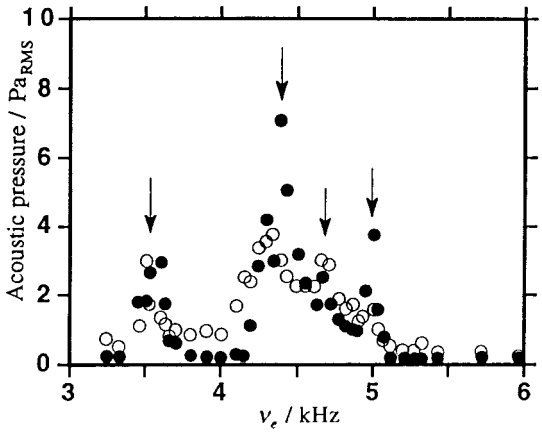



**Fig. 4.7:** Frequency response claimed for an array of four bubbles. (Solid points are at $\nu_i \pm \nu_e/2$, hollow at $\nu_i \pm \nu_e$).Data are from Leighton *et al* 1991a.

Better instrumentation, elucidation of origin of subharmonic modulation, and a solution to the problem of the great variability between experiments were needed.

## IV.2. THE INSTRUMENTATION

### IV.2.1. REQUIREMENTS

The specifications of the signal to be processed are shown in the table below. The 'Preliminary' column gives the original estimates. These were based on results like figure 4.3. The range of modulation frequencies was chosen to cover the natural frequencies of bubbles which would attach to a greased 0.5 mm diameter wire. Output variations of ~0.03 s were intended to be detectable so that the system could be applied to a stream of rising bubbles. The main problems were the variability of $\nu_i$, the small degree of modulation, the asymmetry of the sidebands and the low signal-to-noise ratio. Because $\nu_i$ could vary by ~1 kHz in ten minutes (the Therasonic 1030 was not designed as a measuring tool) the possibility of detecting each sideband by multiplying the signal by a separate carefully tuned fixed reference was not applicable. The small degree of modulation and the relative closeness of the sidebands to the $\nu_i$ carrier precluded direct bandpass filtering of each sideband. The asymmetry of the sidebands would be a complication if demodulating by $\nu_i$ which superimposes $\nu_i + \nu_e/2$ and $\nu_i - \nu_e/2$ etc.. The low signal-to-noise ratio made the electronic design seriously difficult (the ratios in the table are at only the frequencies of the peaks; the peaks appeared to be ~1 kHz wide but the noise stretched to beyond 10 MHz so the signal to noise ratios as normally defined are ~40 dB lower.)

| | Preliminary | Eventual |
|---|---|---|
| Modulation fraction | $\lesssim$ -50 dB | $\lesssim$ -5 dB |
| Hydrophone output | ~5 $mV_{pp}$ | ~50 $mV_{pp}$ |
| Modulation frequency | 1-10 kHz | 0.1-1 kHz and 2-8 kHz |
| Imaging frequency | 3.35 MHz | 3.35 MHz |
| Signal to noise ratio | 10-20 dB | up to 40 dB |
| Asymmetry of sidebands | up to 20 dB | not a problem |
| Detect variations of | 30 Hz (bubble flow) | 30 Hz (erratic behaviour) |

The signal processing instrumentation was built to meet the requirements implied by 'Preliminary' column in the above table. Once the instrumentation was functioning, it was possible to investigate subharmonic modulation further and optimise the effect to produce a much clearer modulation signal. The requirements which would have been set if this optimisation had been possible before the electronic design stage are given in the column headed 'Eventual'.

### IV.2.2. EQUIVALENT REPRESENTATIONS OF MODULATION

Explanation of both the instrumentation and the results will be simplified by first clearly stating the relationships between different representations of amplitude modulation. To save repeated writing of $2\pi$, angular frequencies $\omega$ instead of conventional frequencies $\nu$ will be temporally used. Note that the mathematics of this section is applicable to modulation in general not just ultrasound modulation. (The symbols used are borrowed from the physical sections – hopefully the similarities will aid comprehension rather than confuse it.)

Any oscillation $\Psi$ which consists of two sidebands of amplitudes $q_{-1}$ and $q_{+1}$ some distance, e.g. $\omega_e$, from a centre frequency, e.g. $\omega_i$, is

$$\Psi = q_{-1}\sin((\omega_i - \omega_e)t + \Theta_{-1}) + q_{+1}\sin((\omega_i + \omega_e)t + \Theta_{+1}) \qquad \{4.1\}$$

where $\Theta_{-1}$ and $\Theta_{+1}$ specify the phases. This is how a spectrum analyser presents modulation.

Equivalently, it can be thought of as the sum of two separate oscillations of amplitudes $q_\alpha$ and $q_\beta$, each of which is simple modulation at $\omega_e$ of a carrier at $\omega_i$:

$$\Psi = q_{1\alpha}\sin(\omega_e t + \Theta_{1e})\cos(\omega_i + \Theta_{1i}) + q_{1\beta}\cos(\omega_e t + \Theta_{1e})\sin(\omega_i + \Theta_{1i}). \qquad \{4.2\}$$

This is probably a more instructive way to represent modulation. The parameters are related by:

$$q_{1\alpha} = q_{+1} + q_{-1}, \qquad \{4.3\}$$

$$q_{1\beta} = q_{+1} - q_{-1}, \qquad \{4.4\}$$

$$2\Theta_{1i} = \Theta_{+1} + \Theta_{-1}, \quad \{4.5\}$$

$$2\Theta_{1e} = \Theta_{+1} - \Theta_{-1}. \quad \{4.6\}$$

For describing the instrumentation, a third representation will be useful;

$$\Psi = q_{1A} \sin(\omega_e t + \Theta_{1A}) \sin \omega_i t + q_{1B} \sin(\omega_e t + \Theta_{1B}) \cos \omega_i t \quad \{4.7\}$$

where:

$$q_{1A} \cos \Theta_{1A} = q_{-1} \sin \Theta_{-1} - q_{+1} \sin \Theta_{+1}, \quad \{4.8\}$$

$$q_{1A} \sin \Theta_{1A} = q_{+1} \cos \Theta_{+1} + q_{-1} \cos \Theta_{-1}, \quad \{4.9\}$$

$$q_{1B} \cos \Theta_{1B} = q_{+1} \cos \Theta_{+1} - q_{-1} \cos \Theta_{-1}, \quad \{4.10\}$$

$$q_{1B} \sin \Theta_{1B} = q_{-1} \sin \Theta_{-1} + q_{+1} \sin \Theta_{+1}. \quad \{4.11\}$$

A useful measure of the combined amplitude is $q_1$:

$$q_1 = \frac{\sqrt{{q_{-1}}^2 + {q_{+1}}^2}}{2} = \frac{\sqrt{{q_{1\alpha}}^2 + {q_{1\beta}}^2}}{8} = \frac{\sqrt{{q_{1A}}^2 + {q_{1B}}^2}}{8}. \quad \{4.12\}$$

If the modulation is simple with symmetric sidebands, these three representations reduce to

$$\Psi = q_{-1}(\sin((\omega_i - \omega_e)t + \Theta_{-1}) + \sin((\omega_i + \omega_e)t + \Theta_{+1})), \quad \{4.13\}$$

$$\Psi = q_{1\alpha} \sin(\omega_e t + \Theta_{1e}) \cos(\omega_i + \Theta_{1i}), \quad \{4.14\}$$

$$\Psi = (q_{1A} \sin \omega_i t + q_{1B} \cos \omega_i t) \sin(\omega_e t + \Theta_{1A}). \quad \{4.15\}$$

In the rest of this chapter, amplitudes denoted by $q$ with subscripts will be reserved for pressure amplitudes caused by bubbles. Symbols consisting of $S$ with similar subscripts ($S_1, S_{1A}, S_{1B}$ etc.) will denote the output signals of the devices proportional to the corresponding pressure $q$. Of course, the pressure amplitudes can be obtained from these by calibration and will be done so whenever necessary. Sidebands at other separations will be denoted by replacing the '1' in the subscript appropriately ($q_{1/2}, q_{-1/2}, S_{1/2A}$ etc. for $\omega_i \pm \omega_e/2$ and $q_2, q_{+2}, S_{2A}$ etc. for $\omega_i \pm 2\omega_e$).

### IV.2.3. INSTRUMENTATION MECHANICS

The Mylar® speaker used in the preliminary experiments was replaced by the Gearing & Watson UW60 speaker used for the previous two chapters. The

Therasonic 1030 was out of production and the current model, the Therasonic 1032, has a different oscillator which was found to give strong sidebands at multiples of 0.5 kHz rendering it useless for this work. The Therasonic 1030 used in the preliminary experiments was purchased from Addenbrooke's Hospital, repaired, and modified by the addition of a $\nu_i$ reference output (see Appendix 1). Its transducer was placed underwater instead of outside the tank (figure 4.8). The Dapco hydrophone was also retained.

To retain consistency with the experiments on the Acoustic Bubble Capacitor and Acoustic Re-emission techniques, most of the experiments were performed on bubbles of 0.10 to 3.00 ml injected from a graduated syringe and held under a watchglass as in chapter III. Unless otherwise stated, the experiments were performed on air bubbles in water. Photographic plates 1 and 2 show the system in operation.

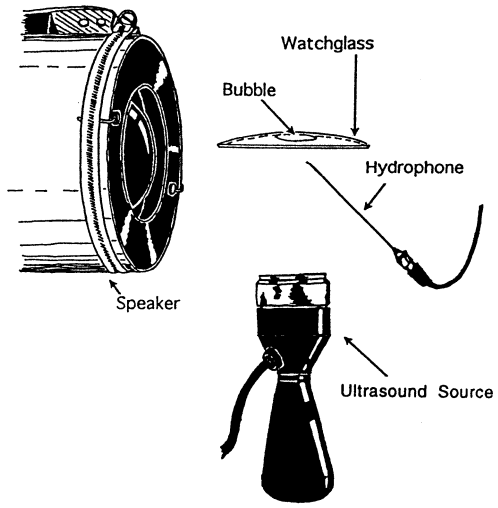



**Fig. 4.8:** Sketch of the sensors in place for a subharmonic modulation experiment.

### IV.2.4. INSTRUMENTATION ELECTRONICS

The setup for the experiments (figure 4.9) was broadly similar to that for acoustic re-emission (chapter III) with the addition of the ultrasound source, more oscilloscopes to simultaneously display several separated components of the output, and the signal processing electronics.

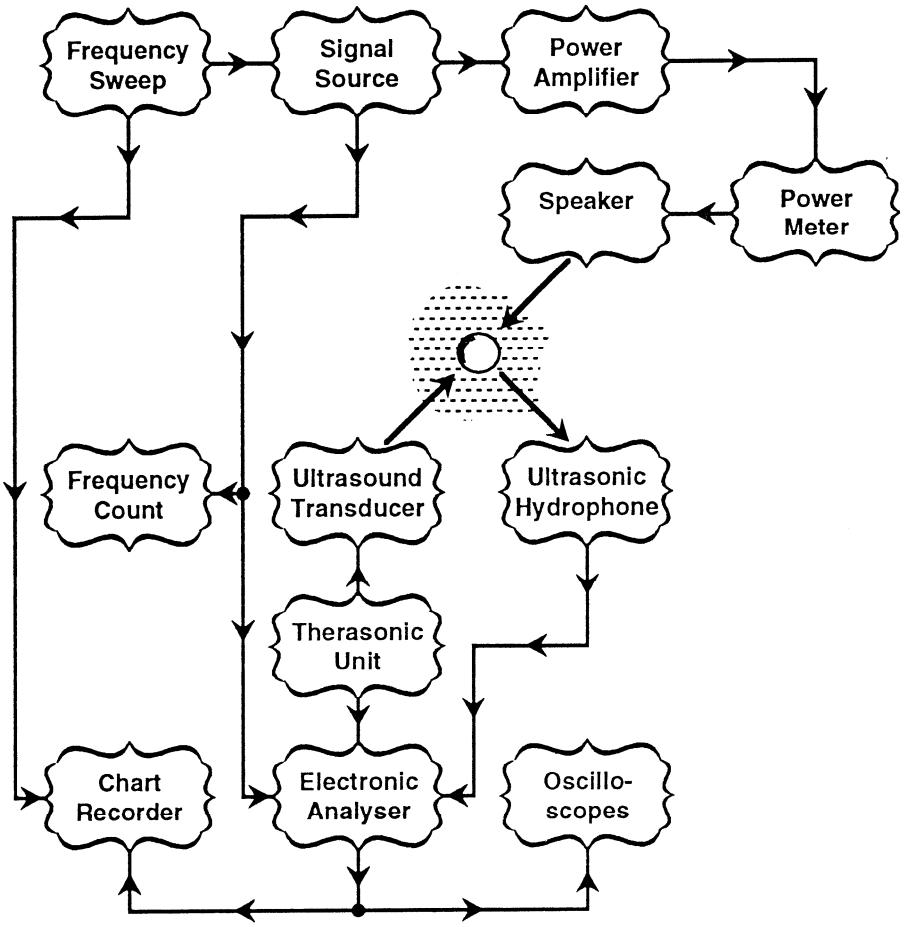



**Fig. 4.9:** Schematic of the subharmonic modulation analysis setup (greatly simplified).

The greatest simplification in figure 4.9 is the 'Electronic Analyser'. This is described in a little more detail here.

The signal from the hydrophone can include not only sidebands at $\omega_i \pm \omega_e/2$, $\omega_i \pm \omega_e$, $\omega_i \pm 3\omega_e/2$ etc. but the stronger carrier at $\omega_i$, electromagnetic pickup for the speaker at $\omega_e$, mains pickup at 50 Hz, radio pickup at tens of megahertz and general broadband noise. From this, the electronic analyser produces voltages proportional to ${q_1}^2$ and ${q_{1/2}}^2$.

The electronic analyser works by demodulation. The method is shown in figure 4.10. A signal is extracted from the Therasonic 1030 and is buffered and filtered to provide a clean $\omega_i$ reference. In the quadrature demodulator, the reference is split and phase shifted to $\sin\omega_i t$ and $\cos\omega_i t$. The amplified signal from the hydrophone is then multiplied by these two. A modulation component at $\omega_e$ in the signal, described in the form of {4.7}

$$S_{1A}\sin(\omega_e t + \Theta_{1A})\sin\omega_i t + S_{1B}\sin(\omega_e t + \Theta_{1B})\cos\omega_i t, \qquad \{4.16\}$$

becomes the two signals

$$\left\{\begin{matrix} S_{1A}\sin(\omega_e t+\Theta_{1A})\sin^2\omega_i t+\tfrac{1}{2}S_{1B}\sin(\omega_e t+\Theta_{1B})\sin 2\omega_i t \\ \tfrac{1}{2}S_{1A}\sin(\omega_e t+\Theta_{1A})\sin 2\omega_i t+S_{1B}\sin(\omega_e t+\Theta_{1B})\cos^2\omega_i t \end{matrix}\right\} \qquad \{4.17\}$$

when thus multiplied. Since the $\omega_i >> \omega_e$, components at $\omega_i$ and above can be filtered out. This is done by the pair of audio filters leaving

$$\left\{\begin{matrix} \tfrac{1}{2}S_{1A}\sin(\omega_e t+\Theta_{1A}) \\ \tfrac{1}{2}S_{1B}\sin(\omega_e t+\Theta_{1B}) \end{matrix}\right\}. \qquad \{4.18\}$$

Other modulation components, at $2\omega_e$ for example, are removed at this stage by tightly bandpass filtering at $\omega_e$. The filters which perform this are designed to follow changes in $\omega_e$ via a reference taken from the signal source. The sinusoid outputs at $\omega_e$ are then converted to RMS:

$$\left\{\begin{matrix} S_{1A}/2\sqrt{2} \\ S_{1B}/2\sqrt{2} \end{matrix}\right\}. \qquad \{4.19\}$$

Finally these are squared and added together to give, by {4.12} a single amplitude which does not depend on the phase of the modulation:

$$\left(S_{1A}{}^2/8\right)+\left(S_{1B}{}^2/8\right)=S_1{}^2. \qquad \{4.20\}$$

As well as the square of the modulation amplitude $S_1{}^2$, the voltages $S_{1A}$ and $S_{1B}$ were useful and could be recorded to show some phase information. The oscillatory signals of {4.18} were also usefully displayed on oscilloscopes. A separate set of filters centred on $\omega_e/2$ lead to outputs of $S_{1/2}$, $S_{1A}$ and $S_{1B}$.

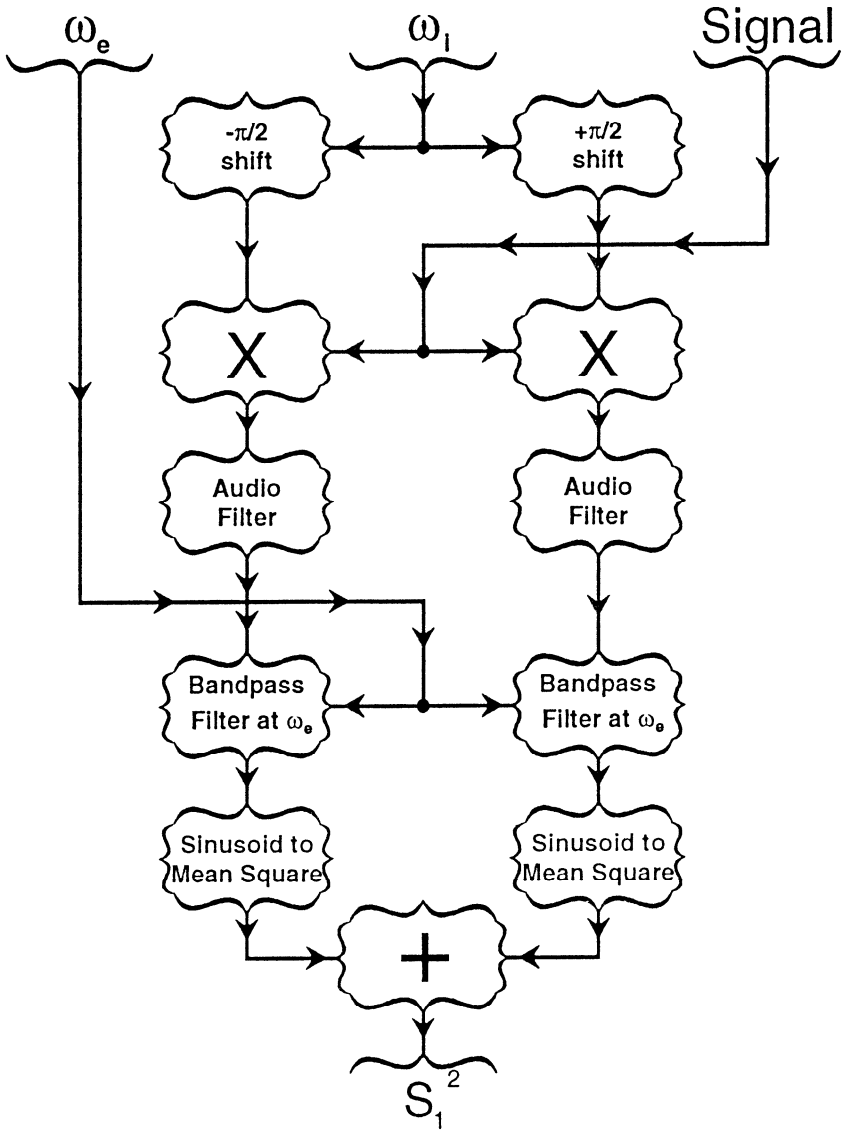



**Fig. 4.10:** The demodulation scheme.

The constituents of the electronic analyser are shown in figure 4.11 where each box represents an electronic circuit which is described in more detail in Appendix 1.

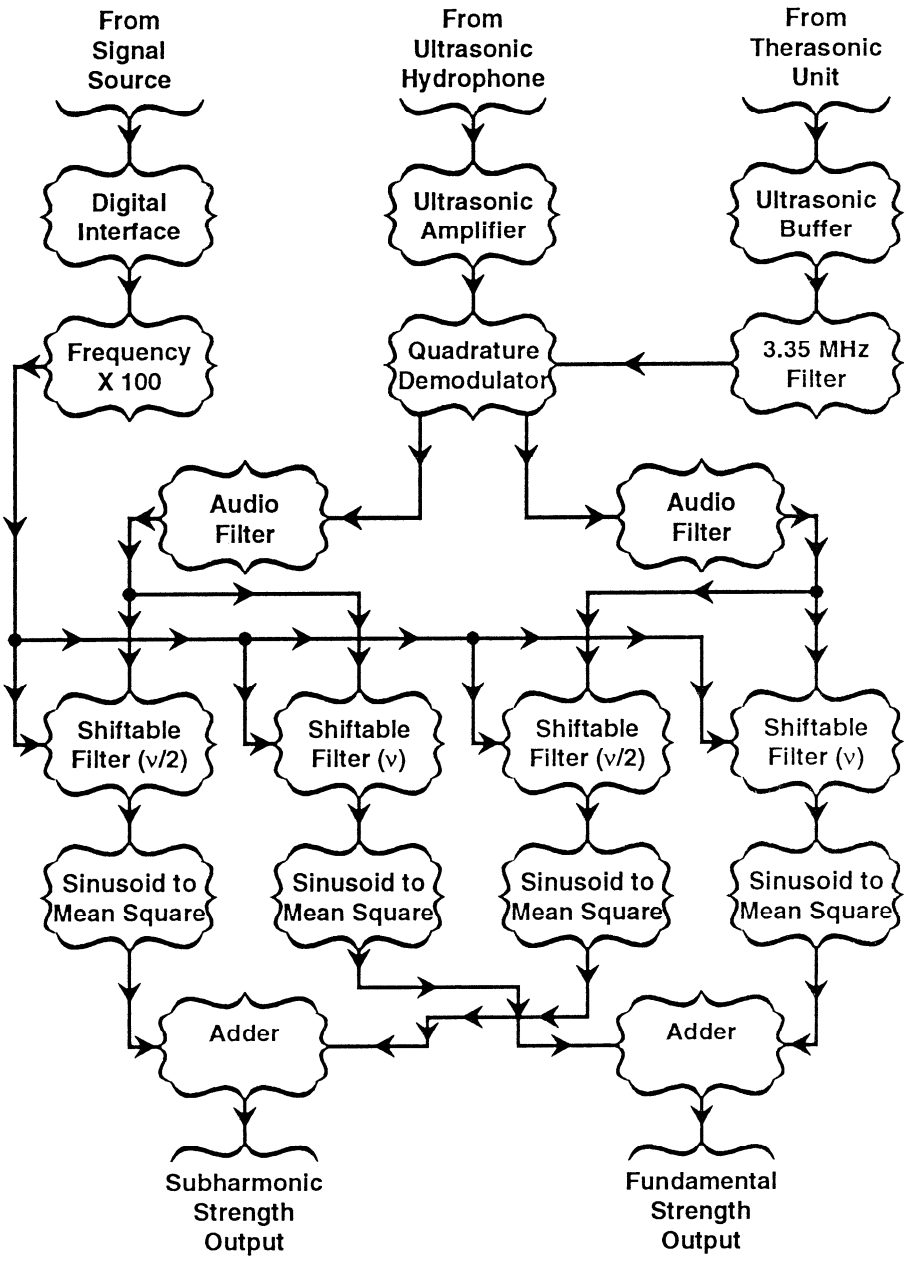



**Fig. 4.11:** Schematic of the electronic analysis system.

## IV.3. THE ORIGIN OF SUBHARMONIC MODULATION EXPLAINED

### IV.3.1. THE PROPOSED MECHANISM:

Recently, the subharmonic breathing oscillation mechanism has been brought into increasing doubt by the realisation that the experimental threshold sound pressure required for the subharmonic modulation ($\lesssim 10^2$ Pa) was far smaller than that theoretically expected for bubbles in water at atmospheric pressure to oscillate subharmonically (~$3\times10^4$ Pa based on Eller and Flynn 1969).

The actual mechanism is due to the surface waves. Though these radiate little sound at $\nu_e/2$ themselves, their wavelength is of the same order of magnitude as the ultrasound wavelength used. Therefore, they affect the spatial distribution of scattered ultrasound. As the surface shape oscillates at $\nu_e/2$, so does the amplitude of ultrasound scattered to any particular point in the liquid.

Figure 4.12 explains this diagrammatically. The hydrophone detects the sound at a point. The amplitude of ultrasound at any particular point depends on the shape of the bubble which scatters it. The figure shows specular reflection varying with the bubble shape over two cycles of the forcing sound. In reality, diffraction and interference were also important.

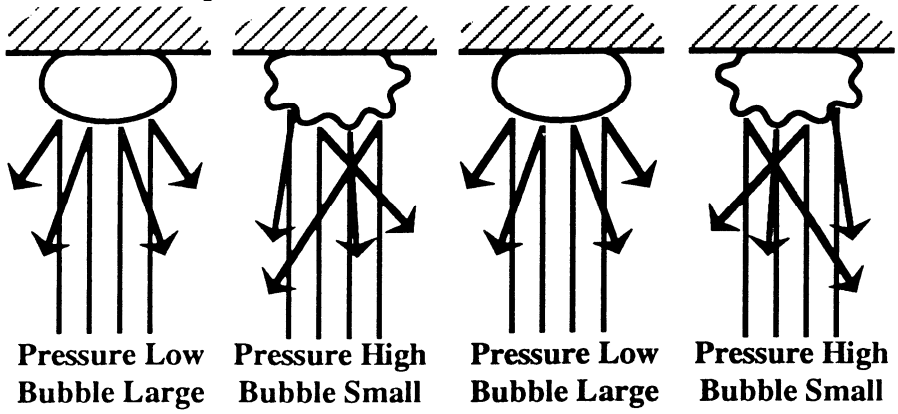



**Fig. 4.12:** Simplified explanatory diagram for subharmonic modulation.
(Note that the second and fourth parts of this figure are different.)

### IV.3.2. THE EXPERIMENTAL EVIDENCE:

The most convincing evidence for this mechanism is that subharmonic modulation and surface oscillations *always* occur together. When the ultrasound is being modulated at $\nu_e/2$ by a bubble, the bubble looks shimmery because of surface waves and vice versa. Though, of course, if the hydrophone is too far from the bubble, the modulation may be too weak to detect with a particular analysis system.

One of the many possible illustrative examples of the coincidence of shimmer with subharmonic modulation is presented in figure 4.13. The experimentally found acoustic pressure thresholds for subharmonic modulation (points) at various frequencies for a 0.90 ml air bubble in water are superimposed on the observed shimmer threshold (line) – the correlation is obvious. The lowest threshold is, understandably, at the bubble's breathing mode resonance $\nu_0$. Figure 4.14 is an expansion of this region of figure 4.13. The instrumentation is as described in the previous section. Shimmer was easily detected by naked eye.

Below the shimmer thresholds only modulation at $\nu_e$ from the breathing mode is observed, not at $\nu_e/2$.

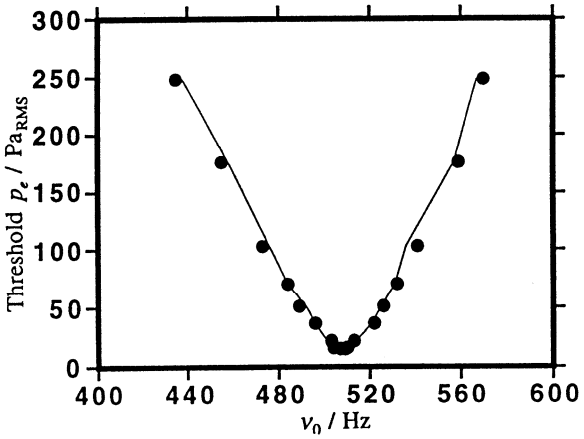



**Fig. 4.13:** Threshold of subharmonic modulation (points) and shimmer (line) for a 0.90 ml bubble as a function of frequency.

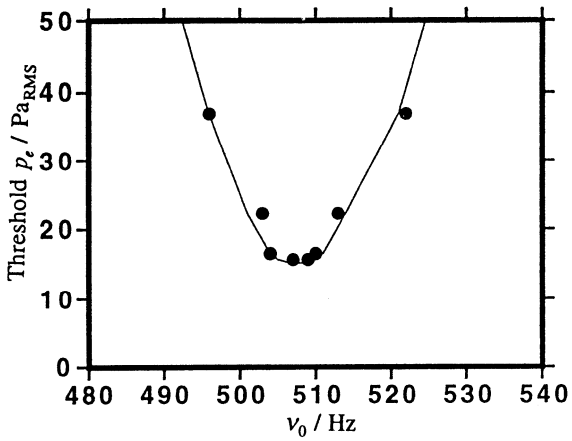



**Fig. 4.14:** Detail of 4.13 near resonance.

In addition, period doubling in the bubble's breathing mode can be demonstrated not to occur by monitoring the re-emitted sound at $\nu_e/2$ and $\nu_e$ using a hydrophone which is sensitive to audio frequencies (Brüel & Kjær 8103). Breathing mode oscillations emit sound and substantial re-emission at $\nu_e$ was detectable when $\nu_e = \nu_0$ but $\nu_e/2$ emission was absent implying absence of a $\nu_e/2$ component in the breathing mode oscillation.

When $p_e$ was raised, the $\nu_e/2$ modulation became comparable to the $\nu_e$ modulation before the $2\nu_e$ modulation did. This would not be expected from non-linear breathing mode oscillations but is totally consistent a surface oscillation mechanism.

Further evidence includes the inability to detect subharmonic modulation when the water was replaced by vegetable oil. The oil's viscosity ($\mu$ = 0.2 to 0.9 Pa s) was sufficient to raise the surface oscillation threshold above the acoustic pressure available but was insufficient to significantly increase the breathing mode damping.

Photographic plate 3 shows surface waves on a 3 ml bubble held under a brass block with various illuminations. With a long exposure and continuous lighting (Plate 2a) the nodes and antinodes of the surface waves are apparent whereas illumination by a single flash (Plate 2b) reveals the surface waves themselves. Strobe illumination and a long exposure time at $\nu_e$ (Plate 2c) just shows the nodal pattern but strobe lighting at $\nu_e/2$ (Plate 2d) 'freezes' the wave motion because the surface waves are at $\nu_e/2$.

The surface waves occur most readily when $\nu_e = \nu_0$ because a spherical cavity shape is somewhat unstable during the collapse half of a bubble's oscillatory cycle. That the surface modes closest to $\nu_e/2$ in natural frequency are preferentially excited can be explained most succinctly by Bernoulli's theorem which implies that a liquid gaining a speed $v$ experiences a pressure drop proportional to $v^2$. This is the mechanism by which a surface wave interacts with the excitation sound pressure since surface waves cause no net compression. Squaring a sinusoidal oscillation doubles its frequency so a surface oscillation which interacts with a pressure variation at $\nu_e$ has a surface displacement oscillating at half that, $\nu_e/2$. A more graphical explanation derived from Faraday 1831 is that humps of water projecting into the bubble are flattened out by the diverging radial flow as the bubble expands. The inertia of the water flowing sideways to flatten the humps keeps the water flowing that way as the bubble collapses so the next set of humps form between the position of the humps in the previous forcing period. This repeats so giving the humps (surface oscillations) twice the period of the breathing mode.

### IV.3.3. IMPLICATIONS:

For those trying to use subharmonic modulation to size bubbles, knowledge of this mechanism is important. The often erratic nature of surface oscillations, especially when driven significantly at above the threshold acoustic pressure, explain the erratic variations of modulation amplitudes which have been found. The apparent asymmetry of the sidebands on the early spectra, such as figure 4.3, were due to the amplitude varying whilst the spectrum analyser was scanning through the frequencies. Hope for overcoming these problems is seriously diminished by the revelation that the cause is physical rather than in the instrumentation.

## IV.4. CHARACTERISING THE SUBHARMONIC MODULATION

### IV.4.1. THE SOUND FREQUENCY DEPENDENCIES

The change in the modulation behaviour as the excitation frequency $\nu_e$ varies is displayed in figures 4.15 to 4.19. The arrows in these figures show the frequencies $\nu_i \pm \nu_e/2$. The ultrasonic hydrophone was 9 mm below a 0.3 ml air bubble ($\nu_0$ = 692 Hz) which was held under a watchglass. The excitation pressure was well above the threshold for shimmer at resonance. When excited well below the resonant frequency ($\nu_e$ = 626 Hz), there was no shimmer visible and the ultrasound spectrum showed only the central frequency $\nu_i$ and weak modulation sidebands at $\nu_i \pm \nu_e$ (figure 4.15). When closer to resonance ($\nu_e$ = 658 Hz) but still not shimmering, the $\nu_i \pm \nu_e$ sidebands were more substantial and the $\nu_i \pm 2\nu_e$ sidebands arising from non-linearities in the breathing mode oscillations were visible (figure 4.16). At the value of $\nu_e$ where shimmer was first observed ($\nu_e$ = 668 Hz), the $\nu_i \pm \nu_e/2$ sidebands first appeared (figure 4.17). When closer still to $\nu_0$ ($\nu_e$ = 674 Hz) and shimmering well, the $\nu_i \pm \nu_e/2$ sidebands were stronger even than the $\nu_i \pm 2\nu_e$ ones (figure 4.18). When at resonance ($\nu_e = \nu_0$) and shimmering erratically, a large number of sidebands at $\nu_i \pm n\nu_e/2$, n = 1, 2, 3, …, were present; their amplitudes varied whilst the spectrum was being recorded so the sidebands looked asymmetrical (figure 4.19). Increasing $\nu_e$ further caused the form of the spectrum to pass back through these stages in reverse.

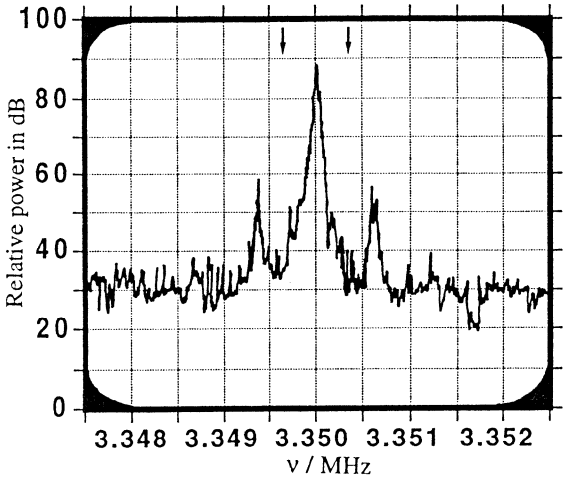



**Fig. 4.15:** Spectrum when excited well below the resonant frequency.

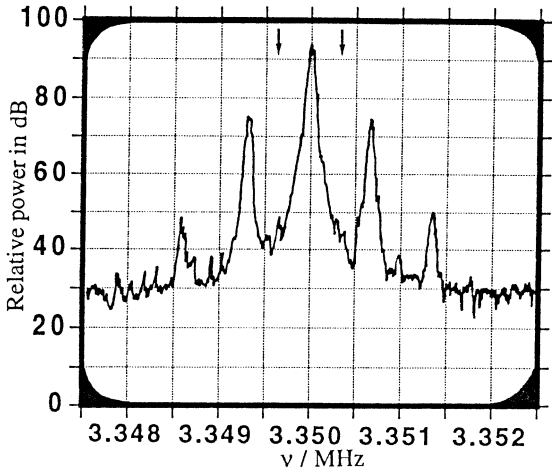



**Fig. 4.16:** Spectrum when excited just below the frequency needed for shimmer.

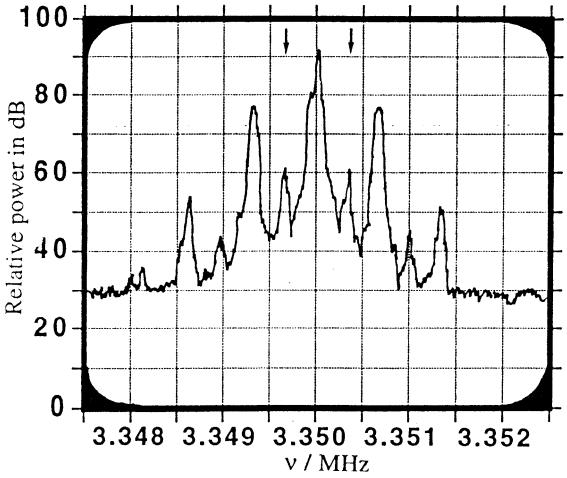



**Fig. 4.17:** Spectrum when excited at the frequency needed for shimmer.

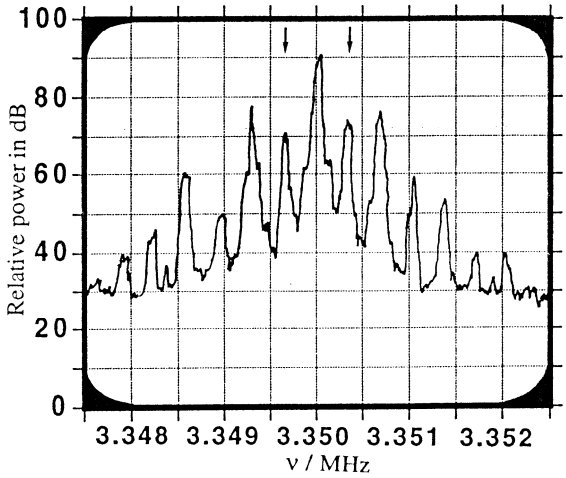



**Fig. 4.18:** Spectrum when excited just above the frequency needed for shimmer.

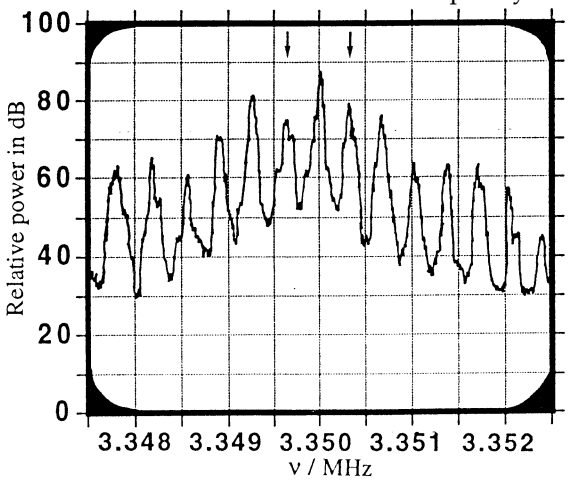



**Fig. 4.19:** Spectrum when excited at the resonant frequency.

dThe following frequency responses for modulation at $\nu_e$ and $\nu_e/2$ were obtained by use of a pair of two channel chart recorders to record $S_{1A}$, $S_{1B}$, $S_{1/2A}$ and $S_{1/2B}$ simultaneously as $\nu_e$ was swept. Figures 4.20 and 4.21 each show the four simultaneous outputs for a 0.90 ml air bubble. Figure 4.20 was

recorded with $p_e$ insufficient to excite surface waves even when $\nu_e = \nu_0$ so $S_{1/2A} = S_{1A} = 0$ throughout. For figure 4.21, $p_e$ was high enough to produce surface waves so all four traces have peaks where $\nu_e \approx \nu_0$.

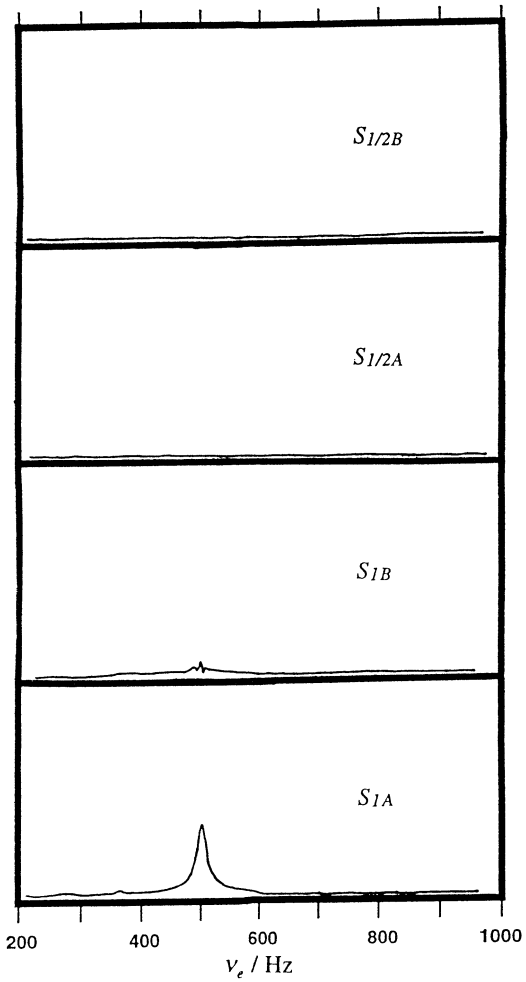



**Fig. 4.20:** Spectrum when excited at the resonant frequency.

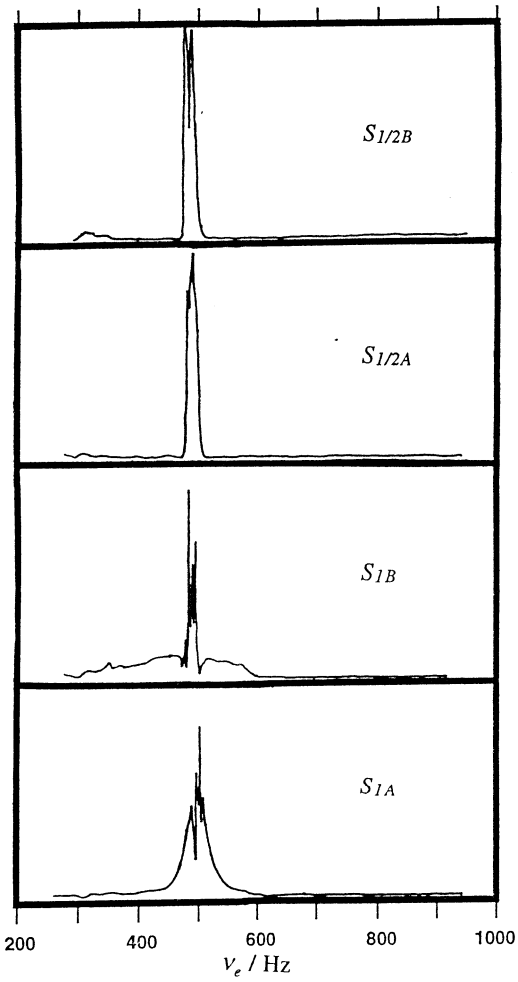



**Fig. 4.21:** Simultaneous frequency responses of four separate modulation components. Excitation pressure above shimmer threshold.

The combined squared modulation amplitudes, $S_1^2$ and $S_{1/2}^2$, would be simpler to use for sizing bubbles because they are insensitive to phase changes in the modulation. The $S_1^2$ and $S_{1/2}^2$ frequency responses of three individual bubbles of different sizes are shown in figure 4.22. The response in the absence of bubbles would not be visible on this scale. Since the geometry of the bubble holder was almost identical to those used in section III.1.2 for testing the acoustic re-emission method, the relationships between $\nu_0$, the bubble volume and gas type are likewise very similar. The variation of $\nu_0$ with bubble volume found by subharmonic modulation is essentially identical to figures 3.5 and 3.6.

The fine structure of the peaks in figures 4.20 to 4.22 were not repeatable features but were effectively random ones caused by the erratic variations of the surface oscillations during the frequency sweep. This erratic behaviour seriously reduces the potential of this technique for reliable bubble sizing. For example, figure 4.23 is the result of slowing the frequency sweep rate to a tenth of the rate used for all other figures (the normal rate was 1 kHz/min). Instead of expanding the detail of the peak, it allows time for more erratic variation which could easily be mistaken for the resonances of several neighbouring bubbles. Conversely, if the sweep rate was increased, the bubble response could be missed altogether.

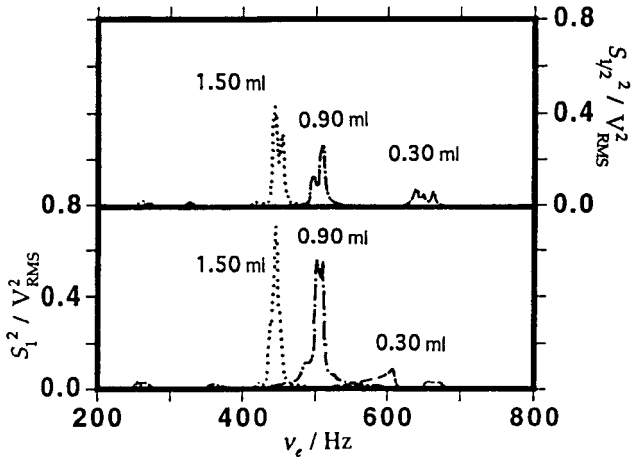



**Fig. 4.22:** Frequency responses of the squared amplitudes of modulation components for three different bubble sizes.

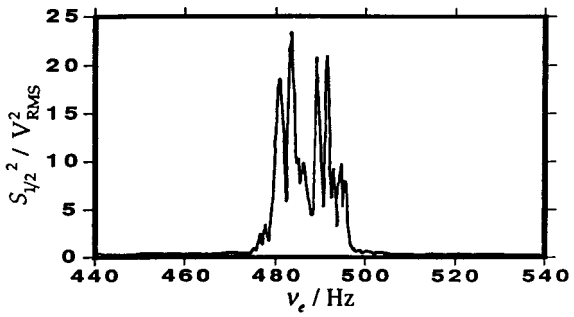



**Fig. 4.23:** Frequency responses of the square amplitudes of subharmonic modulation. The slow frequency sweep reveals erratic behaviour.

Subharmonic modulation does not crucially depend on the imaging frequency. Though $\nu_i$ = 3.35 MHz was used for all the experiments reported here, 1 MHz was found to work comparably well.

### IV.4.2. THE SOUND AMPLITUDE DEPENDENCE

Subharmonic modulation is a non-linear effect so its behaviour can depend upon the amplitudes of sound at $\nu_i$ and $\nu_e$ in a non-proportional manner. The main characteristic, the threshold with respect to the frequency $\nu_e$ and amplitude $p_e$ of the excitation, has already been described in section IV.2.2 and shown in figures 4.13 to 4.14.

The dependence upon the amplitude $p_i$ of the imaging sound is less interesting. If $p_i$ is sufficiently high to disturb the shape of the bubble through radiation pressure and streaming of the liquid then the threshold with respect to $p_e$ is slightly reduced. This is apparent in figure 4.24. The power emitted from the ultrasound source $W_i$, which is proportional to $p_i^2$, was recorded from the ultrasound source's built-in meter.

The threshold in $p_e$ increased with decreasing bubble size (figure 4.25).

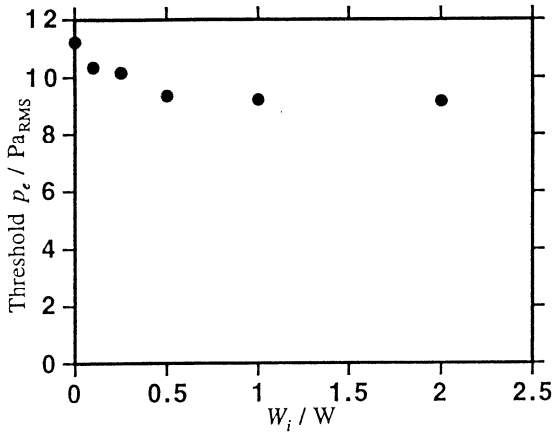



**Fig. 4.24:** Shimmer threshold with respect to excitation amplitude decreasing as the ultrasound power is increased. A 0.90 ml air bubble in water forced at resonance.

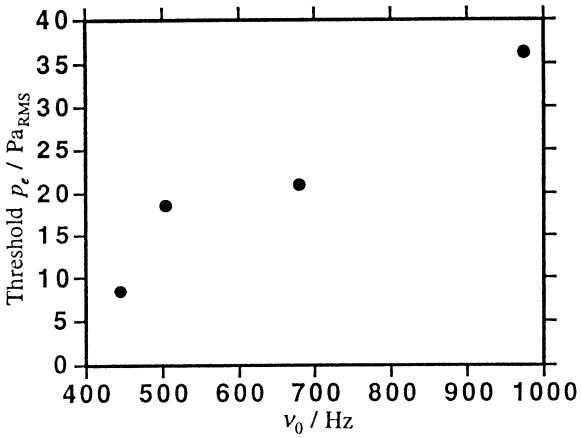



**Fig. 4.25:** Shimmer threshold with respect to excitation amplitude increasing as the bubble size decreases (i.e. resonant frequency rises). Various individual air bubbles in water.

The threshold in $p_e$ and the erratic variation in modulation strength are both demonstrated in figures 4.26 to 4.28. The data were from a 0.90 ml air bubble excited at its resonance at various $p_e$. Eight readings of the modulation percentage were recorded from the spectrum analyser at each $p_e$. Each cross on the figures represents either a single datum or more than one coincident data. The threshold at 18 $Pa_{RMS}$ for modulation at $\nu_e/2$ is clearly visible on 4.26. Figure 4.28 shows the threshold neighbourhood in more detail. The $\nu_e$ modulation (figure 4.27) exhibits no threshold, just a slight dip as the subharmonic effect comes into action.

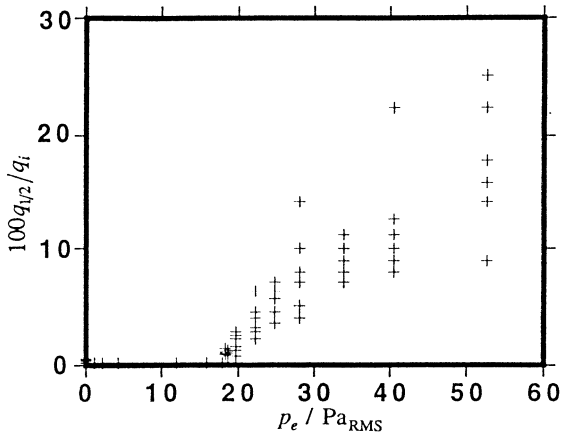



**Fig. 4.26:** Subharmonic modulation percentage versus excitation amplitude for 0.90 ml air bubble in water forced at resonance.

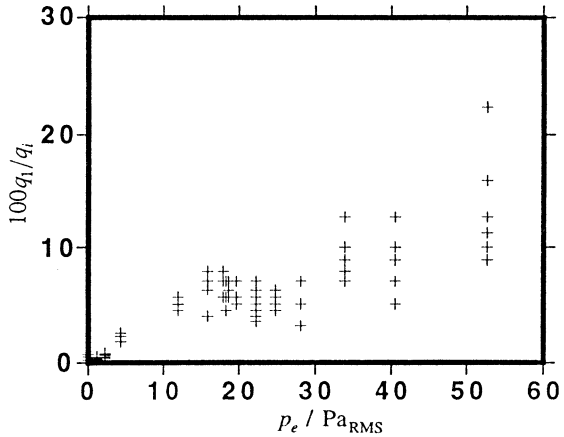



**Fig. 4.27:** Fundamental modulation percentage versus excitation amplitude for 0.90 ml air bubble in water forced at resonance.

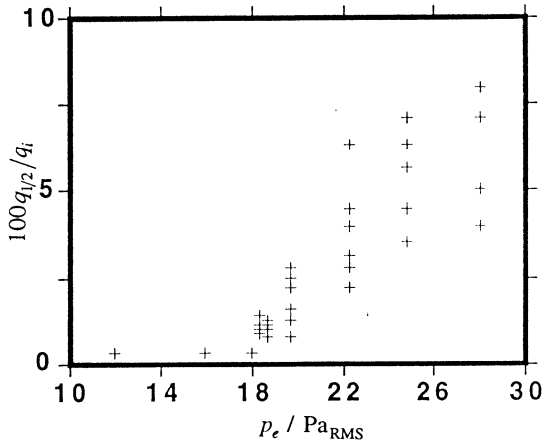



**Fig. 4.28:** Threshold detail from figure 4.26.

### IV.4.3. FURTHER DESCRIPTION OF THE ERRATIC BEHAVIOUR

The erratic modulation amplitudes caused by fluctuations of the surface oscillation have been mentioned earlier. Usually the variations appear to have little significant structure. Variations were observed on time scales from under 0.3 s to over a minute. A typical sample of the variation is reproduced as figure 4.29. The two traces, for $\nu_e/2$ and $\nu_e$ modulation, were simultaneously recorded for a 0.90 ml air bubble excited at 54 $Pa_{RMS}$.

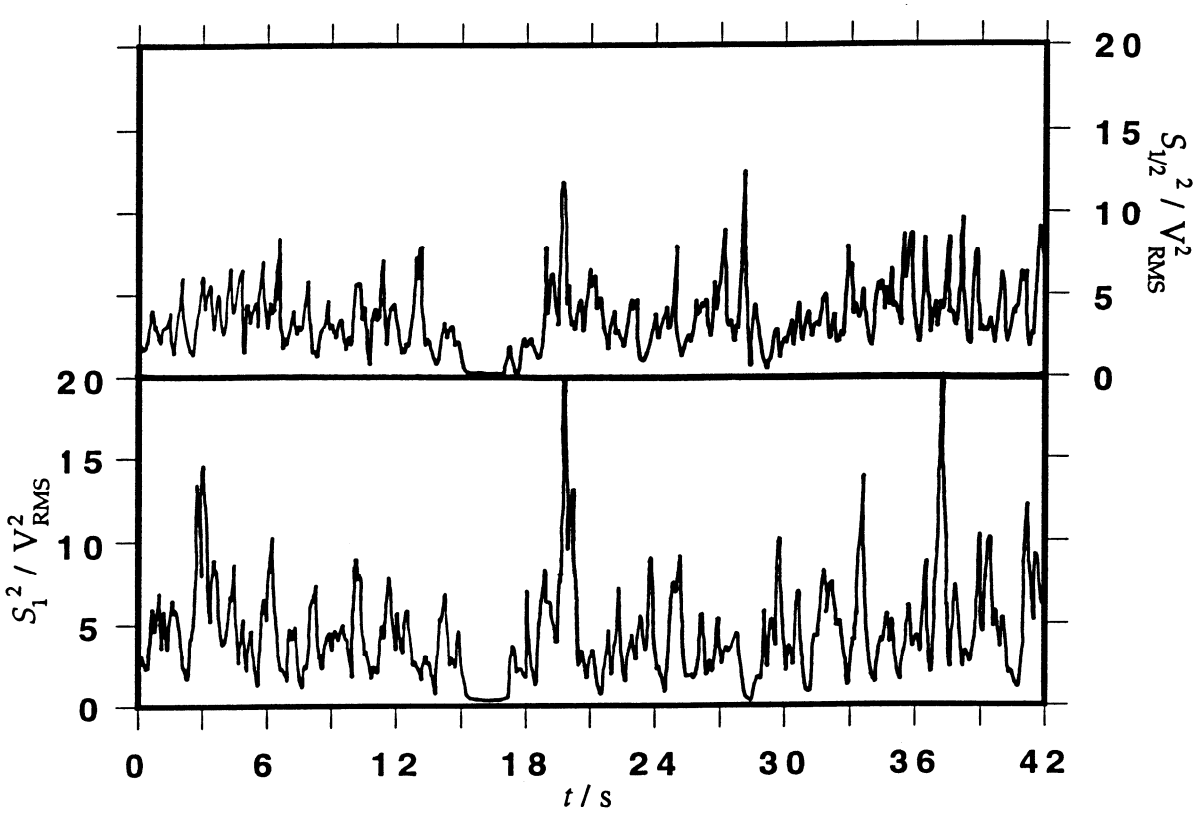



**Fig. 4.29:** Erratic temporal variation of modulation component amplitudes for a bubble excited well above its threshold.

A more interesting variation can occur provided that $p_e$ is only just above the threshold. Under this condition, the variation sometimes became quasiperiodic. A sample of quasiperiodic changes in $\nu_e/2$ modulation is reproduced as figure 4.30. The situation was the same as for figure 4.29 except that $p_e$ was reduced to 21 $\mathrm{Pa_{RMS}}$. The sample chosen shows the variation spontaneously settling from an nonperiodic state to a quasiperiodic one.

Coakley (1971) found that a periodic variation could occur in the strength of a subharmonic resulting from acoustic cavitation. Though R.C.Chivers insisted that Coakley's paper was refered to in this context, Coakely's work involved subharmonic emission not subharmonic modulation, which is the subject of this chapter, so it is largely irrelevant to the current topic.

The appearance of a bubble differs corresponding to whether the modulation varies nonperiodically or quasiperiodically. When nonperiodic, the pattern of nodes and antinodes of the shimmering surface jittered about haphazardly. When quasiperiodic, the pattern appeared to be almost static except for a slow rotational motion about the vertical axis of the bubble. The passage of each antinode through a position corresponded to a modulation amplitude oscillation (with period around 2 s).

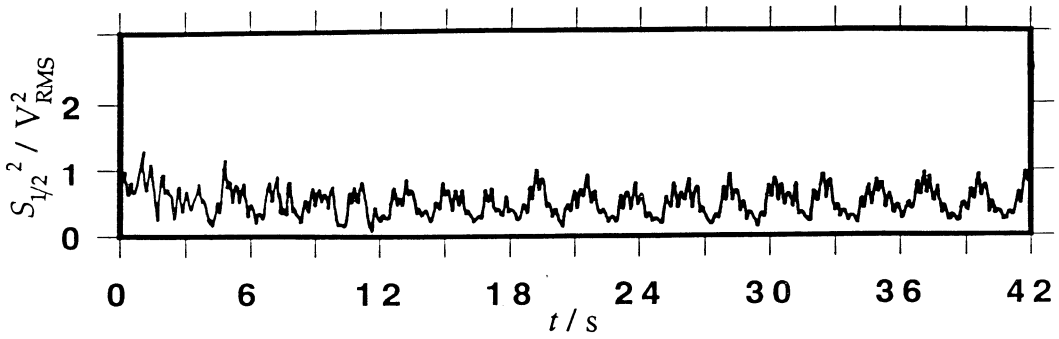



**Fig. 4.30:** Quasiperiodic temporal variation of modulation component amplitudes for a bubble excited just above its threshold.

The quasiperiodic state is easily overlooked because it only occurs for a small range of $p_e$ and $\nu_e$, and it can take tens of seconds to settle down. The domain of the parameter space over which it occurs for a 0.90 ml air bubble is shown below (figure 4.31). Except close to $\nu_0$, the transition as $p_e$ is raised is directly from no shimmer or subharmonic modulation below the threshold to nonperiodic erratic behaviour above it.

In a few cases when testing very close to the threshold, it has been possible to achieve a variation so slow (period ~10 s) that it almost appeared to be unvarying.

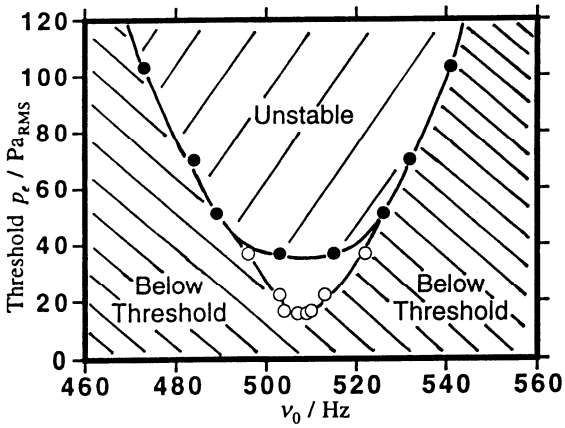



**Fig. 4.31:** The domain for quasiperiodic modulation (unshaded region) for a 0.90 ml bubble.

### IV.4.4. PHASE SHIFTS

As mentioned in chapter I, a similar system was investigated earlier but with only modulation at integer multiples of $\nu_e$ considered (Chapelon *et al* 1988). They found that the frequency response for a single bubble usually comprised two peaks rather than one. They correctly deduced "As the output is the result of the upper and lower sideband we suspected a phase difference in these signals." (Chapelon *et al* 1988) and cured it by a quadrature demodulation scheme. The origin of the phase shift between sidebands was not explained.

The explanation is simple if the effect is considered as a modulation of a $\nu_i$ carrier at $\nu_e$ rather than a pair of sidebands at $\nu_i \pm \nu_e$. In this representation, antiphase sidebands (if adopting the demodulation system of Chapelon *et al* 1988) becomes simply a phase difference of $\pi/2$ rad between the $\nu_e$ modulation envelope and the excitation sound. This is the $\pi/2$ rad shift expected for a simple harmonic oscillator excited at resonance.

Figure 4.32 shows this occurring in the frequency response of a 0.90 ml air bubble. The two quadrature demodulated components $S_{1A}$ and $S_{1B}$ were recorded simultaneously. The excitation amplitude was below the shimmer threshold so there was no subharmonic modulation and the structure of the response was not erratic but repeatable. The hydrophone was positioned so that most of the response was recorded on the upper trace but when $\nu_e = \nu_0$ that trace dipped as the response transferred to the other trace.

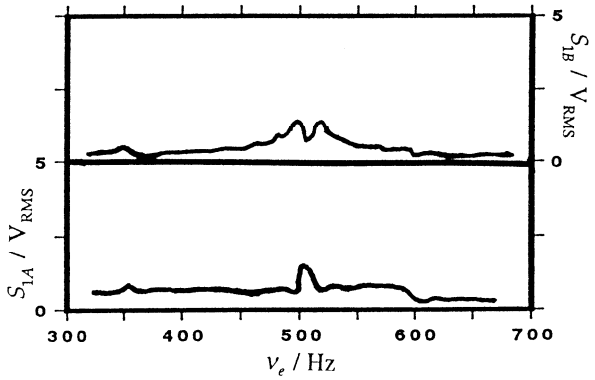



**Fig. 4.32:** The effect of phase change at resonance upon the demodulation components.

### IV.4.5. BUBBLES ON WIRES

This study started with bubbles held on wires. Once the electronic analysis system was functioning and the origin of subharmonic modulation had been explained, the early experiments were repeated more successfully.

As before, air bubbles were pippetted onto a waxed wire and later measured by travelling microscope. This time, the wire was horizontal (an innovation of A.D.Phelps) which increased the time which the bubbles stayed attached. Figure 4.33 shows the dependence of $\nu_0$ on the bubble volume. These volumes were much less than those bubbles used for the studies in chapters II and III. Figure 4.34 is the corresponding graph of $\nu_0$ against the reciprocal of the effective radius. The four largest bubble sizes had greater diameters than had the wire (1.4 mm) so those bubbles behaved almost as if they were in an unbounded liquid. This explains why the line through those points on figure 4.34 fits so well with Minnaert's prediction {1.16}. The straight line through the origin has gradient $3.20 \pm 0.03$ Hz m which matches the predicted 3.24 Hz m.

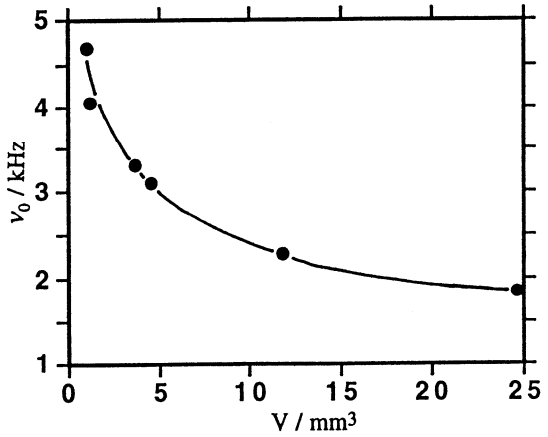



**Fig. 4.33:** Resonant frequency as a function of bubble volume for air bubbles attached to a wire in water.

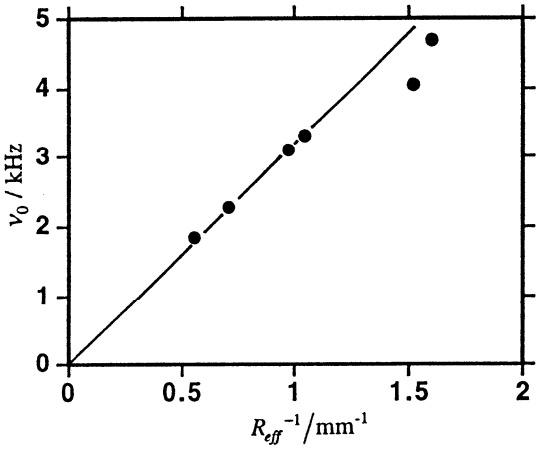



**Fig. 4.34:** Resonant frequency versus the bubble's effective radii reciprocated.

As found for the larger bubbles of figures 4.13 and 4.14, the shimmer and subharmonic modulation thresholds were the same. The plot of this (figure 4.35) is for a bubble resonant at 2.74 kHz. The apparent skew of the threshold curve is an artefact of calibrating the excitation pressure only at $\nu_0$. No regular dependence was found between the threshold when forced at resonance and the size of the bubble (figure 4.36).

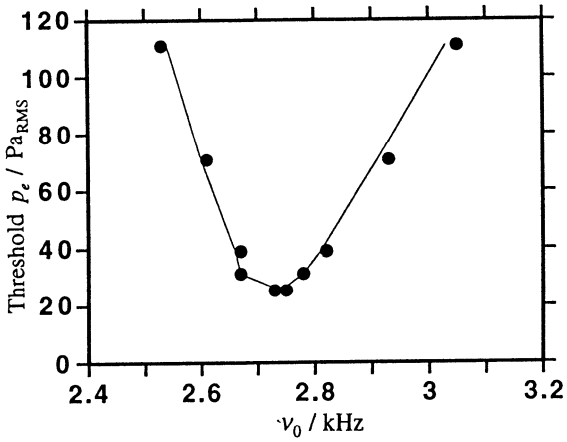



**Fig. 4.35:** Threshold of subharmonic modulation (points) and shimmer (line) for a bubble on a wire as function of excitation frequency.

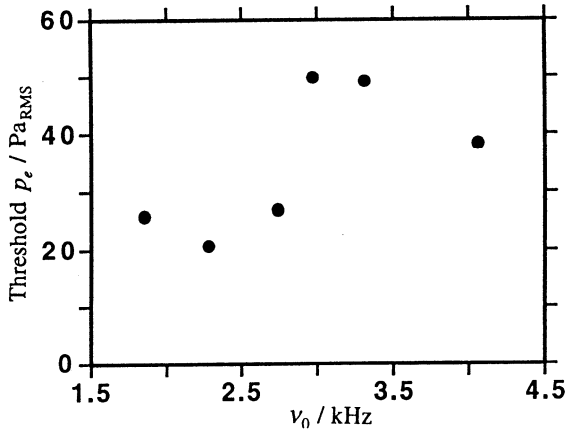



**Fig. 4.36:** Excitation threshold for subharmonic modulation for different size bubbles versus their resonant frequencies.

Because subharmonic modulation is best detected with the hydrophone very close to bubbles, it is difficult to obtain a frequency response of a bubble array unless the bubbles are small. Figure 4.37 was obtained from an array of three bubbles on a wire. The hydrophone was 4 mm from the smallest bubble and 11 mm from the other two. Three peaks are just visible. Several traces had to be made to guard against false multiple peaks from the erratic amplitude variations. Each peak corresponded visually to a different one of the three bubbles shimmering.

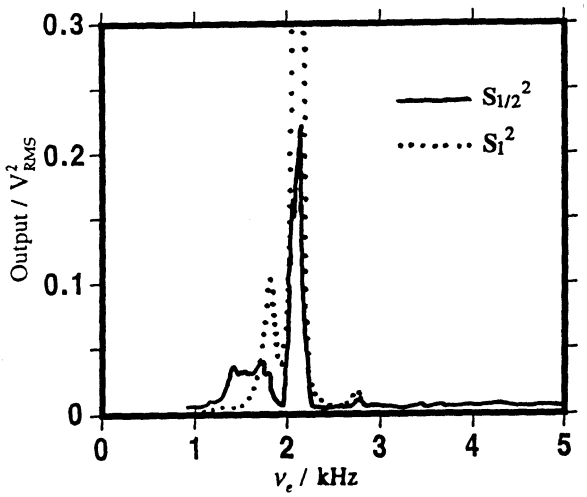



**Fig. 4.37:** Frequency responses for three bubbles on a wire.

## IV.5. CONCLUSION

Subharmonic modulation is not a good technique for measuring bubble sizes. It has many drawbacks:

(a) It does not work at low sound pressures below a bubble's shimmer threshold.

(b) At higher sound pressures the range of excitation frequencies giving subharmonic modulation is increased so the sizing accuracy is reduced. Keeping just above the threshold is not a solution because the threshold depends on the bubble size.

(c) The threshold increases greatly if the liquid is viscous.

(d) The detected modulation amplitude varies highly for displacements of the order of the ultrasound wavelength and falls rapidly as the hydrophone is moved away from the bubble.

(e) The modulation strength varies erratically with time so bubble resonances can easily be mistaken for several separate resonances or missed completely. The quasiperiodic state takes several seconds to settle after, for example, hitting the table on which the tank rested so it is probably irrelevant for bubbles in flow.

(f) The random variations also prevent the peak amplitudes being used to determine numbers of equal-sized bubble present as was originally hoped.

(g) Bubbles in flow lead to other problems. The flow causes natural shape oscillations at frequencies other than half the breathing mode resonance which give spurious modulations. Therefore the excitation pressure is required to be even higher for the subharmonic modulation to be noticeable.

The analogue electronic signal processing system was difficult to design but worked well; the random nature of the output was not from the instrumentation but was intrinsic to subharmonic modulation.

The origin of subharmonic modulation has been discovered – implications of this have been mentioned in section IV.3.3. The mechanism was conceived whilst testing the signal processing system. The perfect correspondence of small erratic changes in shimmer and amplitude changes in the modulation components strongly indicated surface waves as the mechanism. This is an example of real-time analogue instrumentation being more advantageous for investigation than merely digitising a signal and later analysing it computationally.

# CONCLUSIONS

This project has demonstrated that bubble sizes can be measured by means of acoustic excitation and use of the breathing-mode resonance. The three techniques studied in detail have all been shown to work though their abilities differ considerably. The conclusions about them are summarised together below with a few suggestions for further development.

## C.1 COMPARISON BETWEEN THE TECHNIQUES

The Acoustic Bubble Capacitor is electronically and mechanically simple. It measures the resonant frequencies of individual bubbles reproducibly to within 1 % and so, with suitable calibration, could measure effective radii similarly well. This technique is wholly novel and demonstrably works so a patent (number 9406341.9) has been filed with Cambridge University as intellectual property right holder, PSTI as potential royalty receiver, and A.J.Walton and myself as co-inventors.

The acoustic re-emission technique has been shown to work similarly well. It needs only components which are readily commercial available. It is, of course, more sensitive to extraneous acoustic noise than the ABC but less sensitive to extraneous electrical noise; in either case most of the noise could be filtered out in practice.

Regrettably, the subharmonic modulation technique which originally inspired this whole project cannot justifiably be said to work well as a method of bubble sizing. The erratic variations in the amplitude of the subharmonic modulation seriously reduce its utility for bubble sizing. The necessity of high excitation sound pressures is another drawback. Nevertheless, some discoveries have been made which are interesting from a physical viewpoint. These include the threshold behaviour, the quasi-periodic state in the erratic behaviour, and the mechanism of subharmonic modulation.

The figure below shows superimposed traces from applying the three techniques to 0.90 ml bubbles. The peak for the ABC trace is at a lower frequency that the other two simply because the shape of the ABC differed from that of the watchglass which retained the bubble in the other two cases. The subharmonic modulation trace shows a sharper peak with less response away from resonance than the other traces but the peak exhibits a spurious double structure resulting from the erratic behaviour.

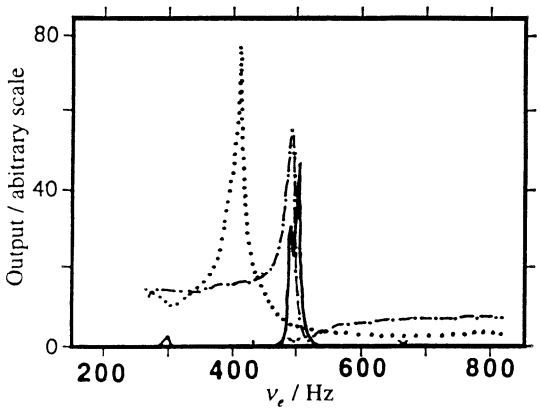



**Fig. C.1:** Frequency responses for a 0.90 ml air bubble from the three techniques: dotted line from ABC, chain from acoustic re-emission, and solid line from subharmonic modulation. (Data from figures 2.9, 3.3 and 4.22.)

## C.2 COMPARISON TO OTHER TECHNIQUES

The three methods can be compared to five the other methods mentioned as "promising" in section I.6.

Wolf's Ultrasonic Tomographer requires an array of ultrasonic transducers which makes it is far more costly than any of the three techniques of this project. It is more suited to detecting bubble streams than sizing individual bubbles.

Farmer and Vagle's Four Frequency Echo-sounder is applicable to a different type of situation. It can estimate size distributions in bubble clouds whereas the techniques studied here were designed to measure individual bubbles with high accuracy. Because it relies on pulsing the interrogating signal, it is limited to bubbles whose resonant wavelengths are much less than the size of the system.

Breitz and Medwin's Resonator takes advantage of cavity resonances to detect bubbles resonant at many particular frequencies simultaneously though this limits its ability of accurately sizing individual bubbles. The ABC and acoustic re-emission techniques could have been similar optimised – for example by exciting with a fixed-frequency square wave and using a spectrum analyser to separate the responses.

Miller's Resonant Bubble Detector needed large sound pressures to induce sufficiently non-linear oscillations and so is principally limited to bubbles with resonances at ultrasonic frequencies where high sound amplitudes are easier to attain.

Newhouse and Shankar's Frequency Mixing Method requires electronics which are far more sophisticated than those needed for the ABC and acoustic re-emission techniques. However, it has been developed through several projects to also incorporate both Doppler and echo-sounding principles in the same device. It has an advantage over the subharmonic modulation technique (which is an off-shoot of Newhouse and Shankar's method and requires similar electronics) in that the erratic amplitude variations were not a problem.

## C.3 COMMON FEATURES

Some features are common to all three techniques of this project, and any others which rely on breathing-mode resonance. One is that the resonant frequency of a bubble depends somewhat upon the shape and nature of any boundaries to the liquid which are close to the bubble. If the position of the bubble is known and the device is calibrated with bubbles at that particular position then this is not a problem. Even if this not the case then there are still several ways to overcome this problem. For example, the surroundings may be such that the bubble environment remains the same as it passes the measuring device; this would be the case if the device were built flush with wall of a pipe and the flow were laminar. Alternatively, two or more devices with different shapes could interrogate the bubbles in turn. The combination of the responses could be used to yield both size and position data.

Another feature of acoustic resonance techniques is that the resonant frequencies of bubbles shift if two or more bubbles are close together. The theoretical analysis of section III.3 solved the problem for a pair of bubbles provided that the bubble separation can be found. One way to detect the bubble positions would be to have an array of capacitors or hydrophones working with a single excitation source. Position information would then be contained in the different amplitudes detected by elements of the array. The two bubble resonance theory needs to be extended to cases with three or more bubbles – I expect that it will be possible to do so in a similar manner, at least for three bubbles in an arrangement with high symmetry, though the resulting expression may not be as elegant.

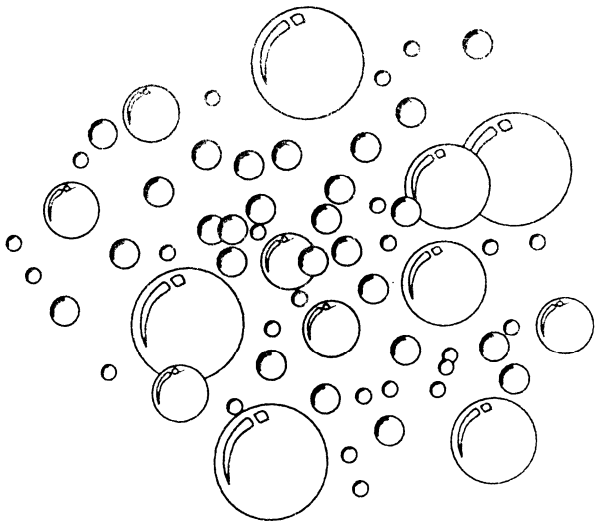
Even if that complications of shifting resonant frequencies are ignored, breathing-mode resonance still gives a reasonable estimate of bubble size. For example naïve approximations for a pair of bubbles are: the resonance is that of the larger bubble alone; and the resonance is if the two bubbles were coalesced into one. These two extreme approximations only give a difference in combined effective radius of $\approx 25$ % at worst.

## C.4 PUBLICATIONS

Publications resulting from this completed work (Hardwick 1994b) will include a description of the Acoustic Bubble Capacitor (Hardwick and Walton 1994a), a didactic report of the acoustic re-emission technique (Hardwick and Walton 1994b), an explanation of the mechanism of subharmonic modulation (Hardwick 1994a) and a paper on the analytic theory of the resonant frequencies of pairs of bubbles (Hardwick 1995).

## C.5 FINAL REMARKS

The different methods all have advantages and disadvantages. Their suitability also depends on conditions in which one desires to measure bubbles and the type of information one wants. The Acoustic Bubble Capacitor and acoustic re-emission techniques are both simple and effective ways to accomplish the acoustic sizing of bubble in liquids.



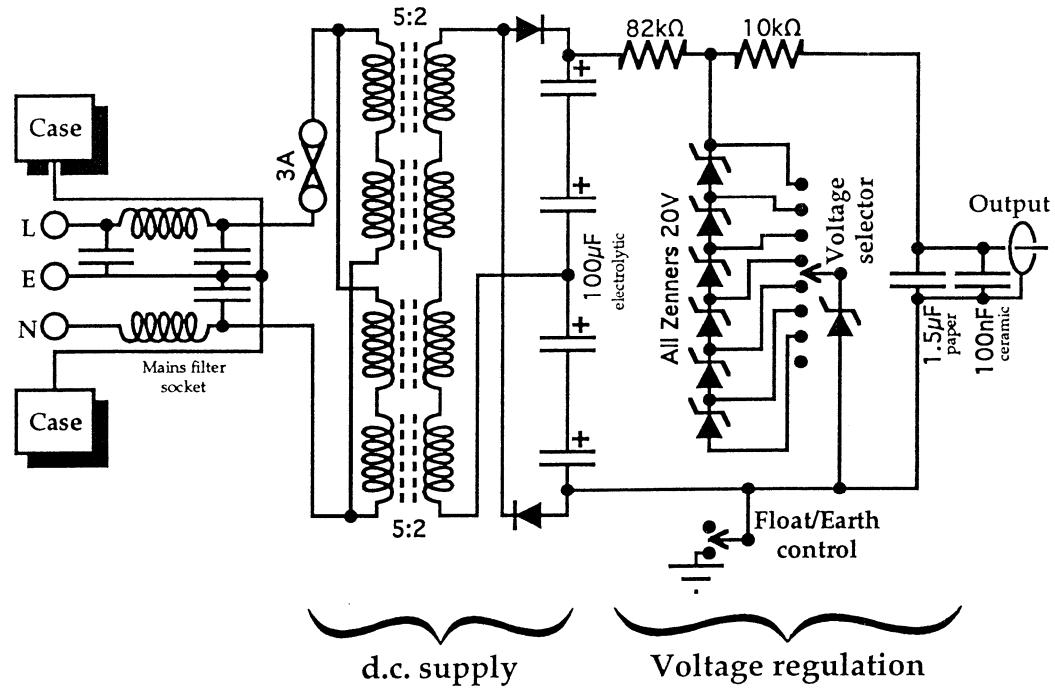
# APPENDICES

## A.1. APPENDIX 1: ELECTRONIC CIRCUITS

### A.1.1. THE SCREENING

Most of the following circuits were contained in earthed aluminium die-cast boxes. BNC coaxial connectors were used for all terminals except dual polarity and mains electric supplies. The standardisation of connectors allowed the analysis system to be adapted for different experimental situations. All the circuits which involved high-frequency signals or high-speed components were constructed on double-sided printed circuit boards so that the upper sides could be devoted to ground planes.

### A.1.2. THE BIAS SUPPLY




A stable low-noise supply of ~ 100 V was required to bias the acoustic bubble capacitor through a 1 GΩ resistor. It had to be sufficiently safe for the capacitor to be used underwater.

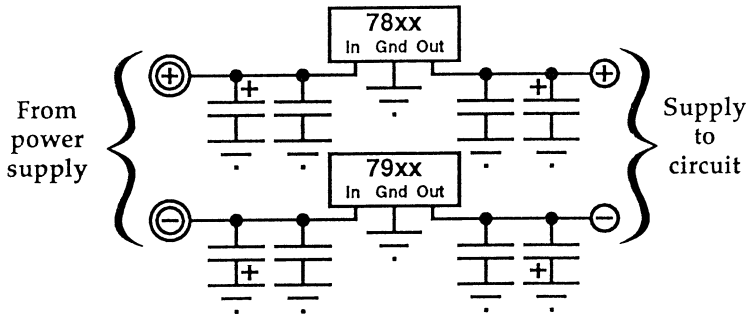
The switchable chain of Zener diodes and the 82 kΩ resistor fixed the voltage between 20 and 160 V in 20 ± 3 V steps. The mains filter, earthed casing and output filtering reduced electrical noise. The circuit was air-wired and constructed so that it could have been electrically floated had earth loops had caused problems. Safety features included: isolation of the output from the mains: fuse linking; and $10^5$ Ω

output impedance. (Additionally, all the equipment – except two oscilloscopes and the spectrum analyser – was powered through a residual current circuit breaker.)

### A.1.3. THE POWER SUPPLY

A dual polarity 15 V 0.5 A supply was constructed for testing the circuits during development. When the subharmonic modulation analyser of chapter III was running simultaneously, additional current was needed. A commercial bench power supply provided this.

### A.1.4. THE VOLTAGE REGULATION

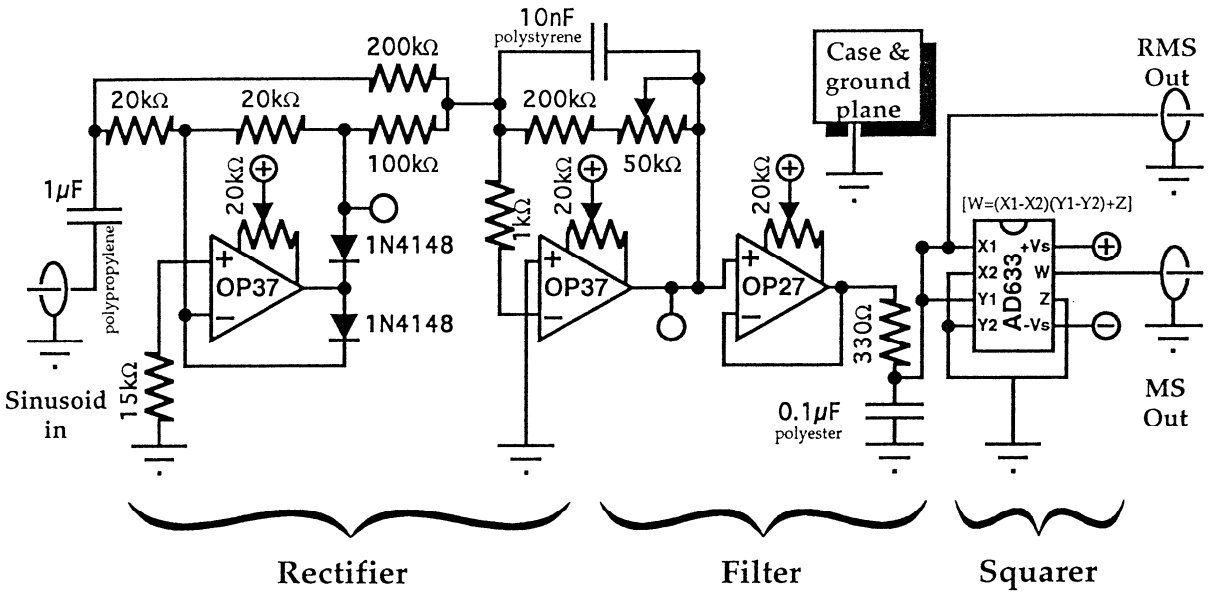



All polar capacitors are 10μF tantalum, the rest are 0.1μF ceramic.

(xx is the p.d. needed (05, 08, 09, 12, or 15) in volts.)

All the active (powered) circuits which follow were regulated in supply voltage by 78xx and 79xx series integrated circuits (or 78Lxx and 79Lxx low current alternatives). The connections are shown above instead of being displayed on each separate circuit diagram. The tantalum capacitors provided the a.c. bypassing which prevented these high-gain devices from oscillating. The ceramic capacitors take over this function at high frequencies for which the tantalum ones become inductive. Supplies to the circuits are ± 12 V unless otherwise stated.

### A.1.5. THE SINUSOID TO MEAN SQUARE AND ROOT MEAN SQUARE CONVERTERS




Sinusoid to d.c. converters were needed in order to record the amplitudes of signals on a chart recorder. They needed to convert oscillations of up to 10 kHz with amplitudes between 1 m $V_{RMS}$ and 1 $V_{RMS}$ whilst substantially allowing through variations with time scales over ~30 ms. The square of the RMS output was also needed for recombining quadrature components. The above circuit actually works reasonably up to 15 kHz at 1 m $V_{RMS}$ rising to 300 kHz at 1 $V_{RMS}$.

The first Op-amp performed inverting half-wave rectification. Active rectification, rather than just a diode, was needed to overcome the 0.6 V 'diode drop' which is often larger than the signal. The inverted rectified signal was then doubled and added to the original signal by the second Op-amp to give full-wave rectification. The 10 nF and 0.1 μF capacitors were parts of the smoothing filter. The third Op-amp buffered the output and was also necessary for the filter. The AD633 multiplier integrated circuit squared the output. It gave the voltage squared divided by 10 V.

An OP27 is a low-noise Op-amp. An OP37 is a high-speed version of an OP27 which was useful to rapidly overcome the 'diode drops' as the input crosses zero volts. Potentiometer symbols with solid arrowheads denote voltage presets in the circuit diagrams. The presets connected to the Op-amps were adjusted to null the Op-amp input offset voltages (~ ± 2 mV, different for each individual integrated circuit). The output to RMS conversion was calibrated by the 50 kΩ preset. 1N4148s are signal diodes; power diodes (such as 1N4007s) have too much internal capacitance to switch polarity rapidly in this circuit. The rectifier part was based largely on Jung 1974.

### A.1.6. THE CHART RECORDER MODIFICATIONS

The inconvenient inaccessible screw terminals were replaced by BNC sockets and switchable attenuators were added to increase the range of voltage scales available.

### A.1.7. THE FREQUENCY SWEEP TIMEBASE

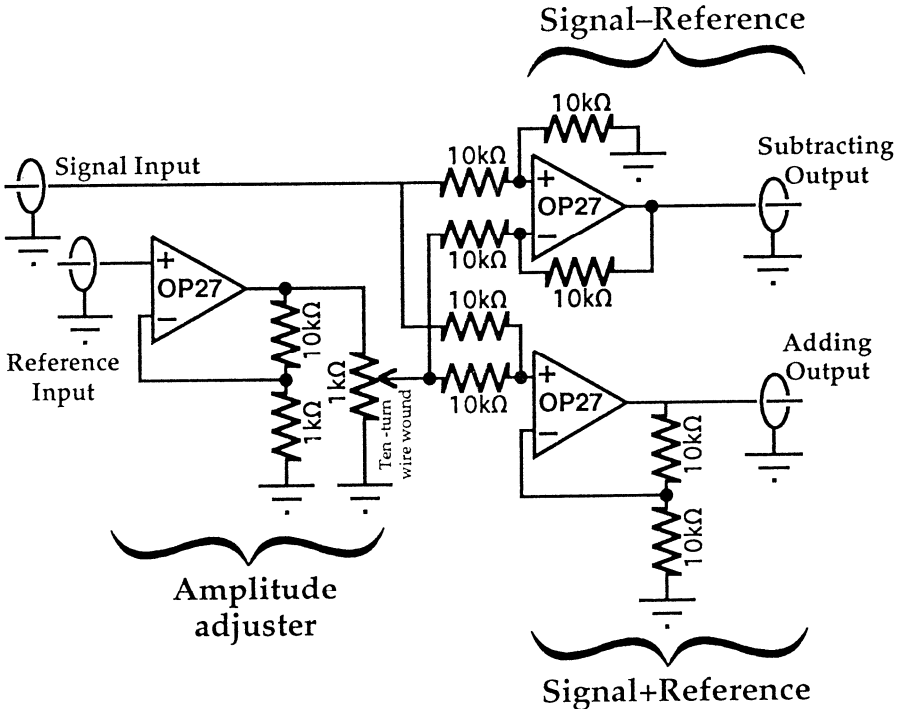
This was required to generate a ramping control voltage for the signal source. Features of the time base included: hold or sweep; reset; six range scales; six preset time scales plus a variable one; adjustable limits; up or down sweep direction; digital voltage display; chart recorder trigger; and reference outputs.

It utilised a 555 timer IC, a transistor current source, a capacitor and a TL071 FET Op-amp to provide the ramping voltage which controlled the signal source. A further 555 and a relay were the basis for the chart recorder trigger. Two LM311 comparator Op-amp delimited the range and five 741 Op-amps (a cheap variety) adapted the signal. It was a mess of wires and components on Veroboard in a folded aluminium box and, hindsightedly, a digital version on a printed circuit board would have been far preferable so the circuit diagram is not included here.

### A.1.8. THE AUDIO FREQUENCY BUFFER

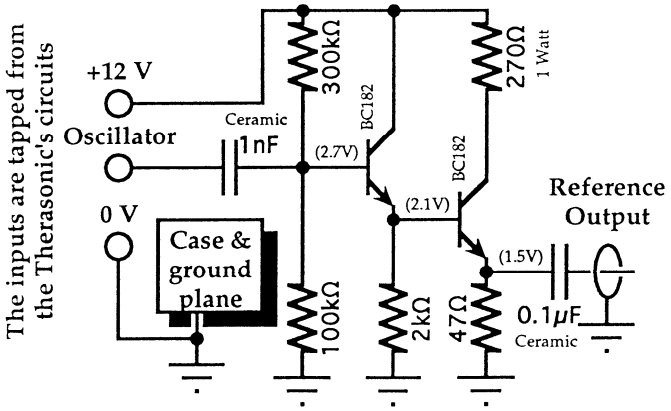
A simple OP27 Op-amp circuit with output connected to inverting input sufficed from 50 Hz to almost 1 MHz.

### A.1.9. THE SPURIOUS SIGNAL CANCELLER




This added between - 10 and + 10 times a reference signal to another signal. No offset zeroing was needed because the devices which used this circuit output ignored d.c..

### A.1.10. THE ULTRASONIC FREQUENCY BUFFER



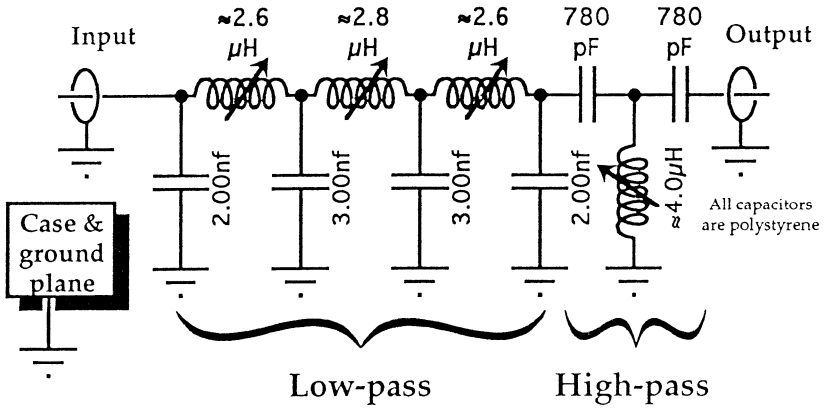

This needed to buffer (current amplify) signals with frequencies from 1 to 3 MHz and amplitudes up to 1 $V_{pp}$ from over 600 Ω input impedance to 50 Ω output impedance. This circuit worked from 50 kHz to 50 MHz, had 100 kΩ impedance inward and (by mistake) 3 Ω outward impedance.

The 1 nF capacitor and the two subsequent resistors re-centred the a.c. signal around 2.7 V and applied it to a pnp transistor's base. A transistor so wired adjusts the current flowing from its collector to its emitter so as to maintain one diode drop between its base and emitter. Thus the signal is reproduced (with lower central

voltage) at the emitter. Similarly for the second transistor. The 270 Ω prevents this transistor overheating.

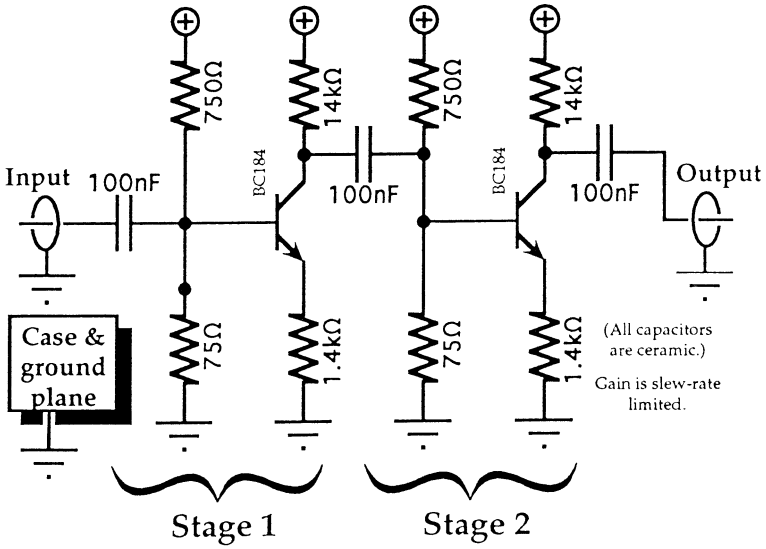
The Therasonic 1030 was modified by wiring one of these parasitically into it to deliver a reference $\nu_i$ signal. (For information: the best place found to tap the signal in the Therasonic was pin 7 of 1IC7.)

### A.1.11. THE 3.35 MHZ FILTER




This needed to let through $\nu_i$ (3.35 MHz) but block $2\nu_i$ (18 dB below $\nu_i$ before filtering), higher harmonics and as much other-frequency noise as possible. It was a six pole Chebyshev low-pass passive filter followed by a three pole Chebyshev high-pass filter. The filters were derived from the tables in van Valkenburg 1982. Though designed with matched 50 Ω input and output, it was possible to tune the filter to accept the 3 Ω output of the buffer as input. It reduced the $2\nu_i$ component to 52 dB below the $\nu_i$ and all the other harmonics to at least 70 dB below the $\nu_i$ component.

### A.1.12. THE ULTRASONIC AMPLIFIER

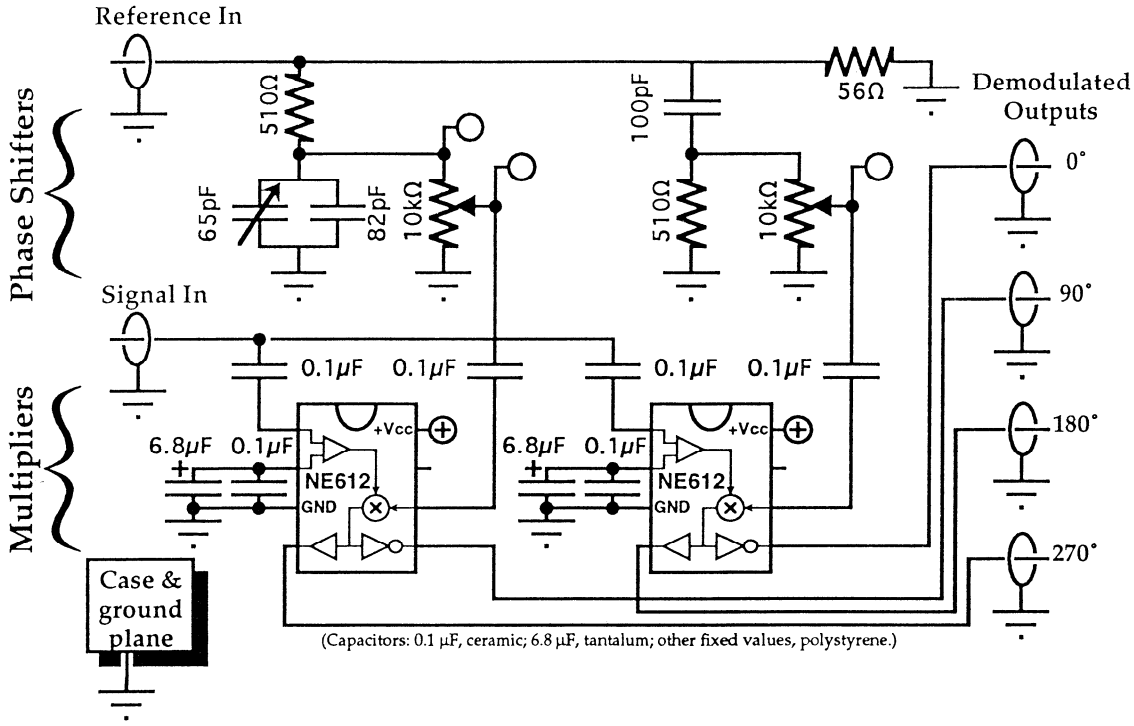



This was intended to amplify 1 to 3 MHz signals by 40 dB. The gain was unintentionally slew-rate limited by the inadequate transistors so it gave 24 dB at

3 MHz. This conveniently counteracted the finding that the hydrophone output could be made significantly greater than was originally planned for; therefore the transistors were not replaced.

It worked in the same manner as the ultrasonic buffer except that the output of each stage was taken from the collector instead of the emitter. Since the current changes were (almost) the same at both but the resistor was greater at the collector, the voltage changes were greater. The signal was re-centred between the stages.

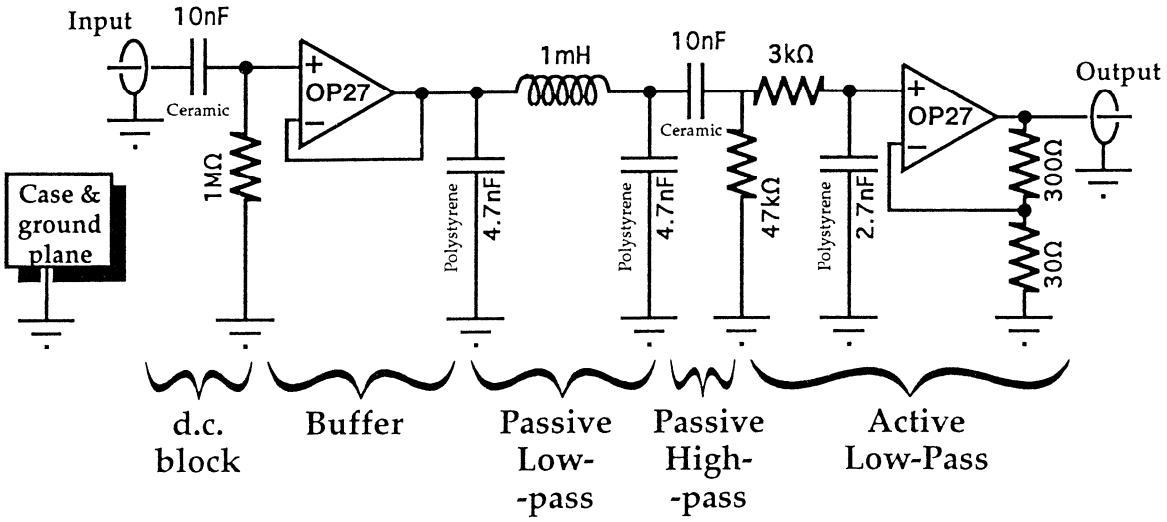
### A.1.13. THE QUADRATURE DEMODULATOR




This demodulated a signal and provides 16 dB gain.

The reference signal was given a 56 Ω termination and was shifted by ±π/4 rad by the two RC networks. The adjustable capacitor was used to make the phase precise. The resistor presets reduced the reference signal to 250 m $V_{pp}$. The NE612s are 4-quadrant Gilbert Cell mixers. Their operation is schematically shown by the detail on the NE612 symbols above. The supply was + 8 V (note that the output was + 8 V biased and so had not be connected to a low resistance).

### A.1.14. THE AUDIO FREQUENCY FILTERS



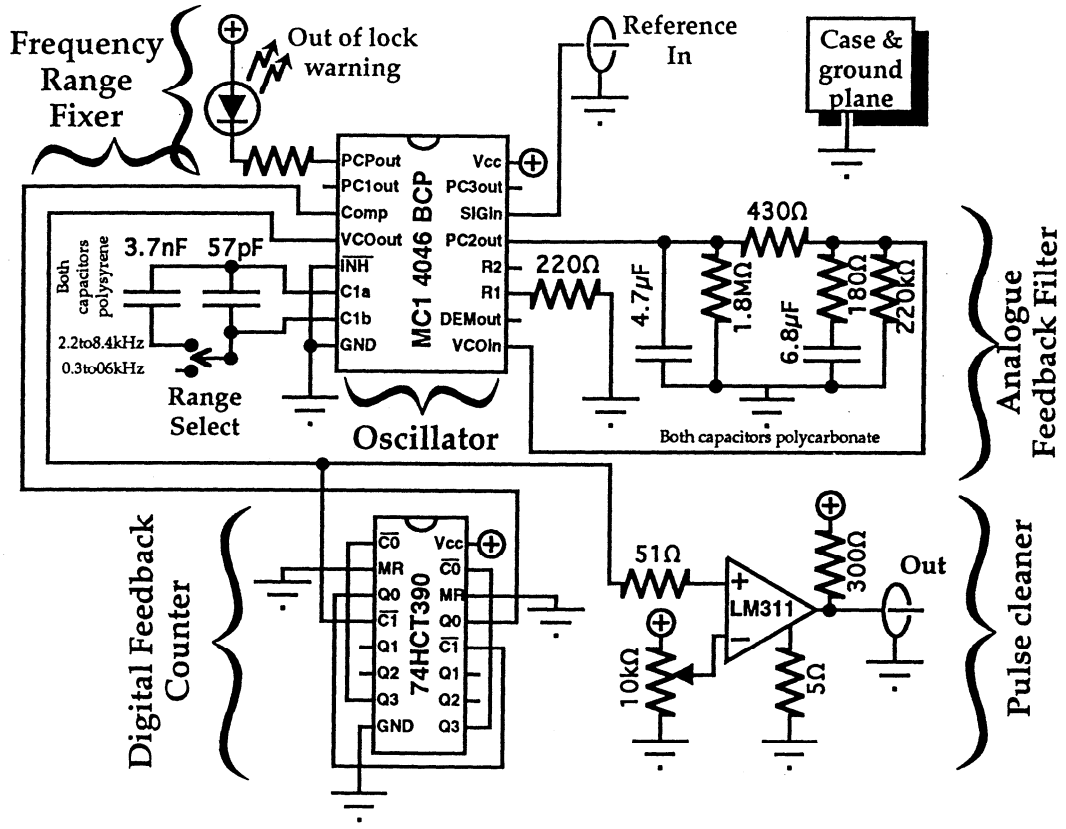

This needed to have little attenuation or ripple below 10 kHz, no noticeable non-linear mixing, at least 90 dB attenuation at 6.7 MHz (based on the modulation being 50 dB below the carrier), and at least 1.5 kΩ input impedance.

The first stage was a one pole passive high pass filter which blocked the demodulator bias. The signal was then buffered and filtered (three pole low pass; one pole high pass). The final stage was intended to be a two pole active filter but, with 10 dB gain, it was intrinsically unstable so the second capacitor was removed leaving a one pole filter which was sufficient.

### A.1.15. THE DIGITAL INTERFACE

This was simply an LM311 comparator Op-amp which converted the signal source's reference output to a square wave to drive the frequency X 100 circuit.

### A.1.16. THE HUNDREDFOLD FREQUENCY CONVERTER




Its purpose was to provide the variable frequency reference for the shiftable filters. This ideally would have subdivided each input pulse into a hundred regular output pulses for all frequencies. For practical reasons, a limited range of frequencies was chosen: 2.2 to 8.4 kHz with no apparent distortion; 1.6 to 15 kHz with acceptable levels of distortion. Later it was modified to also work from 0.3 to 0.6 kHz.

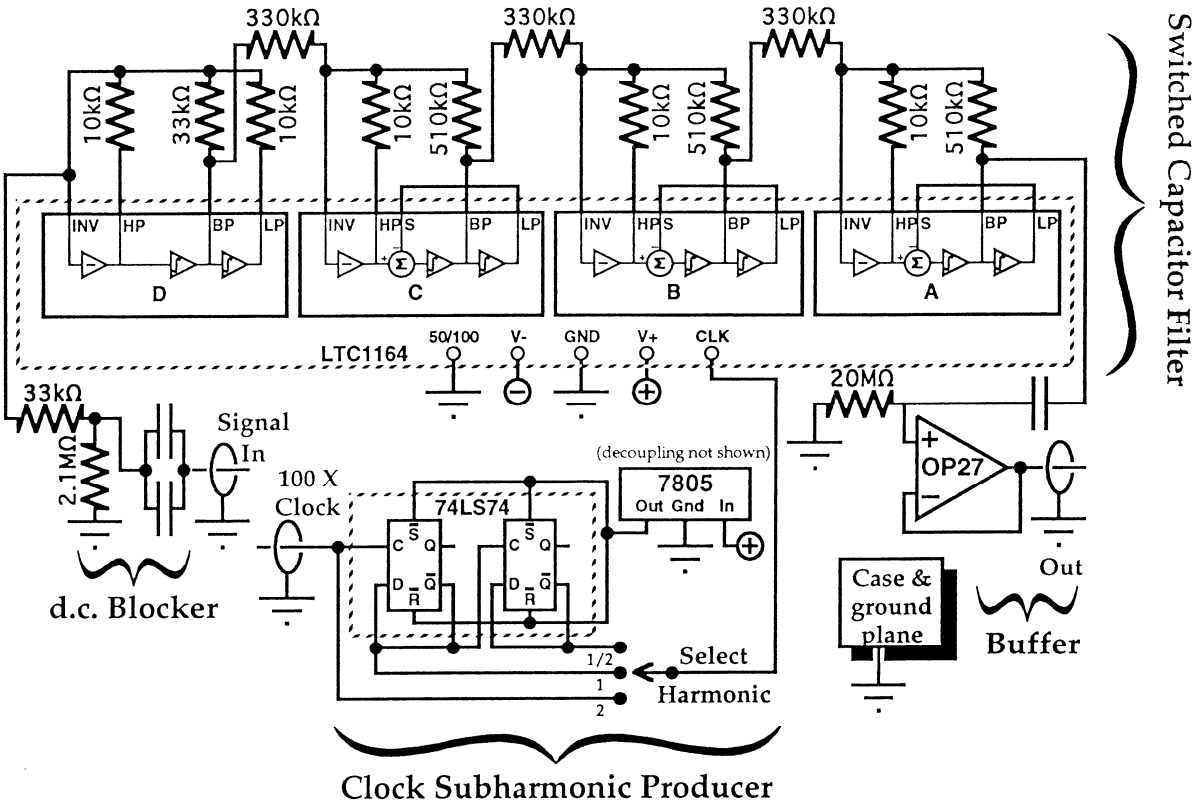
It is based on a phase-locked-loop. The loop consisted of the following components: a voltage controlled variable frequency oscillator (in the 4046; range determined by C1 and R2); a 1 to 100 counter (the 390) in the feedback to the comparator; a comparator (in the 4046) which compared the output pulses, which had been reduced by 100 in frequency, to the reference pulses and produced correction pulses if they did not match; and a filter network in the feedback to the oscillator that smoothed the correction pulses into a control voltage which then went back to control the oscillator.

If the comparator produced a high rate of correction pulses then the LED would light to indicate that the circuit could not multiply the input frequency by a hundred. The Op-amp tidied deformed pulse-shapes. The supply was + 5 V.

This inelegant circuit was designed *ad hoc* after both simple theory and computer packages had failed to design working devices. The difficulty was partly

because the design was attempting to force this style of phase-locked-loop beyond its standard upper frequency limit, its accuracy for one-step hundredfold frequency increase and its ratio of frequency limits. [In the words of C.Moss, "It's not pulling a caravan with a bicycle; it's pulling a caravan with a hamster!".] Nevertheless this *ad hoc* design was eventually made sufficient for the most of the range of frequencies encountered in the experiments.

### A.1.17. THE SHIFTABLE FILTERS



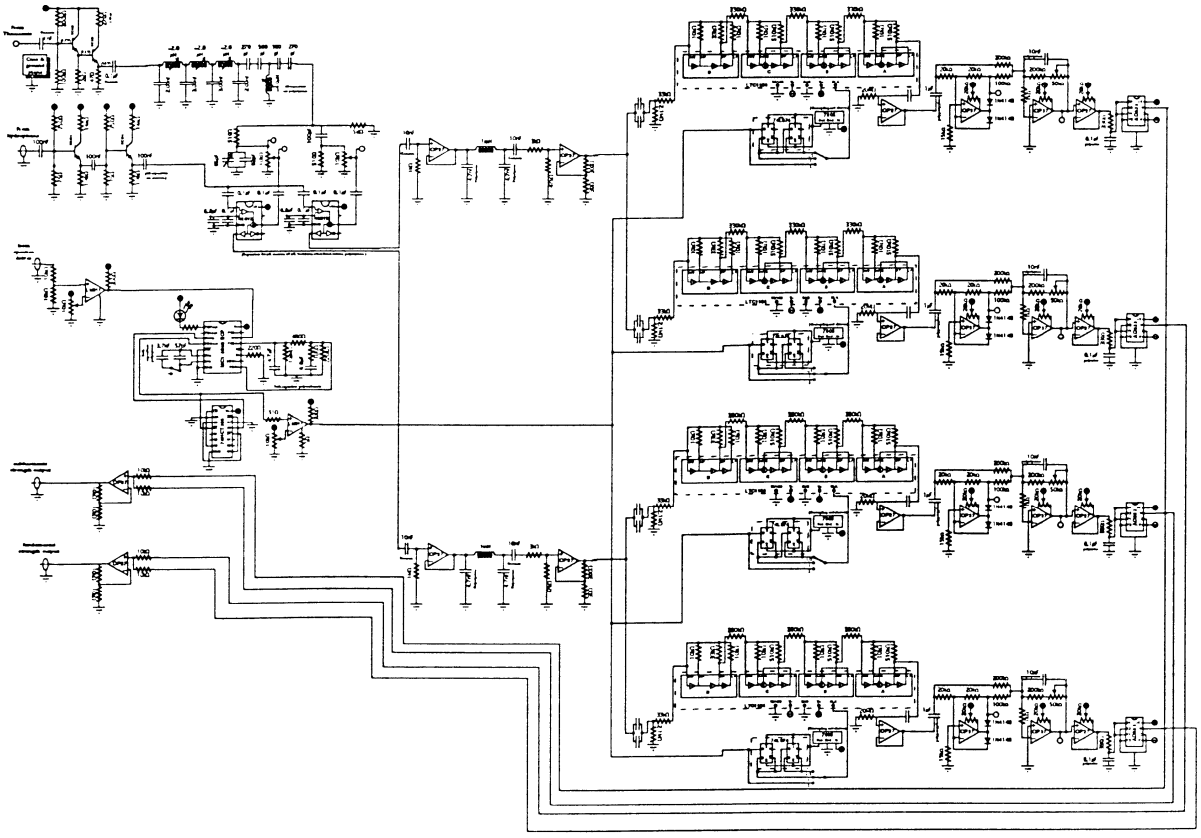

This filtered a signal with eight poles high pass, eight poles low pass, $Q \approx 100$ and 10 dB gain. The centre frequency could vary from 0.1 Hz to 20 kHz and was at ½, 1 or 2 times $\frac{1}{100}$ of the frequency of the 5 V reference square wave (i.e. ½, 1 or 2 times the frequency of the signal source).

The LTC1164 contains elements for four filters. It used clocked switched capacitors as integrators; therefore the whole frequency characteristic could be re-scaled in proportion to the clocking reference frequency. The resistors controlling the filter setup were chosen manually, based on the LTC1164 documentation, because the relevant computer package produced theoretically valid but totally unfeasible designs. The supply was ± 8 V but the D-type flipflops (in the 74LS74) which reduced to clock rate required + 5 V so an additional regulator was used. The LTC1164's output is too high impedance even to drive an unconnected coaxial cable so the output buffer is needed.

### A.1.18. THE ADDER

This was merely an Op-amp arranged like a third of the spurious signal canceller with added offset zeroing.

### A.1.19. THE WHOLE SUBHARMONIC MODULATION ANALYSER



The above shows the resulting circuit when the ultrasonic buffer, ultrasonic amplifier, ultrasonic filter, quadrature demodulator, digital interface, frequency times 100, two audio filters, four shiftable filters, four sinusoid to mean squares and two adders are connected together to monitor the squared amplitudes of $\nu_i \pm \frac{1}{2}\nu_e$ and $\nu_i \pm \nu_e$. For a much more helpful schematic, see figure 4.11.

This gave 70 dB gain followed by squaring and division by 10 V. Thus, with the Dapco NP10-3 hydrophone, the output calibration was 0.20 $\mu V/Pa_{RMS}{}^2$ so typically the output was conveniently ~ $10^{\pm 1}$ V. The accuracy of this system was unnecessarily high because preliminary studies indicated a very poor signal quality, as explained in section IV.2.1. Later the working device enabled the signal to be optimised and the discovery of the modulation mechanism revealed that the erratic results were intrinsic rather than spurious measurement faults.

## A.2. APPENDIX 2: SPEAKER CALIBRATION

### A.2.1. GEARING & WATSON UW60

An extensive series of measurements performed in water in the same tank as was used for the experiments confirmed that the acoustic pressure $p_e$ at $(r_c, \phi, z)$ was proportional to the square root of the power dissipated by the speaker $W_e$ and revealed the spatial dependence. This comprised a Gaussian variation across the speaker's axis and an exponential variation along it:

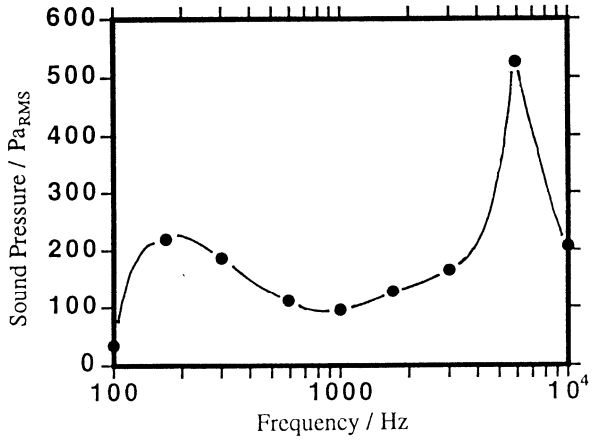
$$p_e[r_c, \phi, z, W_e, \nu_e] \propto F[\nu_e] \cdot \sqrt{W_e} \cdot \exp\left[\frac{-z}{A_0 + A_1\rho + A_2\rho^2}\right] \cdot \exp\left[-\left(\frac{\rho}{A_3 + A_4\sqrt{\nu_e}}\right)^2\right]$$

$$\text{where } \begin{cases} A_0 = 4.5\text{cm} \\ A_1 = 0.14 \\ A_2 = 0.044\text{cm}^{-1} \\ A_3 = 5.8\text{cm} \\ A_5 = 0.085\text{cm Hz}^{-1/2} \end{cases}.$$

Within a few centimetres of the axis, this is reasonably given by

$$p_e[r_c, \phi, z, W_e, \nu_e] \simeq F[\nu_e] \cdot \sqrt{W_e} \cdot \exp[-z/A_0].$$

The frequency response $F[\nu_e]$ is shown by figure A2.1 below. It is fairly smooth over the main range used (300 to 3000 Hz).

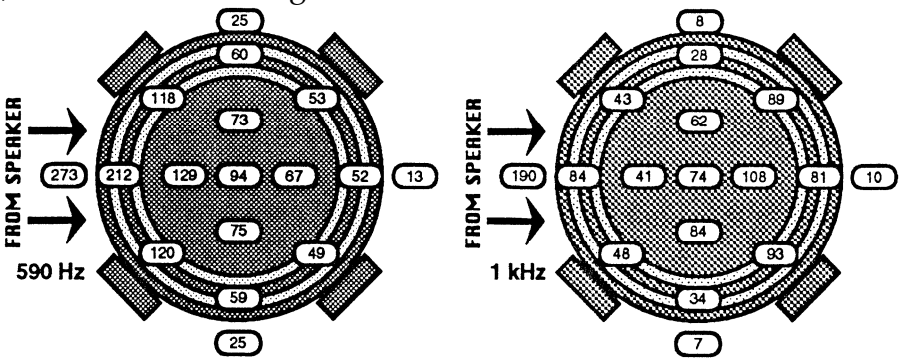



**A2.1:** Sound pressure at 50 mW and 8 cm from the speaker.

### A.2.2. IN THE ACOUSTIC BUBBLE CAPACITOR

The ABC seriously complicated the sound field by adding a resonance at 0.9 kHz (see figure 3.8). Below 800 Hz, the side of the capacitor closest to the speaker

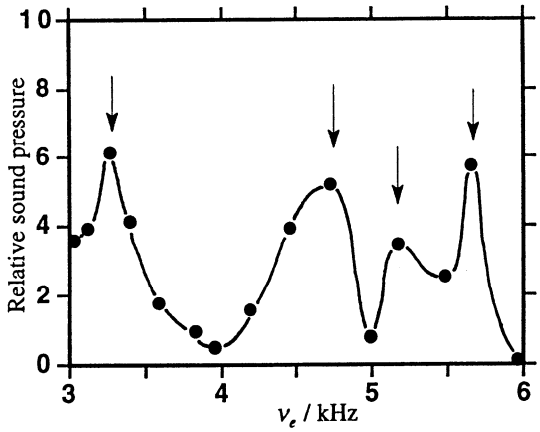
experienced louder sound but the resonance caused a local maximum sound pressure within the ABC at higher frequencies (figure A2.2). In oil it was even poorer (figure 2.4); the UW60 was designed for use in water.




**A2.2:** Relative sound pressure (measured by Brüel & Kjær 8103 hydrophone) in the acoustic bubble capacitor in water.

### A.2.3. MYLAR® SPEAKER

This has a very uneven frequency response. Figure A2.3 shows the response for one particular speaker in the best part of its range. At higher frequencies, little sound was produced. At lower frequencies, numerous closely packed resonances made most frequency response experiments worthless.




**A2.3:** A Mylar®′s frequency response.

## A.3. APPENDIX 3: SYMBOL DEFINITION SUMMARY

In addition to being defined where they are first used, the algebraic symbols used in this dissertation are summarised below. (A 'u' represents any subscript.)

$a_n$ .....Amplitude of the $n$th surface oscillation mode.
$c$.....Speed of sound in the liquid.
$k$ .....Wavenumber ($=\omega/c$ ).
$m$.....'Mass' term.
$n$.....Non-negative integer.
$p$ .....Pressure.
- $p_0$ ..... Equilibrium (ambient) pressure.
- $p_e$ ..... Applied 'excitation' sound pressure amplitude at $\nu_e$ .
- $p_i$ ..... Applied 'imaging' sound pressure amplitude at $\nu_i$ .
- $p_V$ ..... Vapour pressure.
- $p_c$ ..... Pressure centrally between two bubbles.

$q$ .....Detected sound pressure amplitude. It includes the following:
- $q_e$ ..... Re-emitted sound at $\nu_e$ .
- $q_i$ ..... Detected ultrasound at $\nu_i$ .
- $q_{+1}, q_{-1}$ ..... Detected ultrasound at $\nu_i \pm \nu_e$ which is equivalent to
- $q_{1A}, q_{1B}$ ..... Modulating $\nu_i$ components at $\nu_e$ and to
- $q_{1\alpha}, q_{1\beta}$ ..... Modulating $\nu_i$ components at $\nu_e$ .
- $q_1$ ..... $= \frac{1}{2}\sqrt{{q_{-1}}^2 + {q_{+1}}^2} = \frac{1}{8}\sqrt{{q_{1\alpha}}^2 + {q_{1\beta}}^2} = \frac{1}{8}\sqrt{{q_{1A}}^2 + {q_{1B}}^2}$ .
- $q_{+1/2}, q_{1/2A}, q_{1/2}$, etc. similarly relate to $\nu_i \pm \frac{1}{2}\nu_e$

$\underline{r}$ .....Position vector.
- $(r, \theta, \phi)$ ..... $\underline{r}$ in spherical co-ordinates.
- $(r_c, \phi, z)$.... $\underline{r}$ in cylindrical co-ordinates.
- $\underline{r_n}$ ..... $\underline{r}$ with the centre of the $n$th bubble as the co-ordinates' origin.

$s$.....Separation between bubble centres.
$t$.....Time.
$\underline{v}$ .....Liquid velocity vector.
- $v_n$ ..... Liquid velocity due to the $n$th bubble alone.

$w$ .....Gas heat capacity at constant volume per unit volume
- $w_0$ ..... $w$ for a bubble in static equilibrium.
- $w_a$ ..... Oscillation amplitude in $w$ as bubble oscillates.

$(x, y, z)$..... $\underline{r}$ in Cartesian co-ordinates.
$A_0$ to $A_4$ ....Miscellaneous sound field calibration constants.
$C$ .....Capacitance.
$E$.....Electric field strength.
$F$.....Frequency response of loudspeaker.
$K$ .....Gas thermal conductivity.

$M$ .....Minnaert-like constant ($=\nu_0 R_0$)

$M_M$ .....Minnaert's constant.

$N$ .....Number of 'degrees of freedom' of a gas molecule.

$Q$ .....Quality factor ('Q') of oscillator (= reciprocal of damping constant).

$Q_u$ ..... 'Q' as if only the u damping mechanism existed.

$R$ .....Bubble radius.

$R_0$ ..... Equilibrium bubble radius.

$R_a$ ..... Radial oscillation amplitude.

$R_{eff}$ ..... Effective bubble radius ($=\sqrt[3]{3V/4\pi}$).

$R_{initial}$ ..... Initial bubble radius.

$R_{nu}$ ..... Like $R_u$ but for the $n$th bubble.

$S_u$ .....Experimental signal corresponding to $q_u$, i.e. $q_u$ times a scaling factor.

$T$ .....Temperature.

$T_0$ ..... Equilibrium temperature.

$T_a$ ..... Temperature oscillation amplitude.

$V$.....Bubble volume.

$V_0$ ..... Equilibrium bubble volume.

$V_a$ ..... Bubble volume oscillation amplitude.

$W_u$ .....Power used to drive the $\nu_u$ sound source, '$u$' = '$e$' or '$i$'.

$Y_n$ .....Any $n$th order spherical harmonic.

$\alpha$.....Arbitrary constant.

$\beta$.....Arbitrary constant.

$\gamma$.....Ratio of specific heat.

$\varepsilon$ .....Electric permittivity.

$\zeta$.....General purpose oscillation variable.

$\theta$.....See under $r$.

$\kappa$.....Polytropic index.

$\mu$.....Liquid viscosity.

$\nu$.....Conventional ("Hertz") frequency.

$\nu_e$ ..... 'Excitation' frequency (typically in audible domain).

$\nu_i$ ..... 'Imaging' frequency (typically in ultrasonic domain).

$\nu_0$ ..... Resonant frequency.

$\nu_{n0}$ ..... Resonant frequency of the $n$th bubble.

$\nu_-$ ..... Resonant frequency of two bubbles oscillating in phase.

$\nu_+$ ..... Resonant frequency of two bubbles oscillating in antiphase.

$\pi$.....Ratio of circumference to diameter of a Euclidean circle.

$\rho$.....Liquid density.

$\xi$.....Ratio of major to minor axes of an ellipsoid.

$\sigma$.....Electric conductivity.

$\tau$.....Surface tension.

$\phi$.....See under $r$.

$\chi$.....'Stiffness' term.

$\omega$.....Angular frequency ($\omega_u = 2\pi\nu_u$).

$\Gamma$.....General purpose forcing amplitude.

$\Theta_u$ .....Various phase factors.

$\Lambda$.....Displacement of a part of the liquid from its equilibrium position.

$\Psi$.....Wave function.

## A.4. APPENDIX 4: RECOMMENDED READING

This dissertation is complete in itself but the following books are recommended as starting points if the reader desires more detail than it was appropriate to include here.

'Fundamentals of Acoustics' (Kinsler *et al* 1982) is a good general introduction to acoustics.

'The Acoustic Bubble' (Leighton 1994a) is the most comprehensive review yet published of the interactions between bubbles and sound.

'The Art of Electronics' (Horowitz and Hill 1989) is unsurpassed as an introductory book for electronic design because of its practical advice, realistic approach and helpfully explained examples of good and bad circuits.

'Soap Bubbles' (Boys 1911) is not directly relevant to the current dissertation which only concerns bubbles in liquids not bubbles with gas on both sides of thin liquid membranes. Nevertheless, if the reader wishes for an informative and entertaining introduction to soap bubble demonstrations, this classic book is recommended.

## A.5. APPENDIX 5: ALTERNATIVE TEXT

### A.5.1. EXPLANATION OF MAIN DISSERTATION STYLE

Scientific literature can be written in many styles. It can range from formal to colloquial, from terse to verbose, from traditional to innovative, and so on. Personally, I find it easiest to write in the form of a dense mass of facts in a convoluted but logically unambiguous structure of sub-clauses and amalgamated words. Some find this style somewhat difficult to read! Therefore I have tried to largely avoid using it in this work. (The worst remaining example is the explanation of the phase-locked-loop in Appendix 1.16.) I too prefer a style other than that when reading. I like the science to have been written almost biographically and crafted with as much care as a good novel. Unfortunately, writing that way would be incompatible with the current scientific idiom which requires that the person who performs the science is not mentioned and that only the completed outcome, not the endeavour which lead to it, is reported. I could have ignored the idiom and produced a dissertation which was more enjoyable to read but I know people who would take great offence at that small degree of unconventionality. One version of the introduction suffered such a fate and had to be replaced – a relic from it comprises the current foreword.

The style I chose for the main text is one recommended by A.J.Walton, my supervisor. It is not the first person plural style of Walton 1972 but a more traditional form with: the scientist not to be mentioned; colloquial, archaic, poetic and emotive terms to be avoided; the ideas to progress linearly; the sentence structure to be simple; and subtle reminders to be used to aid the reader when the flow is not linear.

The figure styles and sizes in the main chapters are based on the guidelines issued by the Institute of Physics for their journals (in particular, The European Journal of Physics). Word5, Kaleidagraph, MacDrawII, photography, a photocopier, chart recorders, tracing, freehand sketching and glue were used. I hope that the reader does not take offence at the 'etching-style' ABC drawings and the curvilinear boxes of the schematics (some like the way the edges flow into the arrows, others prefer bland rectangles; the scientific content would be the same – it is purely a matter of personal aesthetic taste.)

With some poetic licence, even unfitting literary idioms can be used. An entertaining description of the dissolution experiments written in a heroic style inspired by Poe c.1845, DeQuincy 1822 and Gee 1994 has not been included as light relief, in deference to one who would consider it as ill suited to the traditional decorum of a PhD dissertation. I have included, however, an alternative text for the preliminary subharmonic modulation study on the next two pages. It has proved to be popular in explaining the work to non-physicists so it is not just a novelty.

## A.5.2. THE BUBBLE AND THE MER-SPEAKER

**(A scientific paper and fairy story by A.J.Hardwick)**

Once upon a time an uncaring wizard waved his magic glass staff in the deep waters of a tank as transparent as crystal. Scores of little bubbles were created. All but one were sucked up by the terrible Archimedes force to the very top of the water where they stretched until they could stretch no more. One by one their watery skins burst and they were spread to the four winds. Just one bubble survived – she was a cripple and her small size had given the deathly Archimedes force a weaker grip. She clung desperately to the waxy wire which hung like silver bolt of frozen lightning from way up into the fatal air. Her name was Belinda.

The wizard opened his book of spells and waved his hands over the enchanted dials outside the tank where none but witches and wizards could reach. Belinda felt a tingling sensation as the water pressure rapidly rose and fell and rose and fell about her. She knew she was in no danger from this because it was changing so fast; it merely tickled. Safety was not to last long though. More wizardry produced a peculiar looking monster – half loudspeaker, half waterproof plastic box. It wailed a bloodcurdling sound.

"Please stop. You are hurting me." cried Belinda as the pressure of the wail first squeezed her tightly then tried to rip her apart in an unending cycle.

"I only wish I could." the monster said in a gentle voice without interrupting his wail, "I was once a handsome prince of a loudspeaker who could play the finest music. Songs to make you laugh or cry. Tunes to make you dance or sing. Then I was caught by the wicked wizard. He took his loathsome silicone sealant and epoxy resin. He combined me forever with this ugly waterproof plastic box. I'm now merely an unhappy mer-speaker but the coil of my heart remains as strong as ever, though I now toil to move heavy water instead of fresh light air. I have loved you from afar ever since I you were born from the wizard's glass staff but I am forced to obey the wizard's electric orders and torture bubbles all day long.". The mer-speaker told Belinda that he had blown all the bubbles which had reached the wire earlier into the open water to be burst but the wizard would be appeased if she gave the correct screams. He told her this because her loved her and did not want her to die like the others.

Before he could explain further, the wizard started to change the electrical signals. Sometimes the mer-speaker's thrusting was slow enough to allow Belinda to

just follow – shrinking when high pressure squashed her, growing when low pressure pulled her. Sometimes the mer-speaker's thrusting was fast enough for Belinda to get left behind – growing when high pressure squashed her, shrinking when low pressure pulled her. Insidiously the wizard homed in on the dreadful speed in the middle which would have her ringing like a bell.

When nearly there she started screaming. She was surprised that the pitch of her scream matched that of the tickle but she was not surprised that it enloudened and softened with the in and out thrusting. She still held tightly. The wizard gave a small wicked smile.

When even nearer to having her ring like a bell, her screaming became hoarse. The pitch of her scream still matched that of the tickle but it enloudened and softened at only half as fast as the in and out thrusting. The wizard foolishly believed what his warlock had taught him: that this was because the bodies of bubbles so near the ringing of death balloon out too far to recover before the next squashing so they ring only half as fast as before. Belinda alone knew the real reason, the tickles were only skin-deep and her skin was rippling like a jelly as she grew and shrunk.

She still held more tightly still. The wizard clapped his hands with glee. Belinda had passed the ordeal. Her screams had appeased the wizard.

Before Belinda could thank her love, the mer-speaker, for his help – the wizard broke his unspoken promise and started another ordeal for the lovers. He steadily increased the flow of electric orders to the mer-speaker and the power of the vile thrusting kept increasing. The loudness of her screams were written in the wizard's spell-book.

Just as Belinda decided it was unbearable and prepared to surrender herself to the Archimedes force, the mer-speaker – in his love for her – short-circuited the precious coil of his heart and died in a flash of royal blue light.

The wizard cursed and raged but without the mer-speaker he could torture bubbles no longer. He dared not harm Belinda now for he was due to show his work to a warlock's circle on a far-off land beyond the deep blue sea and white-topped mountains. He sealed her in jar safe from the Archimedes force and a bright white light shone for her.

In old age she became one with the water and at last joined the spirit of her speaker prince. They lived happily ever after.

**THE END**

## A.6. APPENDIX 6: BIBLIOGRAPHY

The few sources which are cited indirectly from accounts or summaries in other works are followed the name of the intermediary source in square brackets.


**A.P.Aleksandrov, E.S.Vaindruck,** 1974; Nauka Publishing Office (Moscow), The Investigation of the Viability of Hydrophysical Fields in the Ocean (Ed. R.Ozmidav), 122-8. [Thorpe 1982]

**S.Almass Tench, D.Hanonge, G.Hayward, C.Kuo,** 1992, A focused array system for cleaning off-shore structures – a preliminary experimental evaluation; The Petroleum Science and Technology Institute Technical Forum (proceedings not published).

**R.E.Apfel,** 1981, Acoustic Cavitation; Methods of Experimental Physics (Ed. P.D.Edmonds), Academic Press, 19, chapter 7, 355-411.

**R.E.Apfel,** 1970, The role of impurities in cavitation-threshold determination; JASA 48(5(II)), 1179-86.

**V.H.Arakeri, V.Shanmuganathan,** 1985, On the evidence for the effect of bubble interference on cavitation noise; JFM 159, 131-50.

**A.A.Atchley, A.Prosperetti,** 1989, The crevice model of bubble nucleation; JASA 86(3), 1065-84.

**C.W.H.Beton,** 1994, Application of the boundary element method to the detachment, oscillation and interaction of gas bubbles in a fluid; PhD dissertation, Department of Physics, Cambridge University.

**E.O.Belcher,** 1980, Quantification of bubble formation in animals and man during decompression; IEEE Trans. Biomed. Eng. BME-27 (6), 330-8.

**T.B.Benjammin,** 1964, Surface effects in non-spherical motions of small cavities; Elsevier Pub. Co., Cavitation in Real Liquids (Ed. R.Davies), 138-46.

**T.B.Benjammin, F. Ursell,** 1954, The stability of a liquid in vertical periodic motion; Proc. Roy. Soc. A 225, 505-15.

**V.F.J.Bjerknes,** 1906; Columbia University Press (New York), Fields of Force. [Walton and Reynolds 1984]

**F.G.Blake,** 1949, Bjerknes forces in stationary sound fields; JASA 21(5), Letters to the editor, 551.

**D.C.Blanchard,** 1963; Prog. Ocean. 1, 71. [Degrois and Baldo 1974]

**C.V.Boys,** 1911, Soap Bubbles; Republished 1959 by Dover Publications, (currently available in soft-back) ISBN 0-486-20542-8.

**W.H.Bragg,** 1921a, Sounds of the town; G.Bell and Sons Ltd. (London), The World of Sound, 68-76.

**W.H.Bragg,** 1921b, Sounds of the country; G.Bell and Sons Ltd. (London), The World of Sound, 129-30.

**N.Breitz, H.Medwin,** 1989, Instrumentation for *in situ* acoustical measurement of bubble spectra under breaking waves; JASA 86(2), 739-43.

**M.J.Buckingham,** 1991, On acoustic transmission in ocean-surface waveguides; Phil. Trans. Roy. Soc. A 335, 513-55.

**F.V.Bunkin, D.V.Vlasov, E.A.Zabolotskaya, Yu.A.Kravtsov,** 1983, Active acoustic spectroscopy of bubbles; Sov. Phys. Acoust. 29(2), 99-100 or Akust. Zh. 29, 169-172.

**O.Ya.Butkovsky, E.A.Zabolotskaya, Yu.A.Kravtsov, V.G.Petnikov, V.V.Ryabikin,** 1986, Possibilities of active nonlinear spectroscopy of inhomogenous condensed media; Acta. Phys. Slov. 36(1), 58-62.

**D.Cathignol, J.Y.Chapelon, V.L.Newhouse, P.M.Shanker,** 1990, Bubble sizing with high spatial resolution; IEEE Trans. on Ultrasonics, Ferroelectrics and Freq. Control 37 (1).

**J.Y.Chapelon, V.L.Newhouse, D.Cathignol, P.M.Shanker,** 1988, Bubble detection and sizing with a double frequency Doppler system; Ultrasonics 26, 148-54.

**J.Y.Chapelon, P.M.Shanker, V.L.Newhouse,** 1985, Ultrasonic measurement of bubble cloud size profiles; JASA 78(1), 196-201.

**N.P.Cheremisinoff** (editor), c.1960, Flow phenomenon and measurement; vol. 6 of Encyclopaedia of Fluid Mechanics, ISBN 0-87201-573-00, Gulf Pub. Co..

**R.Clift, J.R.Grace, M.E.Weber,** 1978, Terminal Velocities of Drops and Bubbles in Liquids; Bubbles, Drops and Particles, published by Harcourt Brace Jovanovich Pub. (NY, SF, Lon), Academic Press, chapter 7: Ellipsoidal Fluid Particles, Part II. Fluid Dynamics, Section B.

**W.T.Coakley**, 1971, Acoustical detection of single cavitation events in a focussed sound filed in water at 1 MHz; JASA 49(3 II), 792-801.

**A.J.Coleman,** 1991, Acoustic shock wave disintegration of urinary and biliary stones; Materials Group colloquium, PCS, Cavendish Labs, Cambridge (unpublished).

**K.Commander, R.J.McDonald,** 1991, Finite-element solution of the inverse problem in bubble swarm acoustics; JASA 89(2), 592-7.

**K.Commander, E.Moritz,** 1989, Off-resonance contribution to acoustical bubble spectra; JASA 85(6), 2665-9.

**G.B.Crawford, D.M.Farmer,** 1987, On the spacial distribution of ocean bubbles; J. Geophysical Research 92(C8), 8231-43.

**L.A.Crum, R.A.Roy, M.A.Dinno, C.C.Church, R.E.Apfel, C.K.Holland, S.I.Madanshetty,** 1992, Acoustic cavitation produced by microsecond pulses of ultrasound: a discussion of some selected results; JASA 91(2), 1113-9.

**M.Degrois, P.Baldo,** 1974, A new electrical hypothesis explaining sonoluminescence, chemical actions and other effects produced in gaseous cavitation; Ultrasonics, 12, 25-8.

**P.P.Dendy,** 1988, Sonoluminescence and the ultrasound hazard debate; Phys. Med. Biol. 33(11), 1233-7.

**T.DeQuincy,** 1822, Confessions of an English Opium Eater; republished in 1989 by Woodstock Books, ISBN 1-85477-020-9.

**A.Detwiler, D.C.Blanchard,** 1978, Ageing and bursting bubbles in trace contaminated water; Chem. Eng. Sci. 33, 9-13.

**C.Devin,** 1959, Survey of thermal, radiation and viscous damping of pulsating air bubbles in water; JASA 31(12), 1654-67.

**D.M.Doskoi, S.V.Zamolin, L.M.Kustov, A.M.Sutin,** 1984, Nonlinear backscattering of acoustic waves in a bubble layer; Acoustics Letters 7(9), 131-4.

**A.I.Eller,** 1970, Damping constants of pulsating bubbles; JASA 47(5 II), letter to editor, 1469.

**A.Eller, H.G.Flynn,** 1965, Rectified diffusion during nonlinear pulsation of cavitation bubbles; JASA 37(3), 493-502.

**A.Eller, H.G.Flynn,** 1969, Generation of subharmonics of order one-half by bubbles in a sound field; JASA 46(3(II)), 722-7.

**P.S.Epstein, M.S.Plesset,** 1950, On the stability of gas bubbles in liquid-gas solutions; J. Chem. Phys. 18(11), 1505-7.

**von R.Esche,** 1952, Untersuchung der Schwingungskavitation in Flüssigkeiten; Acustica 2, 208-18.

**W.M.Fairbank, M.O.Scully,** 1977, A new non-invasive technique for cardiac pressure measurement: resonant scattering of ultrasound from bubbles; IEEE Trans on Biomed. Eng., BME-24(2), 107-10.

**M.Fanelli, A.Prosperetti, M.Reali,** 1984, Shape oscillation of gas-vapour bubbles in liquids: I. mathematical formulation; Acustica 55, 213-23.

**M.Faraday,** 1831, Appendix: On the forms and states assumed by fluids in contact with vibrating elastic surfaces; Phil. Trans. Roy. Soc. (1), 319-40.

**D.M.Farmer, S.Vagle,** 1989, Waveguide propagation of ambient sound in the ocean surface bubble layer; JASA 86(5), 1897-908.

**J.E.Ffowcs Williams, Y.P.Gou,** 1991, On resonant nonlinear bubble oscillations; JFM 224, 507-29.

**E.B.Flint, K.S.Suslick,** 1991, The temperature of cavitation; Science, 253, 1397-9.

**L.Floberg,** 1964, Cavitation in lubricating oil films; Elsevier Pub. Co., Cavitation in Real Liquids (Ed. R.Davies), 138-46.

**L.A.Frizzel, C.A.Linke, E.L.Carstensen, C.W.Fidel,** 1977, Thresholds for focal ultrasonic lesions in rabbit kidney, liver and testicle; IEEE Trans. Biomed. Eng. BME-24(4), 393-6.

**A.M.Gaudin,** 1956, Separating solids with bubbles; Scientific American December, 99-110.

**E.R.G.Gee,** 1994, Reflections on Baptism as a Ritual; first year PhD report for the Faculty of Classics, University of Cambridge.

**M.F.Gillis, M.T.Karagianes, P.L.Peterson,** 1968 Bends: detection of circulating gas emboli with external sensor; Science 161, 579-80.

**J.A.Glazier, D. Wearie,** 1992, The kinetics of cellular patterns; J. Phys.: Condensed Matter 4(7), 1867-94.

**V.E.Gordeev, A.I.Serbinov, Ya.K.Troshin,** 1968; Thermal quality of the luminescence of a cavitating liquid; Sov. Phys. – Acoustics 14(2), 234-5.

**R.F.Graf, G.J.Whalen** (editors), 1974; Souvenir Press Pub., How it Works (Illustrated).

**A.Gresham,** c.1983; indirectly reported lecture from the Cambridge University medical degree course.

**D.R.Gross, D.L.Miller, A.R.Williams,** 1985, A search for ultrasonic cavitation within the canine cardiovascular system; Ultrasound in Med. and Biol. 11(1), 85-97.

**W.Güth,** 1956; Acustica 6, 532-8. [Lauterborn 1976]

**I.Hansson, V.Kedrinskii, K.A.Mørch,** 1982, On the dynamics of cavity clusters; J. Phys. D 15, 1725-34.

**A.J.Hardwick,** 1994a, The mechanism of subharmonic ultrasound modulation by forcibly oscillated bubbles; Ultrasonics, awaiting second referee's reply.

**A.J.Hardwick,** 1994b, The acoustic sizing of bubbles in liquids; PhD dissertation, Department of Physics, Cambridge University.

**A.J.Hardwick,** 1995, (the two-bubble resonance theory, title yet to be decided); to be composed.

**A.J.Hardwick, T.G.Leighton, A.J.Walton, J.E.Field,** 1992, Acoustic bubble sizing through nonlinear combinations involving parametric excitations; European Conf. on Underwater Acoustics, pub. Elsevier Applied Science, ISBN 1-85166-948-5, 153-6.

**A.J.Hardwick, A.J.Walton,** 1994a, The acoustic bubble capacitor: a new method for sizing gas bubbles in liquids; Measurement Sci. and Tech., awaiting second round referees replies.

**A.J.Hardwick, A.J.Walton,** 1994b, Forced oscillations of a bubble in a liquid; Eur. J. Phys., accepted, awaiting publication.

**I.Hashish, W.Harvey,** 1987, Anti-inflammatory and pro-inflammatory mechanisms of therapeutic ultrasound; Proc. Brit. Med. Ultrasound Soc. (probably in Ultrasound in Medicine and Biology), June, 613.

**M.Holness,** 1992, The irresistible fluid and the immovable rock; New Sci. 1813, 41-5.

**R.G.Holt, L.A.Crum,** 1992, Acoustically forced oscillations of air bubbles in water: experimental results; JASA 91(4I), 1924-33.

**P.Horowitz, W.Hill,** 1989, The Art of Electronics; 2nd edition, Cambridge University Press, ISBN 0-521-37095-7.

**D-Y.Hsieh, M.S.Plesset,** 1961, Theory of rectified diffusion of mass into gas bubbles; JASA 32(2), 206-15.

**H.J.M.Hulshof, F.Schurink,** 1985, Continuous ultrasonic waves to detect steam bubbles in water under high pressure.; Kema Scientific and Technical Reports 3(5), 61-9.

**P.A.Hwang, Y-H.L.Hsu, J.Wu,** 1990, Air bubble produced by breaking wind waves: a lab. study; J. of Phys. Oceanography 20, 19-28.

**V.I.Ilyichev, V.L.Koretz, N.P.Melnikov,** 1989, Spectral characteristics of acoustic cavitation; Ultrasonics 27, 357-61.

**Incognito,** 1994; First referee's report for Hardwick 1994a.

**J.B.Jeffies, R.A.Copeland, K.S.Suslick, E.B.Flint,** 1992, Thermal equilibrium during cavitation; Science, 256, 248.

**W.G.Jung,** 1974, Signal processing circuits; IC Op-Amp Cookbook, 3rd Ed, pub. SAMS (Macmillan), ISBN 0-672-22453, Chapter 5, 225-87.

**V.Kamath, A.Prosperetti,** 1989, Numerical integration methods in gas bubble dynamics; JASA 85(4), 1538-48.

**I.S.Kang, L.G.Leal,** 1988, Small amplitude perturbations of shape for a nearly spherical bubble in an inviscid straining flow; JFM 187, 231-66.

**J.B.Keller,** 1964, Growth and decay of gas bubbles in liquids; Elsevier Pub. Co., Cavitation in Real Liquids (Ed. R.Davies), 19-29.

**D.L.Kingsbury, P.L.Marston,** 1981, Mie scattering near the critical angle of bubbles in water; J. Optical Soc. Am., 71, 358-61.

**L.E.Kinsler, A.R.Frey, A.B.Coppens, J.V.Saunders,** 1982, Fundamentals of Acoustics; 3rd edition, pub. John Wiley and Sons Ltd..

**K.Kisman,** 1977, Spectral analysis of Doppler ultrasonic decompression data; Ultrasonics, 105-110.

**J.R.Klepper,** 1982, Ultrasonic methods for detection and sizing of venous gas emboli; IEEE Ultrasonics Symposium, 668-72.

**V.O.Knudsen, R.S.Alford, J.W.Emling,** 1948; J. Marine Res. 7, 410-29. [Medwin and Beaky 1989]

**A.Kolaini, R.A.Roy, L.A.Crum,** c. 1990, The production of high frequency ambient noise by capillary waves; Probably conference pre-print, no information as to place of intended publication but probably dated post-1989.

**E.F.Koraev, K.A.Naugol'nykh,** 1980, Parametric sound radiation in a two phase medium; Sov. Phys. :Acoust. 26(1), 48-51.

**M.S.Korman, R.T.Bayer,** 1988, Nonlinear scattering of crossed ultrasonic beams in the presence of turbulence in water: I. Experiment; JASA 84(1), 339-49.

**M.S.Korman, R.T.Bayer,** 1989, Nonlinear scattering of crossed ultrasonic beams in the presence of turbulence in water: II. Theory; JASA 85(2), 611-20.

**M.Kornfield, L.Suvorov,** 1944, On the destructive action of cavitation; J. Appl. Phys. 15, 495-506.

**I.N.Kozhevnikova, L.Bjørnø,** 1992, Experimental study of acoustical emission from bubble cloud excitation; Ultrasonics 30(1), 21.

**H.Lamb,** 1874, Vibrations of a globule; Cambridge University Press, Hydrodynamics (5th edition, 1924), chapter IX: Surface Waves, §275, 448-50.

**L.D.Landau, E.M.Lifshitz,** 1987, Capillary waves; Course of Theoretical Physics, 6 : Fluid Mechanics 2nd edition (1st edition 1959), §62, 244-7.

**W.Lauterborn,** 1976, Numerical investigation of nonlinear oscillations of gas bubbles in liquids; JASA 59(2), 283-93.

**W.Lauterborn, J.Holzfuss,** 1991, Acoustic chaos; Int. J. of Bifurcation and Chaos 1(1), 13-26.

**W.Lauterborn, U.Parlitz,** 1988, Methods of chaos in physics and their application to acoustics; JASA 84(6), 1975-93.

**T.G.Leighton,** 1989a, Transient excitation of insonated bubbles; Ultrasonics 27, 50-3.

**T.G.Leighton,** 1989b, The enhancement of cavitation effects by acoustic pulsing and by a relative rotation of the sample and beam; Brit. J. Radiology 62 (739) (Proc. Brit. Med. Ultrasound Soc.), 651.

**T.G.Leighton,** 1994a, The Acoustic Bubble, Pub. Academic Press Ltd., ISBN 0-12-441920.

**T.G.Leighton,** 1994b; Personal communication.

**T.G.Leighton, M.Adlam, A.J.Walton, J.E.Field,** 1991c, The non-linear oscillations of multiple bubbles in a simulated acoustic field; Proc. I. O. Acoustics 13(3), 39-47.

**T.G.Leighton, K.J.Fagan, J.E.Field,** 1991b, Acoustic and photographic studies of injected bubbles; Eur. J. Phys. 12, 77-85.

**T.G.Leighton, R.J.Lingard, A.J.Walton, J.E.Field,** 1990a, Bubble sizing by the nonlinear scattering of two acoustic frequencies; Dordrecht (The Netherlands), Kluwer Academic Pub., Natural Physical Sources of Underwater Sound (Ed. B.Kerman).

**T.G.Leighton, R.J.Lingard, A.J.Walton, J.E.Field,** 1991a, Acoustic bubble sizing by combination of subharmonic emissions with the imaging frequency; Ultrasonics 29, 31-24.

**T.G.Leighton, M.J.W.Pickworth, J.Tutor, P.P.Dendy,** 1990d, A search for sonoluminescence in the human cheek; Ultrasonics 28, 181-4.

**T.G.Leighton, M.J.W.Pickworth, A.J.Walton,** 1987, Correlation of sonoluminescence with the standing-wave component of an acoustic sound field produced by a therapeutic unit; Brit. J. of Radiology 60(714), 614.

**T.G.Leighton, M.J.W.Pickworth, A.J.Walton, P.P.Dendy,** 1988, Studies of the cavitation effects of clinical ultrasound by sonoluminescence: I. Correlation of sonoluminescence with the standing-wave pattern in an acoustic field produced by a therapeutic unit; Phys. Med. Biol. 33(11), 1239-48.

**T.G.Leighton, M.J.W.Pickworth, A.J.Walton, P.P.Dendy,** 1989a, The pulse enhancement of unstable cavitation by mechanisms of bubble migration; Proc. I. O. Acoustics 11(5), 461-9.

**T.G.Leighton, A.J.Walton,** 1987, An experimental study of the sound emitted from gas bubbles in a liquid; Eur. J. Phys. 8, 98-104.

**T.G.Leighton, A.J.Walton, J.E.Field,** 1989b, High-speed photography of transient excitation; Ultrasonics 27, 370-3.

**T.G.Leighton, A.J.Walton, M.J.W.Pickworth,** 1990c, Primary Bjerknes forces; Eur. J. Phys. 11, 47-50.

**T.G.Leighton, M.Wilkinson, A.J.Walton, J.E.Field,** 1990b, Studies of non-linear bubble oscillations in a simulated acoustic field; Eur. J. Phys. 11, 352-8.

**F.Leslie, 1985,** Measurements of rotating bubble shapes in a low-gravity environment; JFM 161, 269-79.

**Y.Li, D.Koller, G.George, P.M.Sankar, V.L.Newhouse,** 1992, Underwater bubble sizing using a pulsed double frequency technique; JASA 92(2I), 1117-9.

**R.J.Lingard, T.G.Leighton, A.J.Walton, J.E.Field,** 1990, The sizing of gas bubbles the non-linear scattering of sound; Final year undergraduate experimental project in physics for Cambridge University.

**M.S.Longuet-Higgins,** 1988a, Monopole emission of sound by asymmetric bubble oscillations: I. normal modes; JFM 201, 525-42.

**M.S.Longuet-Higgins,** 1988b, Monopole emission of sound by asymmetric bubble oscillations: II. an initial value problem; JFM 201, 543-65.

**M.S.Longuet-Higgins,** 1990a, An analytic model of the sound produced by raindrops; JFM 214, 365-410.

**M.S.Longuet-Higgins,** 1990b, Bubble noise spectra; JASA 87(2), 652-61.

**M.S.Longuet-Higgins,** 1990c, The sound field due to an oscillating bubble near an indented free surface; JFM 221, 675-83.

**M.S.Longuet-Higgins,** 1991, Resonance in nonlinear bubble oscillations; JFM 224, 531-49.

**M.S.Longuet-Higgins,** 1992, Nonlinear damping of bubble oscillations by resonant interaction; JASA 91(3), 1414-23.

**M.S.Longuet-Higgins, B.R.Kerman, K.Lunde,** 1991, The release of air bubbles from an underwater nozzle; JFM 230, 365-90.

**M.S.Longuet-Higgins, J.S.Turner,** 1974, An 'entraining plume' model of a spilling breaker; JFM 63(1), 1-20.

**N.Q.Lu, H.N.Oğ uz, A.Prosperetti,** 1989, The oscillations of a small floating bubble; Phys. Flu. A 1(2), 252-60.

**T.S.Lundgren, N.N.Mansour,** 1991, Vortex ring bubbles; JFM 224, 177-96.

**R.A.MacArthur,** 1992, Gas bubble release by muskrats diving under ice: lost gas or a potential oxygen pool?; J. Zool. 226, 151-164.

**H.McGee,** 1991b, Wine, beer and distilled liquors; Harper Collins Pub. (Lon), On Food and Cooking: The Science and Lore of the Kitchen, part 1, chapter 9.

**H.McGee,** 1991a, Bread, dough and batters; Harper Collins Pub. (Lon), On Food and Cooking: The Science and Lore of the Kitchen, part 1, chapter 6.

**R.S.Mackay, G.Rubissov,** 1978, Decompression studies using ultrasonic imaging of bubbles; IEEE Trans. Biomed. Eng. BME-25(6), 537-44.

**J.Maddox,** 1993, Sonoluminescence in from the dark; Nature 361, 397.

**A.Mallock,** 1919, Sounds produced by drops falling on water; Proc. Roy. Soc. A, 95, 138-43.

**T.J.Mason,** 1993, Sonochemistry – chemistry induced by cavitation; Seminar to the Physics and Chemistry of Solids group, Department of Physics, University of Cambridge, 1993/12/2.

**T.J.Mason, J.P.Lorimer, D.M.Bates,** 1992, Quantifying sonochemistry: casting some light on a 'black art'; Ultrasonics 30(1), 40-2.

**H.Medwin,** 1977a, Counting bubbles acoustically: a review; Ultrasonics, Jan., 15, 7-13.

**H.Medwin,** 1977b, Acoustical determinations of bubble-size spectra; JASA 62(4), 1041-4.

**H.Medwin, M.M.Beaky,** 1989, Bubble sources of the Knudsen sea noise spectra; JASA 83(3), 1124-30.

**H.Medwin, A.C.Daniel,** 1990, Acoustic measurement of bubbles produced by spilling breakers; JASA 88(1), 408-12.

**M.J.Miksis, L.Ting,** 1984, Nonlinear radial oscillations of a gas bubble including thermal effects; JASA 76(3), 897-905.

**D.L.Miller,** 1981, Ultrasonic detection of resonant cavitation bubbles in a flow tube by their 2nd harmonic emissions; Ultrasonics 19, 217-224.

**D.L.Miller, A.R.Williams, D.R.Gross,** 1984, Characterisation of cavitation in a flow-through exposure chamber by means of a resonant bubble detector; Ultrasonics 22, 224-30.

**M.Minnaert,** 1933, On the musical air-bubbles and the sounds of running water; Phil. Mag. 16, 235-48.

**E.C.Monahan, M.Lu,** 1990, Acoustically relevant bubble assemblages and their dependence on meteorological parameters; IEEE J. of Oceanic Engineering 15(4), Oct..

**K.A.Mørch,** 1977; I. O. Acoustics, Bournemouth, UK, Proc. Conf. on Acoustic Cavitation, 62-70. [Neppiras 1980]

**E.A.Neppiras,** 1969, Subharmonic and other low-frequency emission from bubbles in sound irradiated liquids; JASA 46(3(II)), 587-601.

**E.A.Neppiras,** 1980, Acoustic cavitation; Phys. Rep. (Rev. Sect. of Phys. Let.) 61(3), 169-261.

**E.A.Neppiras, B.E.Noltingk,** 1951, Cavitation produced by ultrasonics: theoretical considerations for the onset of cavitation; Proc. Phys. Soc. B 64, 1032-8.

**V.L.Newhouse, P.M.Shanker,** 1984, Bubble size measurement using the nonlinear mixing of two frequencies; JASA 75(5), 1473-7.

**R.Y.Nishi,** 1972, Ultrasonic detection of bubbles with Doppler flow transducers; Ultrasonics 10, 173-9.

**R.Y.Nishi,** 1975, The scattering and absorption of sound waves by gas bubbles in a viscous liquid; Acustica 33(2), 65-74.

**B.E.Noltingk, E.A.Neppiras,** 1950, Cavitation produced by ultrasonics; Proc. Phys. Soc. B 63, 674-85.

**H.N.Oğuz, A.Prosperetti,** 1990a, A generalisation of the impulse and virial theorems with an application to bubble oscillations; JFM 18, 143-162.

**H.N.Oğuz, A.Prosperetti,** 1990b, Bubble oscillations in the vicinity of a nearly plane free surface; JASA 87(5), 2085-92.

**H.N.Oğuz, A.Prosperetti,** 1990c, Bubble entrapment by axisymmetric capillary waves; Eng. Sci., Flu. Dynamics, 191-202.

**H.N.Oğuz, A.Prosperetti,** 1991, Numerical calculations of the underwater noise of rain; JFM 228, 417-42.

**U.Parlitz, V.Englisch, C.Scheffcyk, W.Lauterborn,** 1990, Bifurcation structure of bubble oscillators; JASA 88(2), 1061-76.

**I.S.Pearsall,** 1972a; Cavitation, Pub. Mills and Boon Ltd (London), chapter 1, 13-4.

**I.S.Pearsall,** 1972b, Hydrofoil cavitation; Cavitation, Pub. Mills and Boon Ltd, chapter 4, 34-8.

**I.S.Pearsall,** 1972c, Cavitation in pumps; Cavitation, Pub. Mills and Boon Ltd, chapter 5, 39-52.

**I.S.Pearsall,** 1972d, Cavitation in water turbines; Cavitation, Pub. Mills and Boon Ltd, chapter 6, 53-8.

**I.S.Pearsall,** 1972e, Ultrasonic and biological cavitation; Cavitation, Pub. Mills and Boon Ltd, chapter 9, 71-2.

**P.O.Pedersen,** 1935, Subharmonics in forced oscillation in dissipative systems; JASA 6, 227-38

**A.D.Phelps, T.G.Leighton,** 1993, Investigation into the use of two frequency excitation to accurately determine bubble sizes; IUTAM Symposium on Bubble Dynamics and Interface Phenomena (Birmingham), pub. Kluwer Academic, ISBN 0-7923-3008-0, 475-84.

**A.D.Phelps, T.G.Leighton,** 1994a, Acoustic bubble sizing using two frequency excitation techniques; Proc. 2nd Conf on Underwater Acoustics (Copenhagen), in press.

**A.D.Phelps, T.G.Leighton,** 1994b, Automated bubble sizing using two frequency excitation techniques; Proc. 3rd Conf. on Sea Surface Sound (San Diego), in press.

**A.D.Phelps, T.G.Leighton,** 1994c, High resolution bubble sizing through detection of the subharmonic response with a two frequency technique; submitted to JASA.

**M.J.W.Pickworth, P.P.Dendy, T.G.Leighton, A.J.Walton,** 1988, Studies of the cavitational effects of clinical ultrasound by sonoluminescence: II Thresholds for sonoluminescence from a therapeutic ultrasound beam and the effects of temperature and duty cycle; Phys. Med. Biol. 34(1), 135-6.

**M.J.W.Pickworth, P.P.Dendy, T.G.Leighton, A.J.Walton,** 1989a, Studies of the cavitational effects of clinical ultrasound by sonoluminescence: Cavitation from pulses of a few μs duration; Phys. Med. Biol. 34(1), 135-6.

**M.J.W.Pickworth, P.P.Dendy, T.G.Leighton, A.J.Walton, R.C.Chivers,** 1989b, Studies of the cavitation effects of clinical ultrasound by sonoluminescence: III. Cavitation from pulses a few μs in length; Phys. Med. Biol. 34(9), 1139-51.

**M.J.W.Pickworth, P.P.Dendy, P.R.Twentyman, T.G.Leighton,** 1989c, Studies of the cavitation effects of clinical ultrasound by sonoluminescence: IV. The effect of therapeutic ultrasound on cells in monolayer culture in a standing wave field; Phys. Med. Biol. 34(11), 1553-60.

**M.J.W.Pickworth, P.R.Twentyman, T.G.Leighton, P.P.Dendy,** 1989d, Absence of sonoluminescence in the human cheek; Brit. J. Radiology (Proc. Brit. Med. Ultrasound Soc.) 62(739), 652.

**A.B.Pippard,** 1989, Radiation from an open end; The Physics of Vibration, omnibus edition, Cambridge University Press, 179-8.

**A.B.Pippard,** 1994; Personal comment.

**I.M.Pfeiler, E.Matura, H.Iffländer, G.Seyler,** 1989, Lithotripsy of renal and biliary calculi: physics, technology and medical-technical application; Electomedica 57(2), 52-63.

**H.Pfriem,** 1940; Akust. Z. 5, 202. [Devin 1953]

**M.S.Plesset,** 1949, The dynamics of cavitation bubbles; J. Appl. Mech. 16, 277-82.

**M.S.Plesset,** 1954, On the stability of fluid flows with spherical symmetry; J. Appl. Phys. 25(1), 96-8.

**M.S.Plesset,** 1964, Bubble dynamics; Elsevier Pub. Co., Cavitation in Real Liquids (Ed. R.Davies), 138-46.

**M.S.Plesset, A.Prosperetti,** 1977, Bubble dynamics and cavitation; Ann. Rev. Flu. Mech., 145-85.

**E.A.Poe,** c.1845, How to write a Blackwoods article; republished in The Complete Tales of Mystery and Imagination, 1981, pub. Octopus Books, ISBN 0 7065 1552 3.

**E.R.Pounder,** 1965, Air bubbling; Physics of Ice, Pub. Pergamon Press, chapter 4: Ice control, §4.3.

**A.Prosperetti,** 1975, Nonlinear oscillations of gas bubbles in liquids and the connection between subharmonic signal and cavitation; JASA 57(4), 810-21.

**A.Prosperetti,** 1977, Thermal effects and damping mechanisms in the forced radial oscillations of gas bubbles in liquids ; JASA 61(1), 17-27.

**A.Prosperetti,** 1988a, Bubble dynamics in ambient ocean noise; Sea Surface Sound (Ed. B.R.Kerman, Kluwer Academic Publishers), 151-171.

**A.Prosperetti,** 1988b, Bubble-related ambient noise in the ocean; JASA 84(3), 1042-54.

**A.Prosperetti,** 1991, Thermal effects behaviour of oscillating gas bubbles; JFM 222, 587-616.

**A.Prosperetti, L.A.Crum, K.W.Commander,** 1988, Nonlinear bubble dynamics; JASA 83(2), 502-14.

**A.Prosperetti, N.Q.Lu,** 1988, Cavitation and bubble bursting as sources of oceanic ambient noise; JASA 84(3), 1037-41.

**H.C.Pumphrey,** c.1987; Private spoken communication recalled by A.J.Walton.

**H.C.Pumphrey,** 1991a, Underwater rain noise – the initial impact component; Proc. I. O. Acoustics 13(3), 192-200.

**H.C.Pumphrey,** 1991b, Sources of underwater rain noise; Dordrecht (The Netherlands), Kluwer Academic Pub., Natural Physical Sources of Underwater Sound (Ed. B.Kerman).

**H.C.Pumphrey, L.A.Crum,** 1990, Free oscillation of near-surface bubbles as a source of the underwater noise of rain; JASA 87(1), 142-8.

**H.C.Pumphrey, L.A.Crum, L.Bjørnø,** 1989, Underwater sound produced by individual drop impacts and rainfall; JASA 85(4), 1518-25.

**H.C.Pumphrey, P.A.Elmore,** 1990, The entrainment of bubbles by drop impacts; JFM 220, 539-67.

**H.C.Pumphrey, J.E.Ffowcs Williams,** 1990, Bubbles as sources of ambient noise; IEEE J. of Oceanic Eng. 15(4), 268-74.

**H.C.Pumphrey, A.J.Walton,** 1988, Experimental studies of the sound emitted by water drops impacting a water surface; Eur. J. Phys. 9, 225-31.

**B.Ran, J.Katz,** 1991, The response of microscopic bubbles to sudden changes in the ambient pressure; JFM 224, 91-115.

**The Third Baron Rayleigh (J.W.Strutt),** 1917, On the pressure developed in a liquid during the collapse of a spherical cavity; Phil. Mag, 34, 94-98.

**R.A.Roy, S.I.Madanshetty, R.E.Apfel,** 1990, An acoustic backscattering technique for the detection of transient cavitation produced by microsecond pulses of ultrasound; JASA 87(6), 2451-8.

**G.Ryskin,** 1990, Dynamics and sound emission of a spherical cavitation bubble in a dilute polymer solution; JFM 218, 239-63.

**G.Ryskin, L.G.Leal,** 1984a, Numerical solution of free-boundary problems in fluid mechanics: I, the finite difference technique; JFM 148, 1-17.

**G.Ryskin, L.G.Leal,** 1984b, Numerical solution of free-boundary problems in fluid mechanics: II, Buoyancy-driven motion of a gas bubble though a quiescent liquid; JFM 148, 19-35.

**G.Ryskin, L.G.Leal,** 1984c, Numerical solution of free-boundary problems in fluid mechanics: III, Bubble deformation in an axisymmetric straining flow; JFM 148, 37-43.

**L.Samek,** 1989, A multiscale analysis of nonlinear oscillations of gas bubbles in compressible liquids: II. 1st and 2nd subharmonics and harmonics; Czech. J. Phys. B39, 136-71.

**R.M.Schmitt, H.J.Schmitt, J.Siegert,** 1987, *In vitro* estimation of bubble diameter distribution with ultrasound; IEEE Eng. in Med. and Biol. Soc., 9th Ann. Conf., Nov. 13-6.

**M.Schott, A.J.Walton,** 1977, A cryostat for measuring contact potential differences; J. Phys. E : Scientific Instruments 10, 226-8.

**P.M.Shanker,** 1991; Private communication to T.G.Leighton, Aug. 1st.

**P.M.Shanker, J.Y.Chapelon, V.L.Newhouse,** 1986, Fluid pressure measurement using bubbles insonified by two frequencies; Ultrasonics 24, 333-6.

**J.Siegert, R.M.Schmitt, H.J.Schmitt, T.Fritzsch,** 1987, Application of a resonance method for measuring the size of bubbles in an echocontrast agent; IEEE Eng. in Med. and Biol. Soc., 9th Ann. Conf., Nov. 13-6.

**T.N.Smith,** 1974, Measurement of drop size in liquid-liquid dispersions; Chem. Eng. Sci. 29, 583-7.

**W.R.Smythe,** 1968a, Charged conducting ellipsoid; Static and Dynamic Electricity, 3rd Ed. (1st Ed. 1939), pub. McGraw-Hill, Lib. Congress 67-28086, §5.02, 122-4.

**W.R.Smythe,** 1968b, Infinite set of images: two spheres; Static and Dynamic Electricity, 3rd Ed. (1st Ed. 1939), pub. McGraw-Hill, Lib. Congress 67-28086, §5.08, 128-32.

**A.A.Stavs, U.von Stochar,** 1985a, Measurement of number and size distribution of reflecting objects by pulsed ultrasound; JASA 77(4), 1419-24.

**A.A.Stavs, U.von Stochar,** 1985b, Measurement of interfacial areas in gas-liquid dispersions by ultrasonic pulse transmission; Chem. Eng. Sci 40(70, 1169-75.

**M.Strasberg,** 1953, The pulsation frequency of nonspherical gas bubbles in liquids; JASA 25(3), 536-7.

**M.Strasberg,** 1956, Gas bubbles as sources of sound in liquids; JASA 28(1), 20-6.

**G.G.Stokes,** 1851, On the motion of pendulums, §IV; Trans. Camb. Phil. Soc. 9 (reprinted as:- C.U.P., G.G.Stokes: Mathematical and Physical Papers, vol. III, 55-75).

**G.G.Stokes,** 1868, On the communication of vibration from a vibrating body to surrounding gas; Phil. Trans. Roy. Soc. (reprinted as:- C.U.P., G.G.Stokes: Mathematical and Physical Papers, vol. IV, 299-324).

**K.S.Suslick , E.B.Flint,** 1987, Sonoluminescence from non-aqueous liquids; Nature 330, 553-5.

**G.Taylor,** 1950, The instability of liquid surfaces when accelerated in a direction perpendicular to their planes: I; Proc. Roy. Soc. A201, 192-6.

**S.Temkin,** 1990, Attenuation and dispersion of sound in bubbly fluids via the Kramers-Kronig relations; JFM 211, 61-72.

**R.M.Tennet** (Editor), 1971; The Open University Science Data Book, pub. Oliver and Boyd (Longman), ISBN 0-05-002487-6.

**H.D.Thoreau,** 1854, Walden; pub. (originally Ticknor and Fields) Penguin 1983, 168-9.

**S.A.Thorpe,** 1982, On the clouds of bubbles formed by breaking wind-waves in deep water and their role in air-sea gas transfer; Phil. Trans. Roy. Soc. A 304, 155-210.

**S.A.Thorpe,** 1984, The effect of Langmuir circulation on the distribution of submerged bubbles caused by breaking wind waves; JFM 142, 151-70.

**D.H.Trevena,** 1987a, Bubble studies; IOP Pub. Ltd., Adam Hilger (Pub.), Cavitation and Tension in Liquids, chapter 5.

**D.H.Trevena,** 1987b, Miscellaneous related topics; IOP Pub. Ltd., Adam Hilger (Pub.), Cavitation and Tension in Liquids, chapter 7.

**D.H.Trevena,** 1987c, Cavitation erosion; IOP Pub. Ltd., Adam Hilger (Pub.), Cavitation and Tension in Liquids, chapter 6.

**E.Tucker** (assistant producer) with help from **A.J.Walton, T.J.Mason, A.J.Hardwick, P.L.Kaye, C.J.Pickles** and the production crew, 1994, Sonoluminescence; Tomorrow's World, British Broadcasting Corporation, screened 1994/2/11.

**P.Turin,** 1964, Supercavitating flows and practical applications; Elsevier Pub. Co., Cavitation in Real Liquids (Ed. R.Davies),55-79.

**M.Vacher, G.Gimenez, R.Gouette,** 1984, Nonlinear behaviour of microbubbles: application to their ultrasonic detection; Acustica 54, 274-283.

**M.E.van Valkenburg,** 1982, Active Filter Design; pub. CBS College Publishing (Holt, Rinehart and Winston), ISBN 0-03-059246-1.

**P.W.Vaughan, S.Leeman,** 1986, Sonoluminescence: violent light or gentle glow?; IEEE Ultrasonics Symposium, 989-92.

**K.Vokurka,** 1988a, A model of spark and laser generated bubbles; Czech. J. Phys . B 38, 27-34.

**K.Vokurka,** 1988b, Evaluation of data from experiments with spark and laser generated bubbles; Czech. J. Phys . B 38, 35-46.

**A.J.Walton,** 1972, Lectures, Tutorials and the Like; Medical and Technical Pub. Co. Ltd., SBN 852 00031 6.

**A.J.Walton,** 1976, The Three Phases of Matter; pub. McGraw-Hill, ISBN 0-07-084063-6.

**A.J.Walton, G.T.Reynolds,** 1984, Sonoluminescence; Advances in Phys. 33(6), 595-660.

**A.J.Watson, R.C.Upstill-Goddard, P.S.Liss,** 1991, Air-sea gas exchange in rough and stormy seas measured by a dual-tracer technique; Nature 349, letters, 145-7.

**D.J.Watmough, H.M.Davies, K.M.Quan, R.Wytch, A.R.Williams,** 1991, Imaging microbubbles and tissues using a linear focused scanner operating at 20 MHz: possible implications for the detection of cavitation thresholds; Ultrasonics 29, July, 312-8.

**F.Weldon,** 1987, The Rules of Life; pub. Hutchinson.

**G.M.Wenz,** 1962; JASA 34, 1936-56. [Medwin and Beaky 1989]

**C.West, R.Howlett,** 1969, Cavitation bubble dynamics; Acustica 21, 112-7.

**P.J.Westervelt,** 1957, Scattering of sound by sound; JASA 29(2), 199-203.

**A.R.Williams, M.Delius, D.L.Miller,** 1989, Investigation of cavitation in flowing media by lithotripter shock waves both *in vitro* and *in vivo*; Ultrasound in Med. and Biol. 15(1), 53-60.

**J.Wolf,** 1988, Investigation of bubbly flow by ultrasonic tomography; Part. and Part. Sys. Characterisation 5, 170-3.

**A.M.Worthington, R.S.Cole,** 1897, VI: Impact with a liquid surface studied by the aid of instantaneous photography; Phil. Trans. Roy. Soc., 137-48 + plates.

**P.Yam,** 1993, The colour of sound: shedding light on sonoluminescence; Scientific American, December, 13-14.

**P.Y.W.Yu, R.L.Varty,** 1988, Laser-Doppler measurement of the velocity of bubbles using the triple-peak technique; Int. J. Multiphase Flow, 14(6), 765-776.

### A NOTE CONCERNING ERRORS

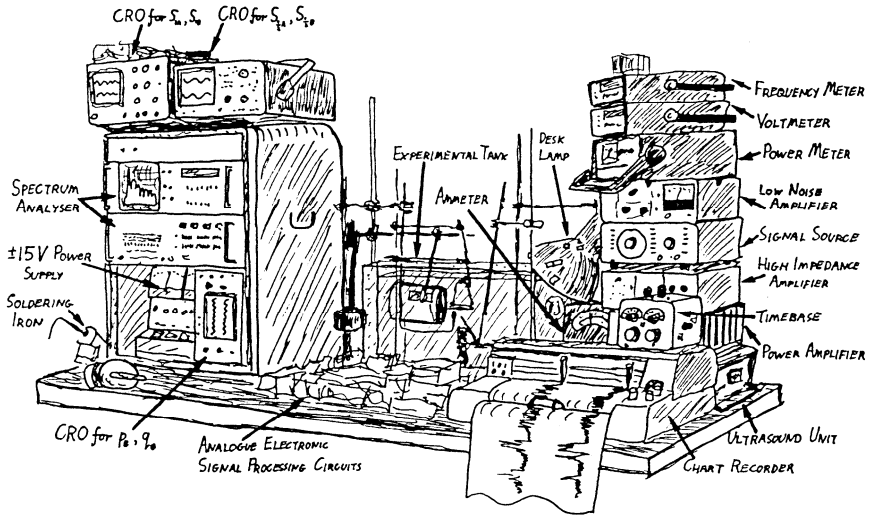
Where an indication of the magnitude of random errors in graphed data would have been appropriate but was neither mentioned in the text nor shown as error bars in the figure, the errors

were sufficiently small that the error-bars would have been smaller than the markers used for the data points.

Unless otherwise stated, numerical results from curve fitting have been obtained by least-squares methods and the corresponding error values are standard deviations from the lines of best-fit. Error values for individual points are based on estimations of the precision of the measuring tools used and, for quantities measured by the specially created devices, the variations found between separate trials under similar circumstances.

## A.7. APPENDIX 7: PHOTOGRAPHIC PLATES

The photographs are at the end because they printed on photographic paper in the first 2 editions of this dissertation and the stiffness of the photographic paper differed from that of the other pages. The apparatus shown in Plate 1 is labeled in the drawing below; for the labels corresponding to Plate 2 see figure 4.8.



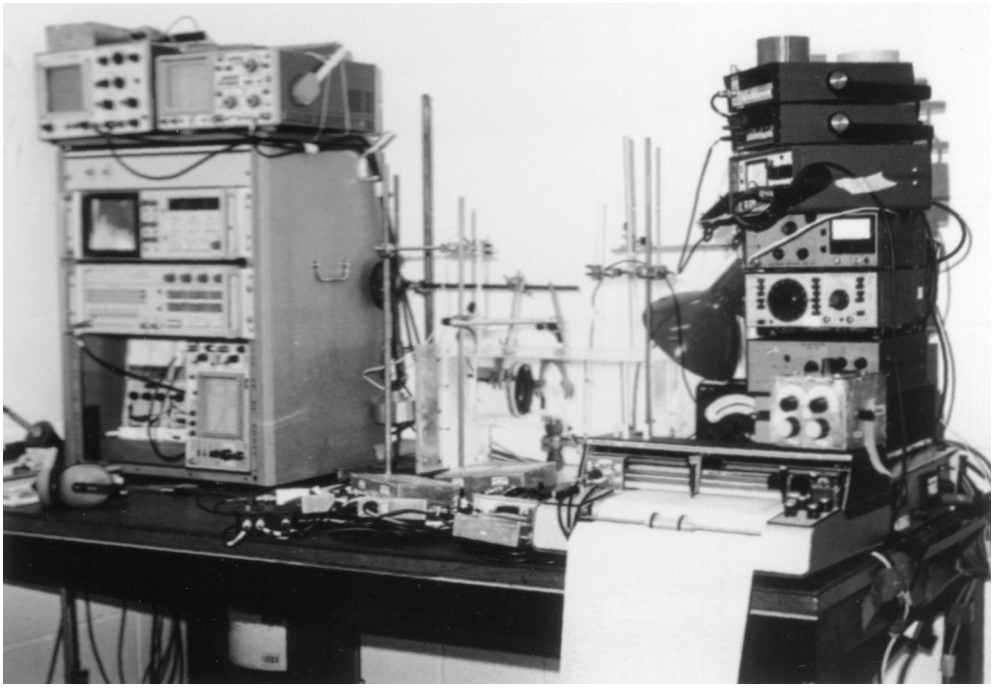


**Plate 1.** The apparatus for the subharmonic modulation experiments in use. (Photograph by Kelvin Fagin.)

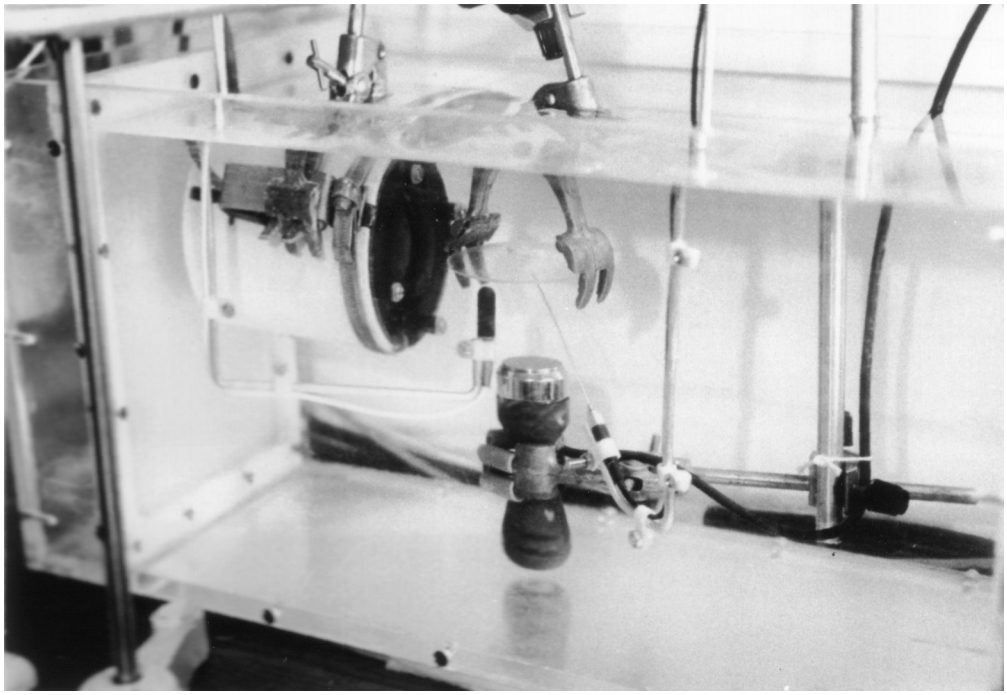


**Plate 2.** Close-up of the tank shown in plate 1. (Photograph by Kelvin Fagin.)

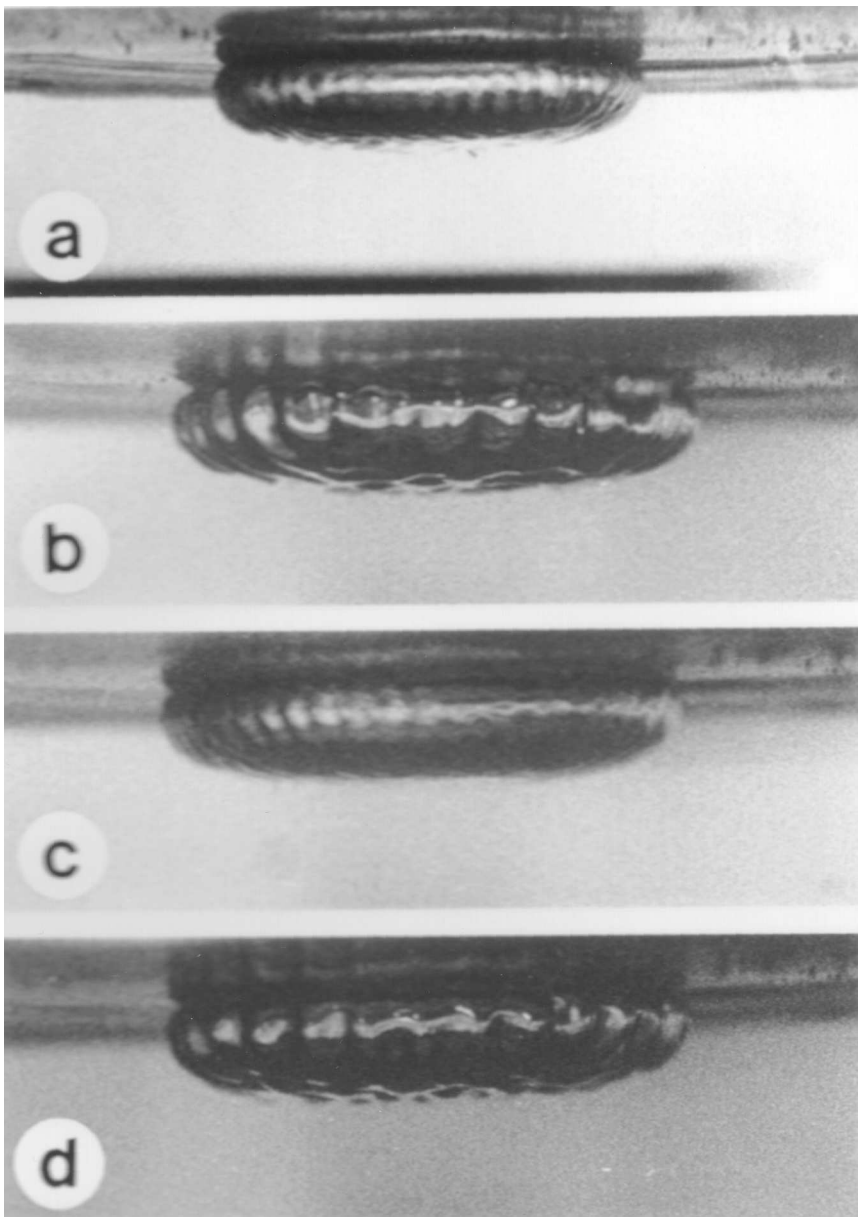



**Plate 3.** A 3 ml bubble exhibiting surface waves when excited by sound at $\nu_e$.
(a) continuously illuminated,
(b) illuminated by a single flash,
(c) strobe lit at $\nu_e$,
(d) strobe lit at $\nu_e/2$.
(Photograph by the author.)